MONASH University

The Synthesis of Arylsulfides from Arylhalides via Visible Light Photoredox Catalysis

by John Burton

Masters of Science

2016

A thesis submitted for the degree of Masters at

Monash University in 2016

Department of Chemistry

In collaboration with CSIRO Australia

Copyright notice

I certify that I have made all reasonable efforts to secure copyright permissions for third-party content included in this thesis and have not knowingly added copyright content to my work without the owner's permission.

Declaration

This thesis contains no material which has been accepted for the award of any other degree or diploma at any university or equivalent institution and that, to the best of my knowledge and belief, this thesis contains no material previously published or written by another person, except where due reference is made in the text of the thesis.

Acknowledgements

First of all, I would like to thank A/Prof David Lupton for all of his help and guidance over the last 2 years. I have learnt more than I would have dreamed possible from being involved with your group.

To Dr Tash Polyzos, thank you for everything you have done for me since starting this project. The last two years have been a rollercoaster of good and bad times and you have been a greater help to me than I ever expected you could be. You were my Supervisor and helped and pushed me with this project, but more importantly you were a friend. For this I thank you and will never forget your kindness, or having to clean that first laboratory.

Thank you to Dr Milena Czyz. Your help and guidance over the last year cannot be overstated. Your help with my education as well as advice and insights into my project will always be appreciated. Especially your help with teaching me how to write my thesis correctly.

Thank you to Dr Martin Brzozowski and the rest of the Polyzos group. You have all been there from pizzas to souvlakis giving help and support.

Lastly I would like to thank my family, especially my mother, for the constant support and care. Being able to leave the stress of my studies and recharge my batteries at home on weekends was more help than I can ever state.

Abstract

This thesis describes the development of a reaction to prepare aryl sulfides from aryl iodides under visible light photoredox catalysis. Visible light is used to excite a photocatalyst which leads to an oxidative catalytic cycle. The excited photocatalyst reduces a chosen aryl iodide forming an aryl radical to undergo electrophilic addition with a disulfide to form a desired aryl sulfide. This research addresses some of the limitations of traditional transition-metal catalysed cross-coupling reactions, through the development of a radical-mediated cross-coupling reaction to afford aryl sulfides.

An introduction to cross-coupling reactions and visible light photoredox catalysis is described in Chapter 1.

Chapter 2 describes the reaction design and mechanistic studies with a focus on eliminating competitive reduction of the starting aryl iodide. Particular interest was taken in examination of Single Electron Transfer (SET) donors and solvents as these would be the most probable source of reduction in the reaction.

A summary of this work and proposed future studies is delineated in Chapter 3. All procedures and results are present in Chapter 4.

Abbreviations

AIBN	azobisisobutyronitrile
Bu_3N	tributyl amine
^tBuOH	*tert*- butyl alcohol
bpy	bipyridine
cat.	catalyst
$CHCl_3$	chloroform
dF	difluoro
DIPEA	*N*,*N*-diisopropyl amine
DiPPF	bis(diisopropylphosphino)ferrocene
DME	dimethoxyethane
DMF	*N*,*N*-dimethylformamide
DMDS	dimethyl Disulfide
DMSO	dimethyl sulfoxide
dtbbpy	di-*tert*-butyl bipyridine
Et_3N	triethyl amine
EtOH	ethylalcohol
eq	Equivalent(s)
GC/MS	Gas Chromatography/ Mass Spectrometry
$HSnBu_3$	tributyltin hydride
Josiphos	1-[*bis*(1,1-dimethylethyl)phosphino]-2-[(1*R*)-1-[*bis*(2-methylphenyl)phosphino]ethyl]ferrocene
LED	light emitting diode
Me	methyl
MeCN	acetonitrile

MeOH	methanol
mol	mole(s)
MLCT	metal to ligand charge transfer
NAS	N-(arylthio)-succinimides
Na^{t}BuO	sodium *tert*-butoxide
NHC	N-heterocyclic carbene
NMP	N-Methyl-2-pyrrolidone
NMR	nuclear magnetic resonance
p-	para-
PFA	perfluoro alkoxy alkane
Ph_3N	triphenylamine
ppm	parts per million
ppy	2-phenylpyridine
$^{i}Pr_3N$	triisopropylamine
^{i}PrOH	Isopropylalcohol
SCE	saturated calomel electrode
S_{EAr}	electrophilic aromatic substitution
SET	single electron transfer
t-	tert-
TFA	trifluoroacetic acid
UV	ultraviolet

Table of Contents

Chapter 1:

Introduction

Chapter 1: Introduction:

The synthesis of aryl sulfides is of importance in modern organic synthetic chemistry owing to a large number of naturally occurring and synthetic materials containing C(sp^2)-S bonds.[1] Aryl sulfides form important building blocks of compounds used in material science and the pharmaceutical industry.[2]

Various pharmaceutical compounds that contain an aryl sulfide or derived from an aryl sulfide group include Sildenafil (**1**), commonly known as Viagra which was worth over US$2 billion in 2012, Nelfinavir (**2**), an HIV antiretroviral drug worth over $US335 million and Salazopyrin (**3**), used for the treatment of Rheumatoid arthritis.

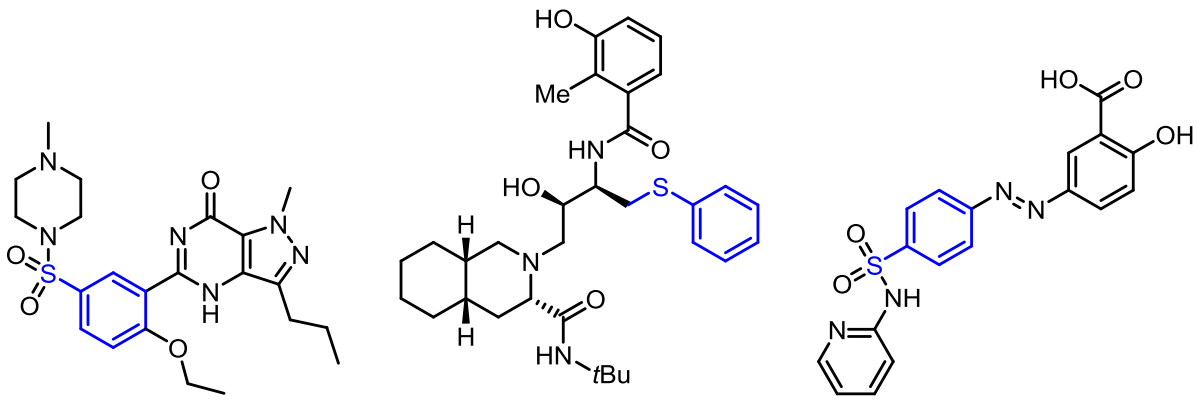

Figure 1: Examples of approved pharmaceuticals containing aryl sulfides

The aryl sulfide scaffold is also present in natural products, such as sunset yellow dye (**4**) and varamine A (**5**) & B (**6**), a secondary metabolite from *Lissoclinum uarea*,[3] (Figure 2). As a consequence, there has been significant interest in discovering efficient catalytic methods for the synthesis of aryl sulfides.

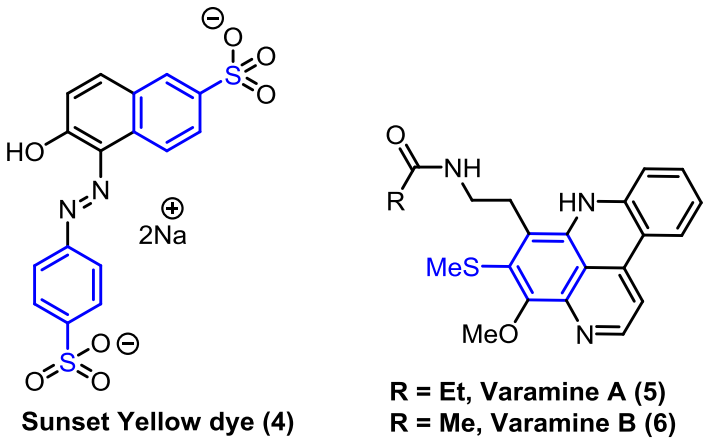

Figure 2: Further examples of aryl sulfides in a dye (left) and natural product (right).

Many current approaches that enable the synthesis of aryl sulfides exploit transition metal catalysed cross coupling reactions. Important examples are summarised in the following section.

1.1 Palladium Catalysed Thiolation of Aryl Halides

Palladium catalysed cross-coupling reaction between aryl halides and thiols to afford aryl sulfides were first reported by Migita in 1978 (Scheme 1).[4] Migita observed that aryl iodides and bromides react with thiolate anions (prepared *in situ* from thiols in the presence of Na^{t}BuO) in DMSO at 100 °C to give aryl sulfides albeit in poor yields (trace to 33%). However, higher yields of 49-98% were obtained in the presence of the Pd[0] catalyst, $Pd(PPh_3)_4$. Further mechanistic insight was reported, in which the reaction was not inhibited when *p*-dinitrobenzene was added to the mixture, suggesting that the mechanism is likely to involve oxidative addition of aryl halide to Pd[0] complex rather than a radical-nucleophilic aromatic substitution reaction.

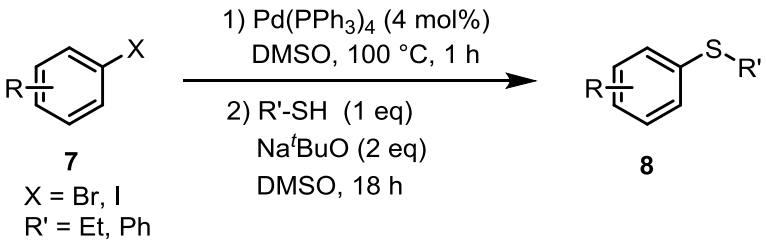

Scheme 1: First reported palladium catalysed formation of aryl sulfides

A general mechanism for the palladium-catalysed cross-coupling reaction between aryl halides and heteroatoms is shown in Scheme 2. This mechanism proceeds through oxidative addition of the aryl halide (step **A**) to Pd[0] to give organopalladium complex **10**. Co-ordination of the thiol (step **B**), followed by transmetallation and reductive elimination (step **C**) yields the newly formed carbon-heteroatom product and regenerates Pd[0] catalyst.

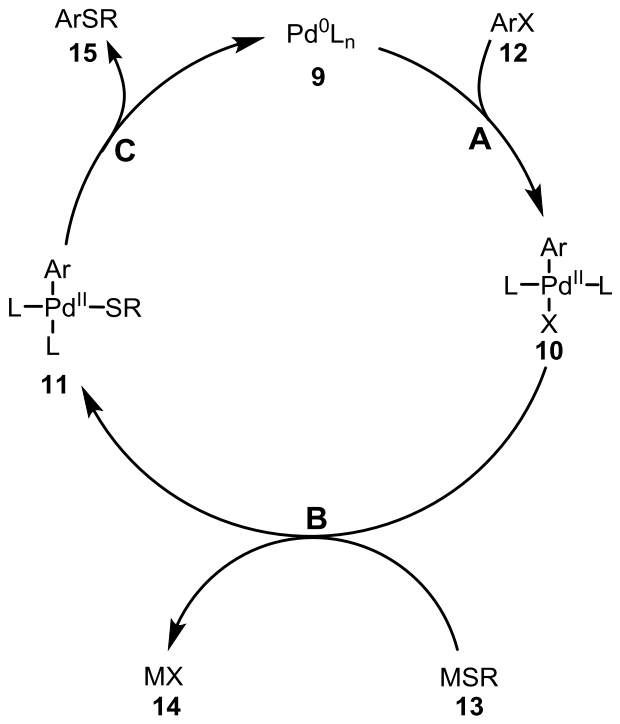

Scheme 2: General mechanism for palladium catalysed carbon-heteroatom bond formation

Migita's method tolerated neutral and electron-poor aryl iodides and bromides, however gave only moderate yields with electron-rich substrates, while less activated aryl chlorides failed to react. Furthermore, the reaction scope was limited to unhindered, *para*-substituted aryl iodides and bromides. To overcome these limitations, in 2004, Buchwald and co-workers tested a variety of monodentate and bidentate phosphine ligands,[5] and have found that the bidentate ligand 1,1'-bis(diisopropylphosphino)ferrocene (DiPPF) was optimal (Scheme 3). The use of bidentate ligands was

rationalised as being more effective for this reaction on the basis that monodentate ligands allow more than one substrate to bind to the catalyst leading to unwanted deactivation. However, the bidentate ligand demanded specific steric bulk and flexibility within the structural design of the catalyst to allow reduction of Pd[II] species to Pd[0]. Using DiPPF as a ligand Buchwald reported couplings of electron-rich and sterically-hindered aryl halides and primary, secondary and tertiary aromatic thiols in excellent yields (82-99%). Despite excellent yields for all substrates reported, Buchwald's method had a limited reaction scope of only 6 substrates and none of these were active functional groups.

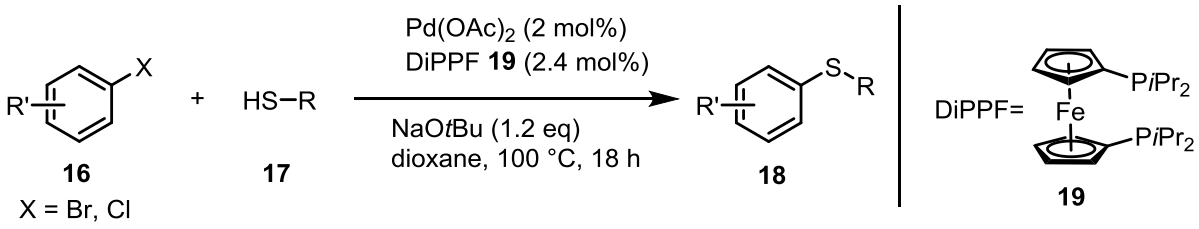

Scheme 3: Buchwald's synthesis of aryl sulfides

In 2006, Hartwig and co-workers reported the use of a related strongly co-ordinating ligand, Josiphos, with palladium acetate to create a highly reactive catalytic system for the C-S bond formation[6] (Scheme 4). Buchwald's methods had previously reported the synthesis of aryl sulfides from chloroarenes but only those containing alkyl, nitrile, ether or ester functionality. Also, the reaction reported has low turnover numbers (≤ 50) and do not include the use of aryl tosylates, limiting the use of these reactions in the preparation of various sulfides. Hartwig's reaction worked at extremely low catalyst loading (0.001-2 mol%) to produce aryl sulfides by the coupling of thiols with aryl chlorides, iodides, bromides, triflates and tosylates at 110 °C in DME (Scheme 4). The reaction worked well with neutral, electron-rich and electron-poor aryl chlorides giving yields between 70-98%. Hartwig also reported the versatility of his method with different arene functionality and thiol coupling partners. The use of neutral bromo-, iodo-, triflic- and tosyl arenes with alkyl or aryl thiols gave high to excellent yields (79-99%). Even though the reaction is shown to give excellent yields with a range of substrates, just like

the other reported Pd[0] catalysed reactions, it still requires the use of high temperatures and long reaction times.

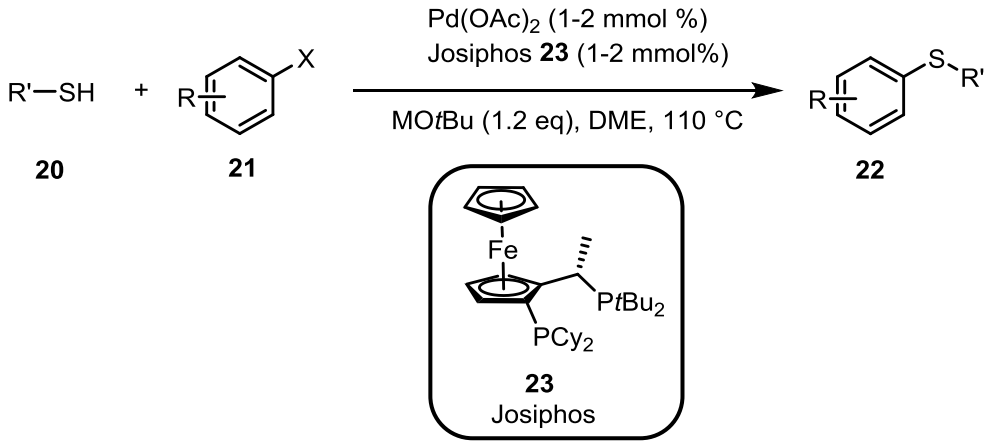

Scheme 4: The palladium catalysed synthesis of aryl sulfides described by Hartwig *et al.*

In 2013 Nolan and Bastug reported the use of a palladium-NHC complex as an alternative to phosphine-based catalytic systems.[7] While Migita, Buchwald and Hartwig had all reported significant advances in the synthesis of aryl sulfides via Pd[0] catalysis, each of them depended on phosphine-based ligands, which are expensive and can be sensitive to reaction conditions. *N*-Heterocyclic carbene (NHC) complexes have already been found to be efficient catalysts in Buchwald-Hartwig amination reactions[8] due to their higher reactivity and thermal stability compared to phosphine ligands. The steric bulk of [Pd(IPr*OMe)(cin)Cl] enabled stabilisation of the low-valent active intermediate and favoured reductive elimination. The strong σ-donor characteristic of the NHC-ligand facilitates the oxidative addition of aryl halides.[9] Nolan and Bastug observed good to excellent yields of aryl sulfides by coupling aryl or alkyl thiols with sterically and/or electronically deactivated aryl halides (69-97%) in dioxane at 110 °C.

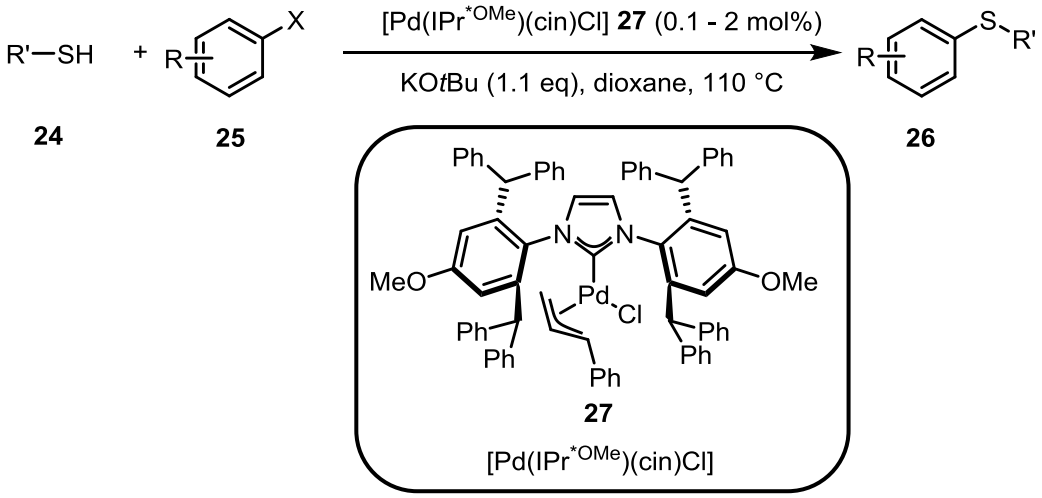

Scheme 5: Pd-NHC catalysed formation of aryl sulfides

1.2 Nickel Catalysed Thiolation of Arylhalides

Nickel has been shown to catalyse formation of aryl sulfides from aryl halides and thiol derivatives. In 1981 Cristau *et al.* reported the use of a nickel (II) complex with a bidentate phosphine ligand[10] at 0.3% catalyst loading to form the corresponding diaryl-sulfide in good to excellent yields (Scheme 6). The reaction does however require significantly higher temperatures than the corresponding Pd-catalysed-methods.

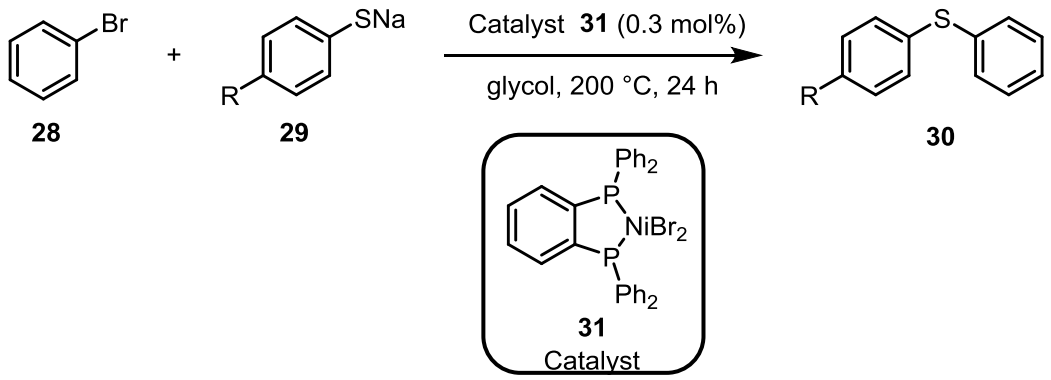

Scheme 6: Nickel catalysed formation of diaryl sulfides

In 2004, Taniguchi reported the use of disulfides as coupling partners with $NiBr_2$-bpy and stoichiometric Zn as a reductant.[11] Taniguchi observed the formation of aryl sulfides from electron-rich and electron-poor aryl iodides and dialkyl sulfides in moderate to good yields (61-92%). It is noteworthy that only 0.5 equivalent of the disulfide was needed to achieve these yields, however, higher catalyst loading (10 mol%) and longer reaction were required under these conditions (Scheme 7).

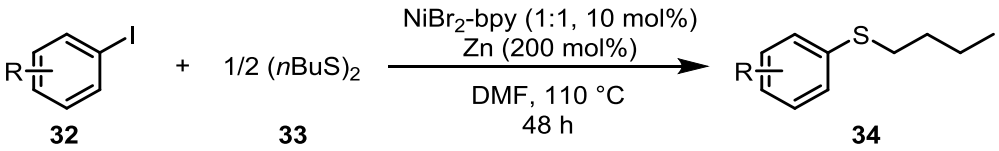

32 **33** **34**

Scheme 7: Nickel catalysed aryl sulfide formation with disulfides.

The reaction has been proposed to involve the initial reduction of the nickel [II] salt by zinc to nickel (0) (Scheme 8). Oxidative addition of either aryl iodide or disulfide produces Ni[II] complex, which is reduced by Zn to Ni[I]. Oxidative addition of the other coupling partner leads to formation of a Ni[III] species, which is postulated to undergo reductive elimination to form Ni[I]. The cycle that utilises the aryl halide as coupling partner 1 and the disulphide as the second coupling partner (Cycle A), then has one last step before the catalytic cycle can repeat. The final complex converts a second equivalent of aryl halide to the aryl sulfide product thereby also regenerating the nickel salt which can be reduced by Zn to repeat the catalytic cycle.

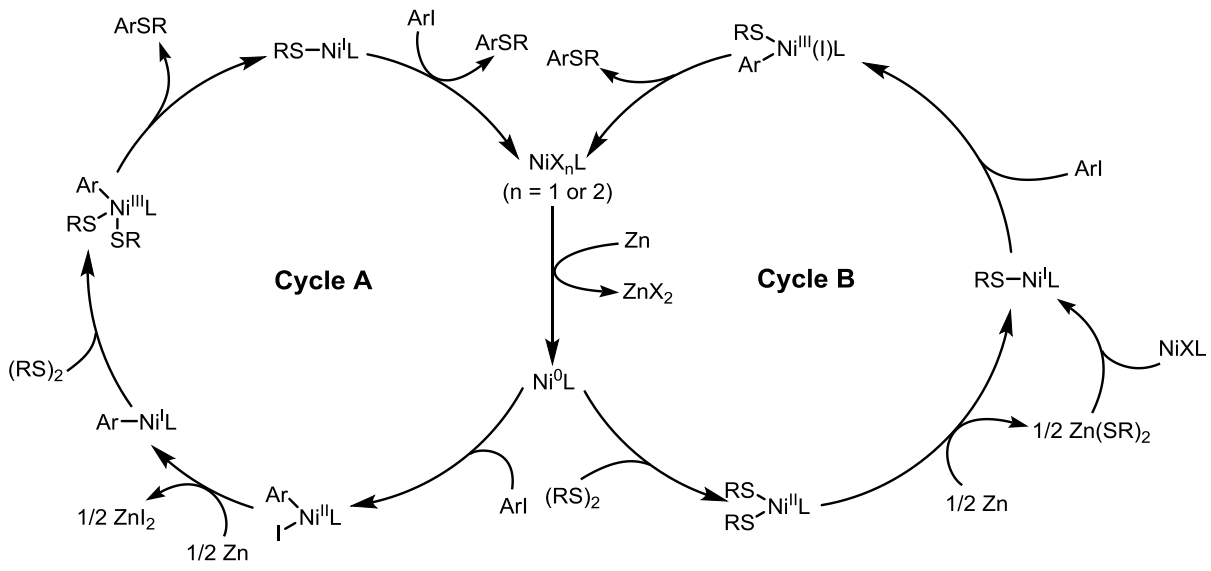

Scheme 8: Catalytic cycle for $NiBr_2$-bpy catalyst

Following Taniguchi's work, Morales-Morales *et al.* also reported the use of disulfides in the Ni-catalysed formation of aryl sulfides (Scheme 9). With the use of a highly functionalised nickel "pincer" catalyst and zinc, Morales-Morales *et al.* were able to form aryl sulfides from iodobenzene and a range disulfides in high yields (60-90%) at 160 °C in DMF in only 4 hours.[12] However, the reaction had a limited substrate scope. Aryl bromides, electron-rich and poor variants, yielded poorer results with a maximum yield of 35%. This was expected as the energy requirements for cleaving a C-Cl or C-Br bond is greater than cleaving a C-I bond.

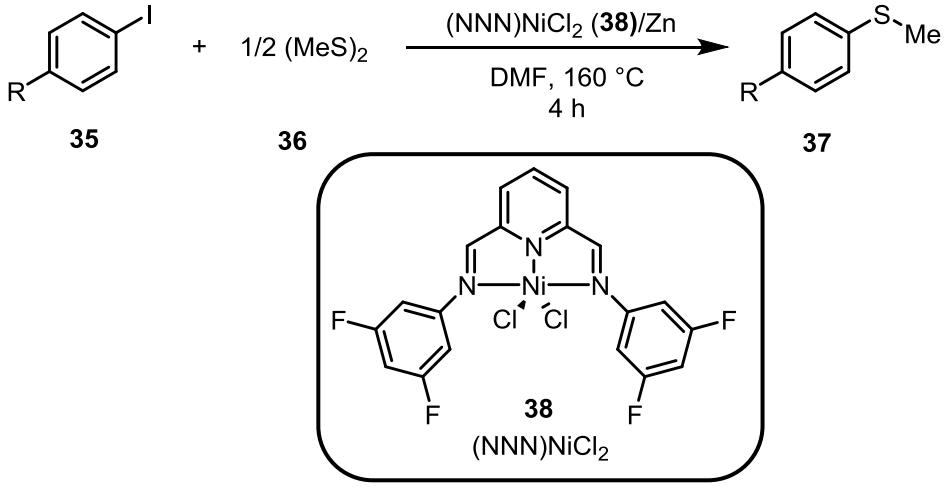

Scheme 9: Nickel "pincer" complex catalysed formation of aryl sulfides

1.3 Copper-Catalysed Thiolation of Arylhalides

Copper-catalysed formation of biaryl ethers was discovered in 1904 and is known as the Ullmann reaction. Copper has advantages over other transition metals such as palladium due to its wider availability and lower cost. In 1998, the Chan-Evans-Lam modification of the Ullman coupling was reported which incorporated the synthesis of biaryl ethers, amines and thioethers[13] from phenols, anilines and thiophenols respectively. In 2013 the reaction scope was further extended, to allow the synthesis of aryl suflides. This was achieved by the use of CuI in the presence of $Zn(OAc)_2$ co-catalyst (Scheme 10). It was proposed that $Zn(OAc)_2$, acted as a Lewis acid, to activate DMSO prior to addition to the copper catalyst and subsequent formation of aryl sulfide with aryl iodide (Scheme 11). Consistent yields of 70-96% were observed when coupling electron-rich, electron-poor or neutral aryl iodides were reacted with DMSO at 130 °C for 24 hours.

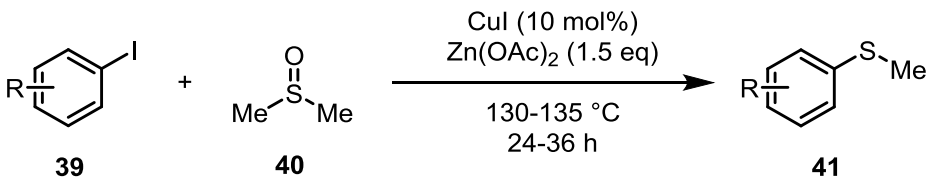

Scheme 10: Synthesis of aryl sulfides by catalytic CuI

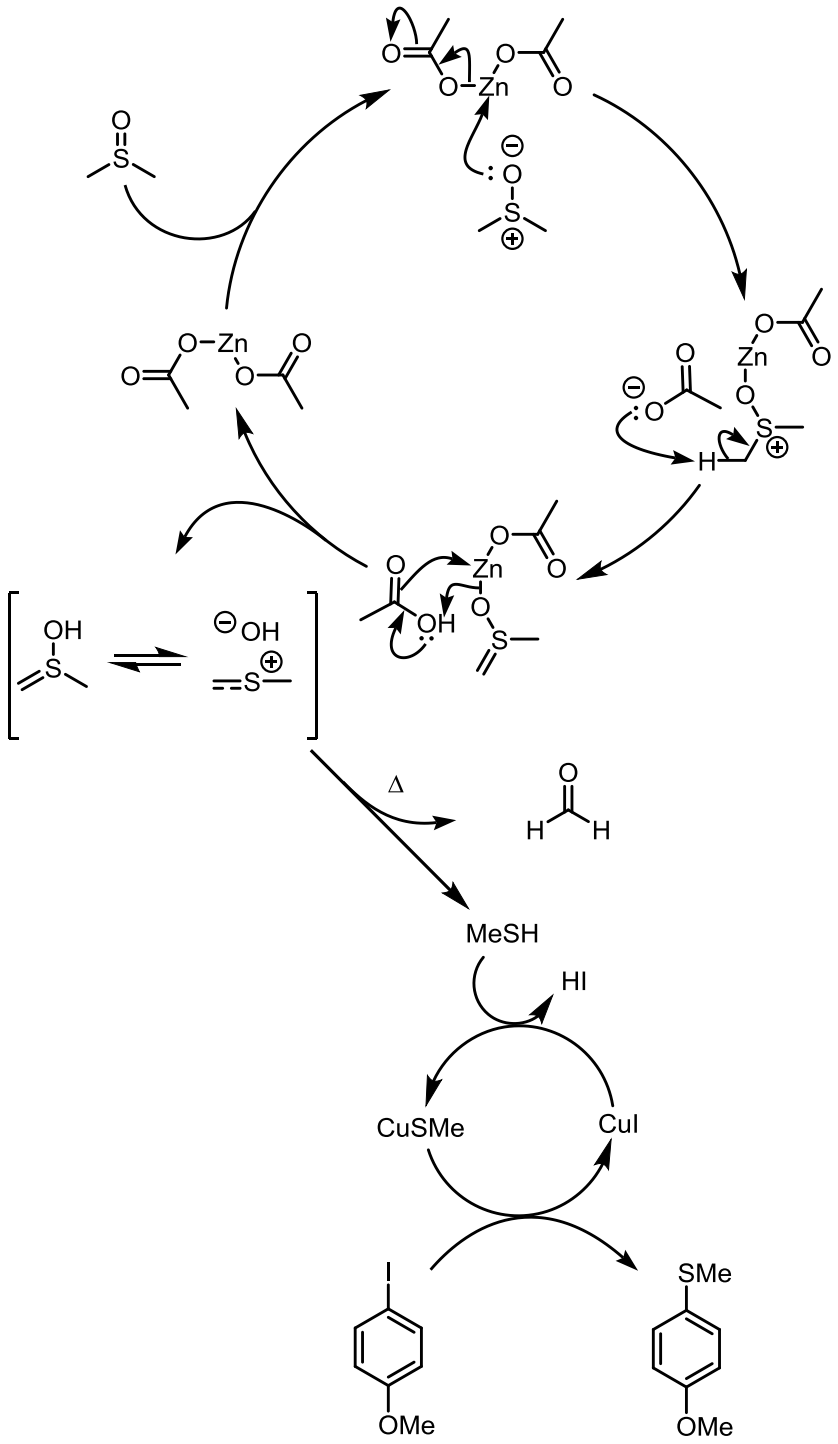

Scheme 11: Zn(OAc)2 activated DMSO thioetherification catalytic cycle

Peñéñory and Castro reported the formation of S-aryl thioacetates by the reaction of inexpensive potassium thioacetate with both electron-rich and electron-poor aryl iodides.[14] The use of CuI with a

bidentate 1,10-phenanthroline ligand in toluene at 100 °C for 24 hours afforded the desired thioacetates in good to excellent yields (73-96% yield).

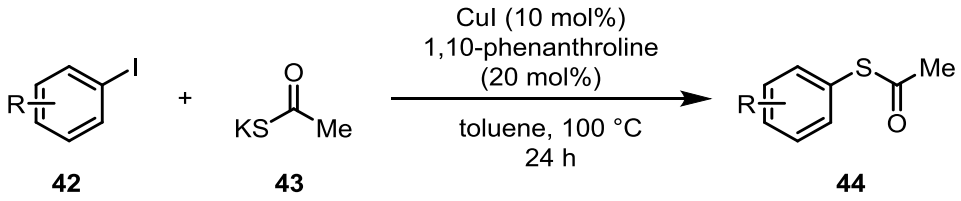

Scheme 11: CuI catalysed formation of S-aryl thioacetates

CuI has also been used as a photocatalyst to form diaryl sulfides from aryl thiols and aryl halides.[15] This methodology harnesses ultraviolet (UV) radiation to activate the catalyst to initiate the catalytic cycle and addresses a significant issue of transition metal catalysed C-S bond formation reactions; the high temperature. By initiating the reaction with UV irradiation, this Ullmann-like reaction was conducted at low temperatures with added NaO*t*-Bu as a single electron transfer (SET) donor. Diaryl sulfides were afforded in moderate to high yields (63-90%) from sterically bulky, electron-rich and electron-poor aryl iodides in less than 8 hours (scheme 12).

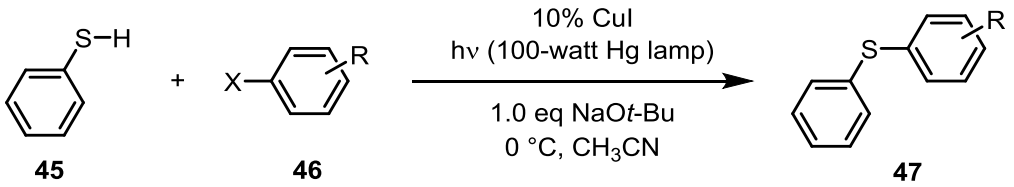

Scheme 12: Photo-induced copper catalysed diaryl sulfide formation

Significant progress has been made towards the development of transition-metal catalysed reactions described in sections 1.1-1.3. In addition to Pd, Ni and Cu-catalysed methodologies, the use of other metal, such as (Co,[16] In,[17] Fe,[18] Rh,[19] Au[20]) as well as nanoparticles[21] have also been reported.

However, the issues associated with high temperatures and long reaction times continue to persist. In an effort to overcome these limitations, transition-metal free methodologies have been developed.

1.4 Transition Metal Free Methods for the Synthesis of Aryl Sulfides

Recently, Cossy *et al*. reported the synthesis of aryl sulfides by direct C-H thiolation.[22] Electron-rich arenes were reacted with N-(arylthio)-succinimides (NAS **49**) and trifluoroacetic acid (TFA) at room temperature to produce the desired aryl sulfide **50** in modest to excellent yields (17-98%) in 6 hours (Scheme 20). The proposed mechanism is shown in Scheme 21. Treatment of arene with NAS in the presence of TFA leads to protonation of NAS and generation of an electrophilic thiol transfer intermediate **53**. This intermediate can participate in electrophilic aromatic substitution with the electron rich arene to produce the aryl cation **54**. The expected aryl sulfide is formed after deprotonation and regeneration of TFA. Consistent with other electrophilic aromatic substitution reactions, substrate scope was limited to electron-rich arenes.

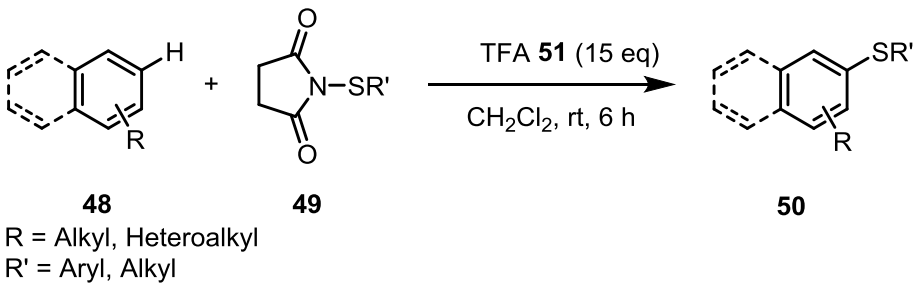

Scheme 20: TFA catalysed aryl sulfide synthesis

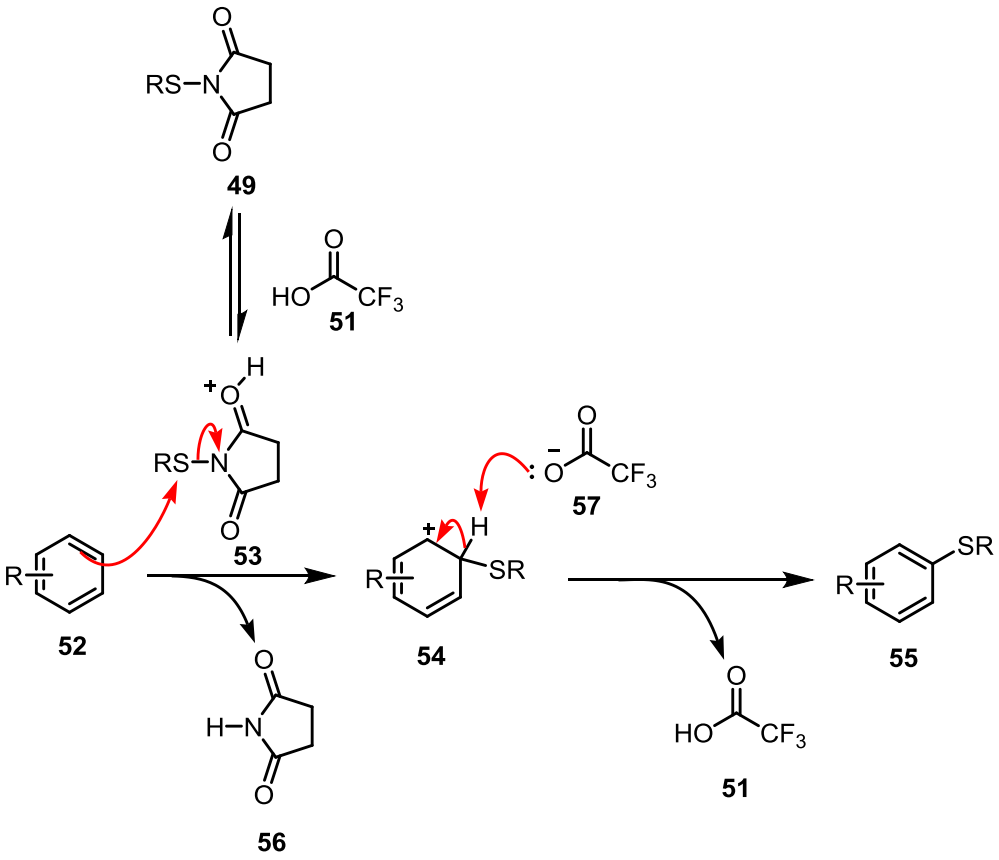

Scheme 21: TFA catalysed mechanism

Radical-based reactions have been reported as a viable option in the synthesis of aryl sulfides. In 2013, von Wangelin and Majek reported the use of light sensitive dye, Eosin Y (**61**), as a photoredox catalyst to irreversibly reduce diazonium salts to arene radicals that could be intercepted by a disulfide .[23] Von Wangelin and Majek observed modest to good yields with both electron-rich and electron-poor arenes (31-89% yield). Diazonium salts were chosen as starting materials as they are easily prepared and can be irreversibly reduced under mild conditions. However, the necessity to prepare the diazonium salt substrates from the corresponding amines limits the scope of the reaction, as demonstrated by the limited array of examples reported. Furthermore, thiol diazonium adducts can be thermally and mechanically unstable, leading to hazardous explosive detonation.

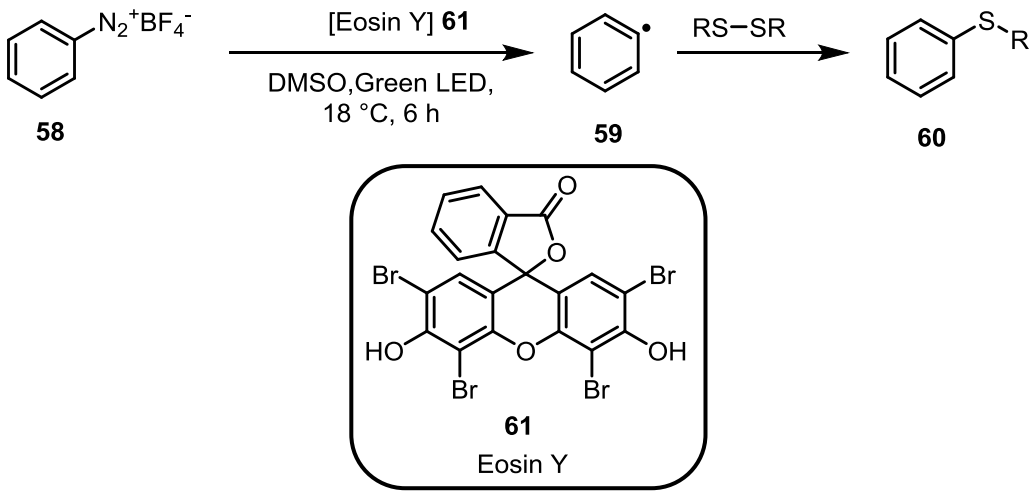

Scheme 23: Visible light photoredox catalysed aryl sulfide synthesis

Scheme 24 shows the mechanism proposed by von Wangelin and Majek. The arene-diazonium salt is irreversibly reduced by SET from the excited photocatalyst (E*), resulting in the formation of an aryl radical and nitrogen gas. The resulting aryl radical (**59**) can then be attacked by the nucleophilic disulfide to give a trivalent sulfur radical **64**. This trivalent sulfur radical would be stabilised by the aryl and sulfur neighbouring groups. Oxidation by SET with the eosin Y radical cation produces an electrophilic species that can undergo substitution with DMSO in large excess (solvent) resulting in the formation of the product (**60**) and a dithiol ether species (**67**).

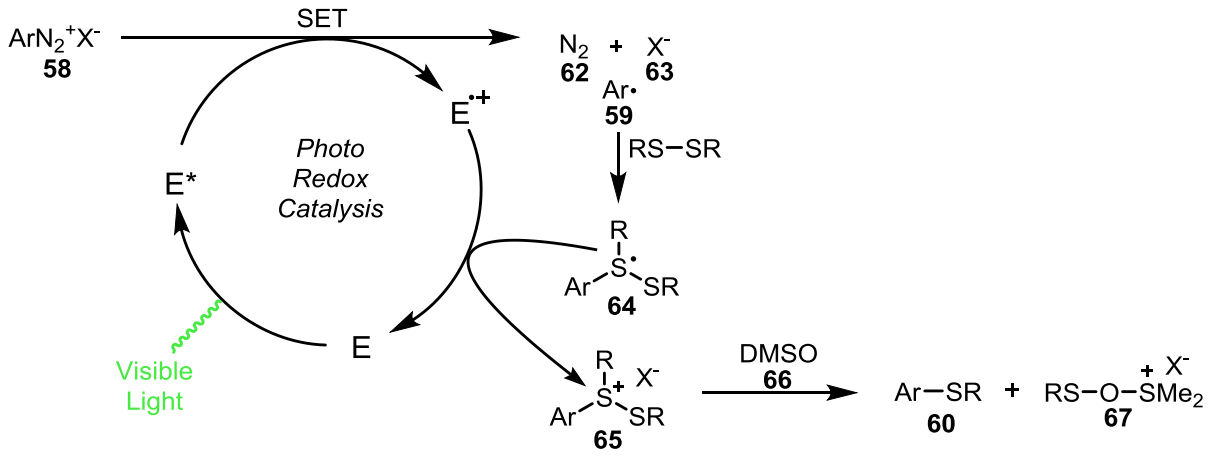

Scheme 24: Mechanism of aryl sulfide synthesis from diazonium salts

The use of radicals in the formation of aryl sulfides has the potential to alleviate many of the issues observed with transition-metal catalysed reactions and with electrophilic aromatic substitution. However radical reactions are still underdeveloped compared to transition-metal catalysis, as they have traditionally required the use of hazardous reagents (eg. $HSnBu_3$, AIBN) often employed in stoichiometric amounts to initiate the reaction. In recent years, photoredox chemistry has emerged as an attractive method for the initiation of radical reactions under mild, catalytic conditions.

1.5 Visible Light Photoredox Catalysis

Photoredox catalysis is a method for the initiation of radical reactions under mild conditions and at room temperature by the activation of a catalyst using visible light. Most commonly used photoredox catalysts are metal centred complexes (usually Ruthenium or Iridium) with polypyridyl ligand, or organic dyes such as Eosin Y (Figure 3).

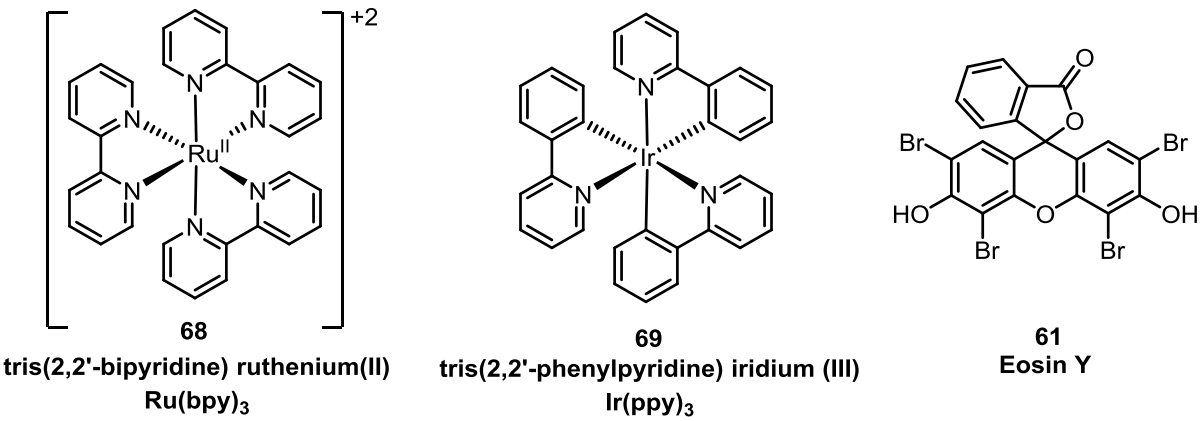

Figure 3: Common photoredox catalysts

Figure 4 illustrates excitation of a prototypical photocatalyst, $Ru(bpy)_3$. Upon absorption of a photon of visible light, an electron undergoes metal to ligand charge transfer (MLCT) from one of the metal-

centred t_{2g} orbitals to ligand-centred π* orbital. This transition results in an Ruthenium species with a long lived excited state (approximately 1100 ns).[24]

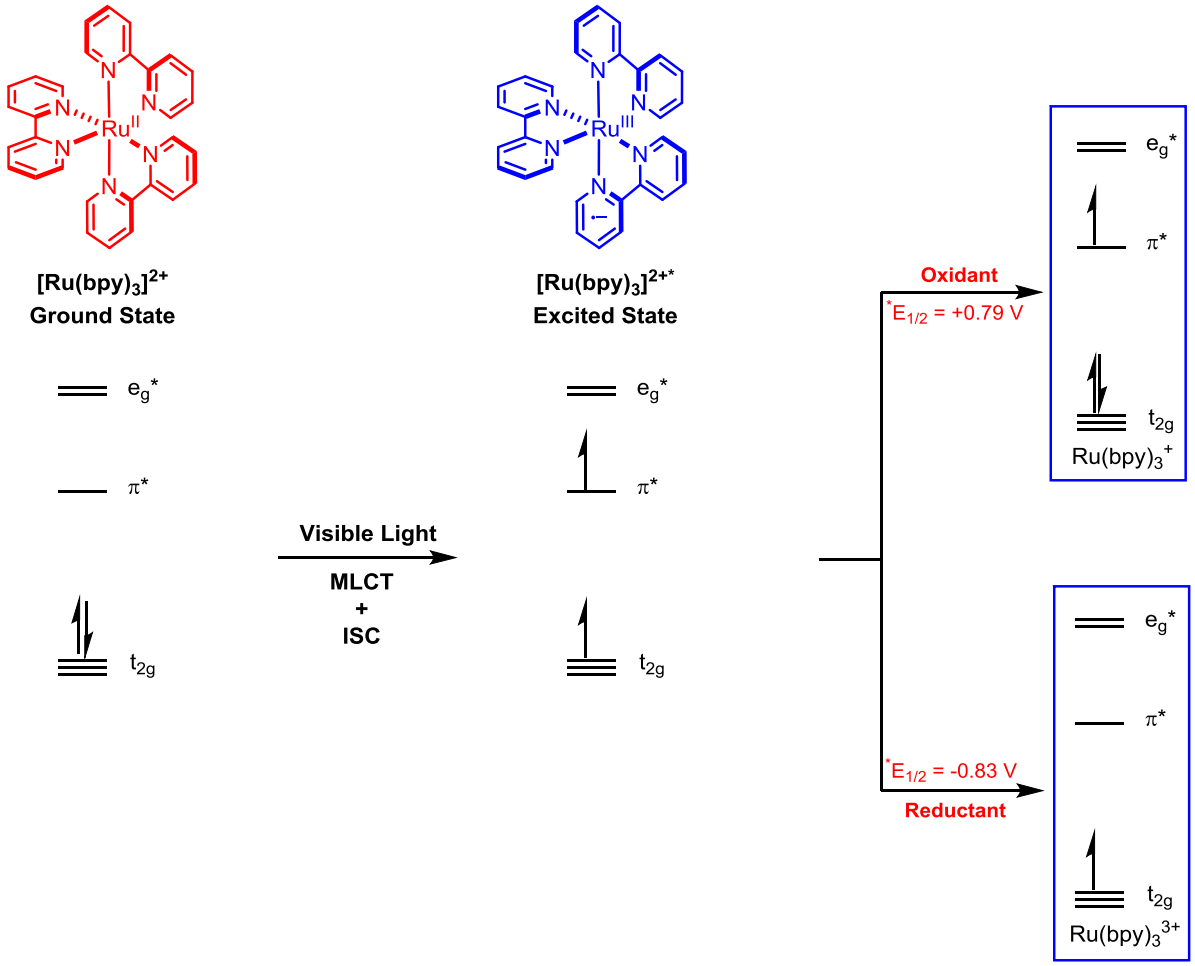

Figure 4: Visible light excitation of $Ru(bpy)_3$[24]

Once in the long lived excited state, the photoredox catalyst can go through either an oxidative or reductive quenching cycle (depending on reaction conditions). This process occurs through the donation of an electron from π* by the excited species to an organic molecule, acting as a reducing agent. The oxidised catalyst will then go through another single electron transfer to be reduced to the ground state (Figure 4 bottom pathway). Alternatively, the excited catalyst species can accept an electron from an organic molecule acting as an oxidising agent. The catalyst will then undergo another SET to be

oxidised back to the ground state (Figure 4, top pathway). Figure 5 shows the full catalytic cycle of $Ru(bpy)_3^{2+}$.

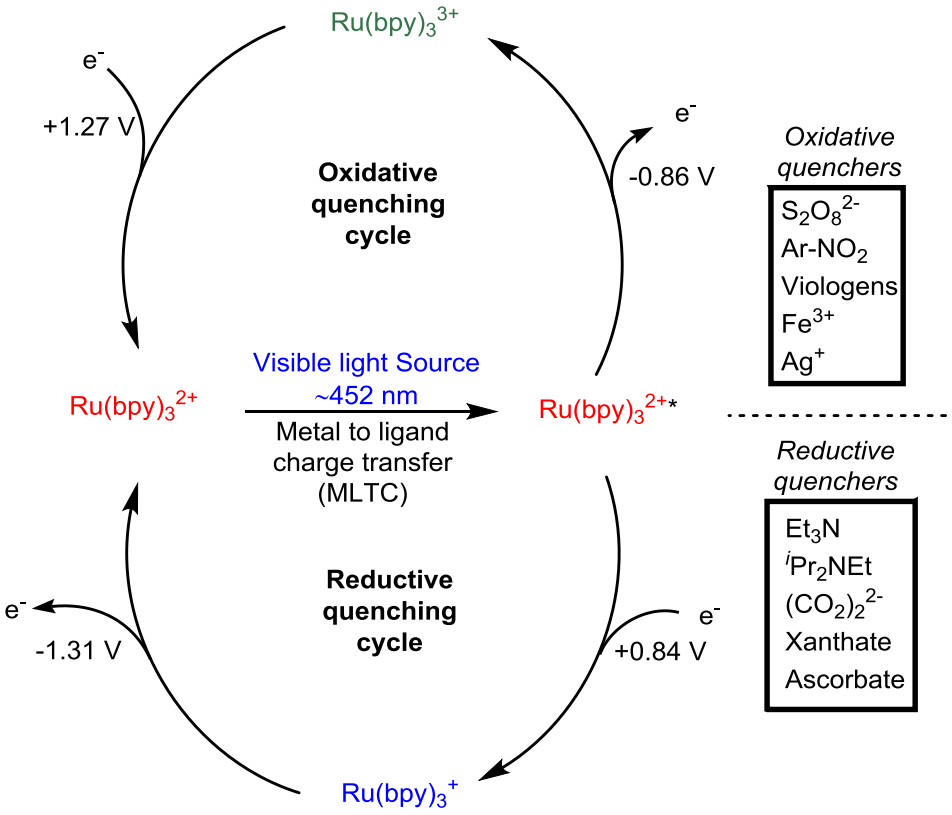

Figure 5: Oxidative and Reductive quenching cycle of $Ru(bpy)_3^{2+}$. [25]

The formation of aryl radicals has been reported by the reduction of aryl halides via visible light photoredox catalysis[26]. Stephenson *et al.* described the use of Iridium or Ruthenium photocatalysts focusing on their reduction potential. *fac*-$Ir(ppy)_3$ with a reduction potential of -1.73 V (versus SCE) was proposed to be the catalyst with appropriate redox potential to reduce aryl halides (Scheme 25), as it has the largest reducing potential out of the four catalysts reported ($[Ir[dF(CF_3)ppy]_2(dtbbpy)]PF_6$, $Ru(bpy)_3Cl_2$ and $Ir(ppy)_2(dtbbpy)PF_6$).

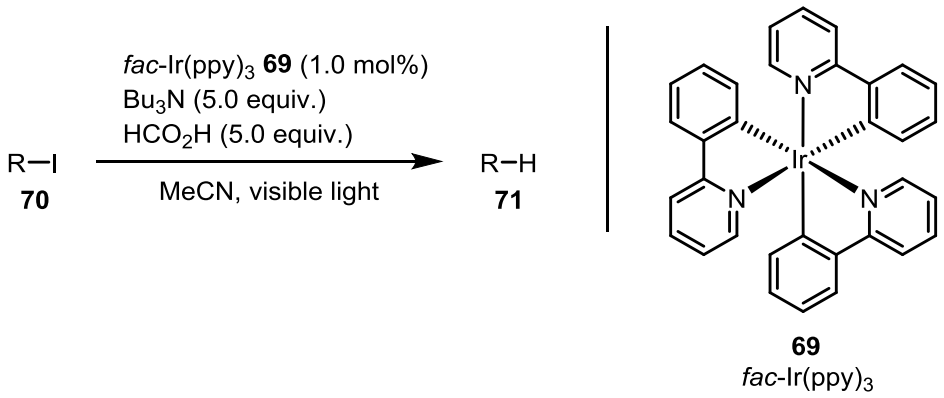

Scheme 25: Visible light reduction of aryl halides

The proposed mechanism for this reaction (Scheme 26) involved excitation of $Ir(ppy)_3$ via irradiation with blue light. Oxidative quenching of the excited-state catalyst by the alkyl, alkenyl or aryl-iodide results in reductive cleavage generating a carbon-centred radical. The carbon-centred radical can undergo cyclisation and/or hydrogen atom abstraction resulting in the product. Regeneration of the catalyst from $Ir(ppy)_3^+$ occurs from the oxidation of tributylamine, Hantzsch ester or formate.

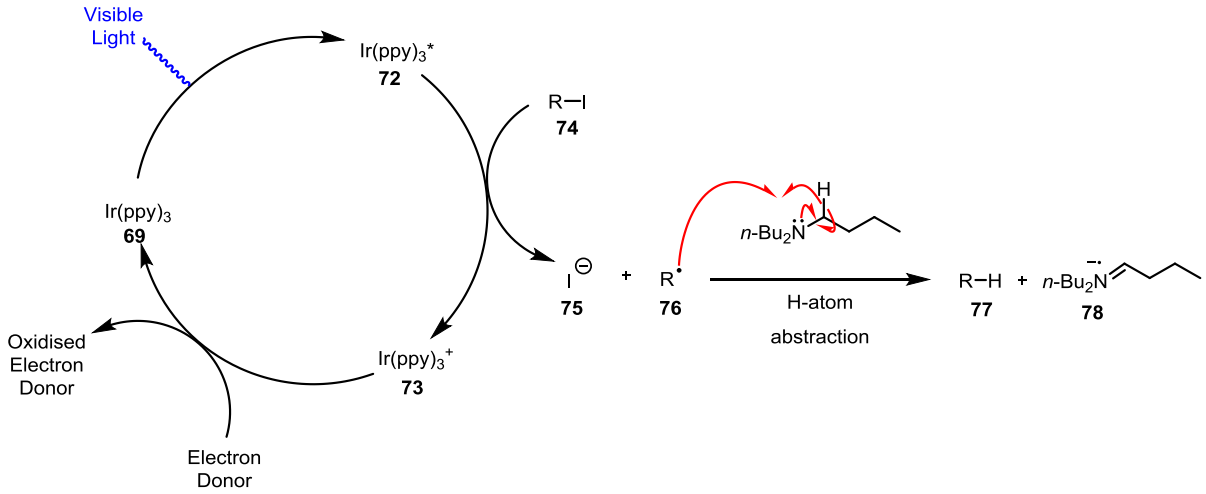

Scheme 26: Proposed mechanism for reduction of aryl halides

1.6 Research Design

The methodology established by Stephenson *et al.* provides an efficient route for the generation of carbon-centred radicals from alkyl and aryl iodides under mild conditions. We hypothesised that the generation of aryl radicals from aryl iodides under photoredox conditions would ameliorate the limitations of von Wangelin and Majek's approach for the formation of aryl sulfides (Scheme 27). Specifically, this proposed method would have the potential to proceed at ambient temperatures without the need of strong bases and excess DMSO. Also, as the substrates would be aryl halides, and not diazonium salts, a broader scope could potentially be accessed by this method. Furthermore, the replacement of diazonium salts with aryl halides would increase the safety of this reaction and eliminates the risk of forming hazardous diazonium sulfide intermediates.

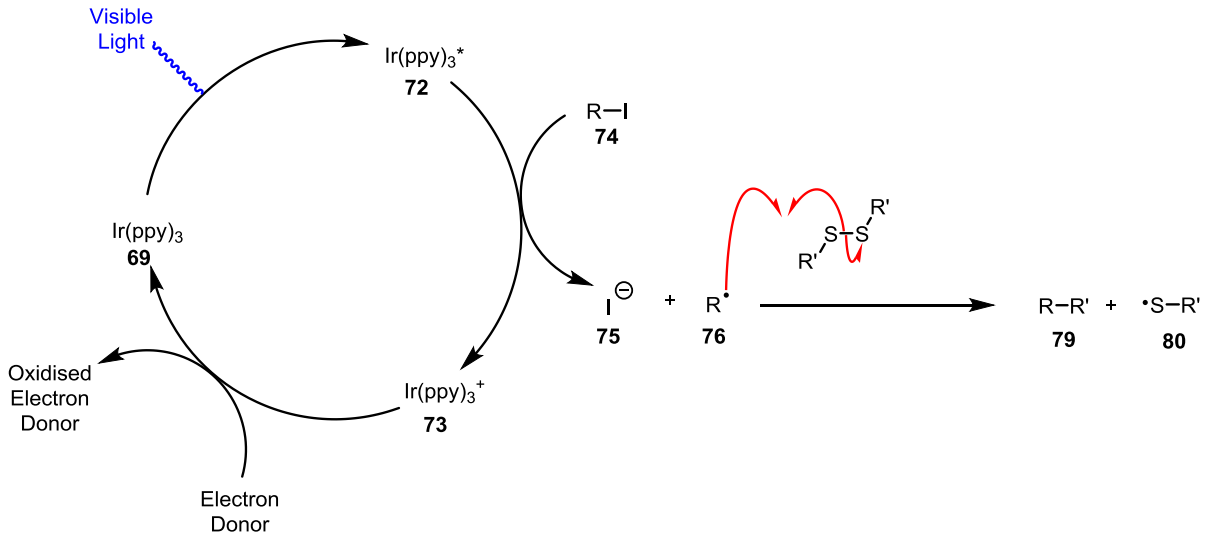

Scheme 27: Proposed synthesis of aryl sulfides via visible light photoredox catalysis

1.7 Research Goals

The general aim of this project is to address the limitation of transition metal catalysed and current photochemical approaches for the synthesis of aryl sulfides through the application of visible light photoredox catalysis. The specific aims of the project are to:

- To develop a novel method for the synthesis of aryl sulfides from readily available aryl halides via visible light photoredox catalysis.
- To develop a reaction that proceeds under mild conditions; ambient temperature, in the presence of weak bases and short reaction times, and with broad substrate scope.

Chapter 2:

Results and Discussion

2.1 Optimisation

4-Methyl iodobenzoate was selected as the substrate to examine this chemistry as it has been shown to be readily reduced in 6 hours.[26] Using reaction conditions reported by Stephenson with the addition of 10 equivalents of DMDS (**82**), the reaction was stirred at room temperature for 16 hours under 5 W blue LED irradiation (Scheme 27). ^{1}H NMR spectroscopic analysis of the crude reaction mixture revealed that it contained 2 major products, identified as the desired aryl sulfide **83** and the reduced aryl iodide **84**. The ^{1}H NMR ratio of **83**:**84** was 1:1. Given that these reaction conditions were specifically designed for the reduction of aryl iodides, the observed 50% conversion to aryl sulfide was highly encouraging.

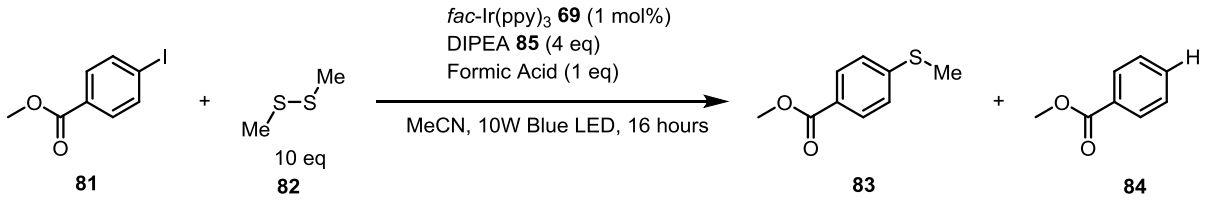

Scheme 28: Stephenson's reaction with DMDS

The excessive reduction of 4-methyl iodobenzoate (**81**), although not unexpected, demonstrated that the reaction conditions would need to be re-optimised to minimise formation of **84**. As discussed in section 1.5, the aryl radical is reduced by abstracting a hydrogen atom from the tertiary amine (the SET donor), its radical cation derivative, or the corresponding formate salt (Scheme 29). As a consequence, screening of SET donors was conducted in order to determine whether a suitable reagent that suppressed the rate of hydrogen atom transfer could be used to increase the yield of the desired product **83**.

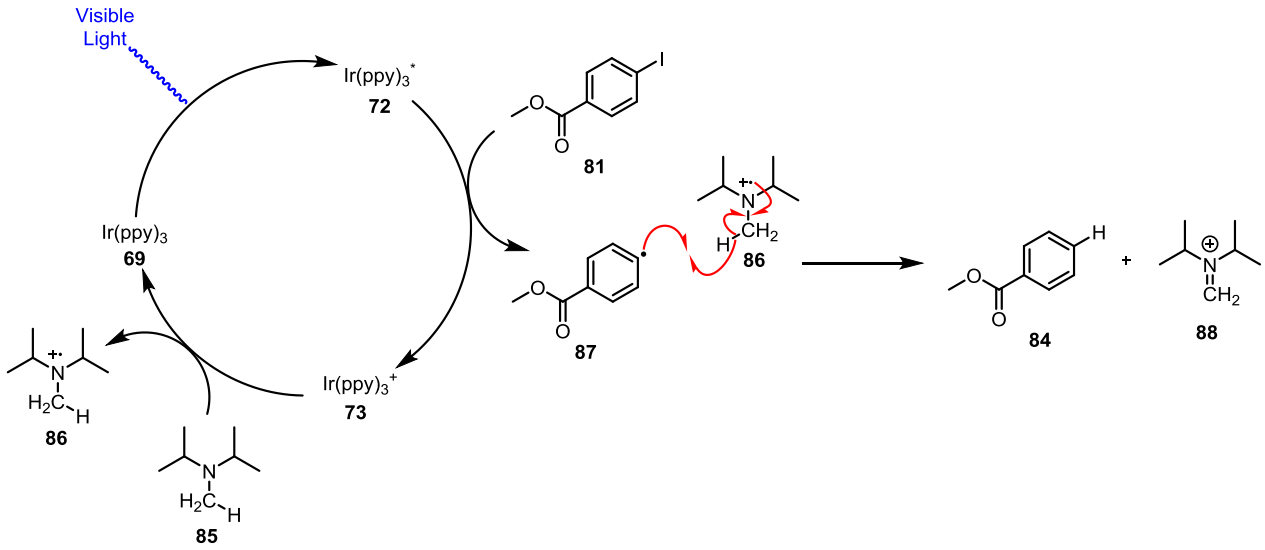

Scheme 29: Proposed mechanism for reduction of 4-methyl iodobenzoate **81**

Commonly used sacrificial reductants in photoredox catalysis include diisopropylethylamine (DIPEA), trimethylamine (Et_3N), triisopropylamine ($^iPr_3N$) and tributylamine (Bu_3N). Therefore, the reaction was conducted with 4 equivalents of each of these amines in acetonitrile (Table 1, entries 1-4). Although the 4-methyl iodobenzoate (**81**) was fully consumed in each case, the isolated were 50% for DIPEA, and 33% for Et_3N and 41% for $^iPr_3N$, respectively. Unfortunately, although dehalogenated product **84** was observed in ^1H NMR analysis of the crude material, isolation proved challenging despite best efforts. Interestingly, unprotonated DIPEA instead of the formate salt (Table 1, entry 1 cf. Scheme 27) did not reduce the rate of reduction. Furthermore, consistent with Stephenson's studies, Bu_3N, an efficient hydrogen atom donor for the reductive dehalogenation of aryl and alkyl halides, gave a poor yield of 19%. Further examination of the literature revealed that unwanted competitive reduction of aryl and alkyl halides has been reported previously.[25] Stephenson *et al.* observed that the use of trialkyl amines as the electron donor resulted in preferential reductive dehalogenation of the aryl/alkyl halide. To counter the preferential reductive dehalogenation, triaryl amines were investigated, in which the absence of a transferable hydrogen donors atoms should eliminate the reductive dehalogenation pathway.

However, when 2,6-lutidine, Ph_3N and derivatives of Ph_3N were examined as electron donors, all gave no reaction (Table 1, entries 5-8). The lack of reactivity could be associated with a kinetically competitive charge recombination event.[25] With the observed results of the SET donor screen, DIPEA was clearly the most efficient SET donor for the production of the desired aryl sulfide **83**. Therefore, optimisation was continued with DIPEA as the chosen SET donor.

Table 1: SET donor screen

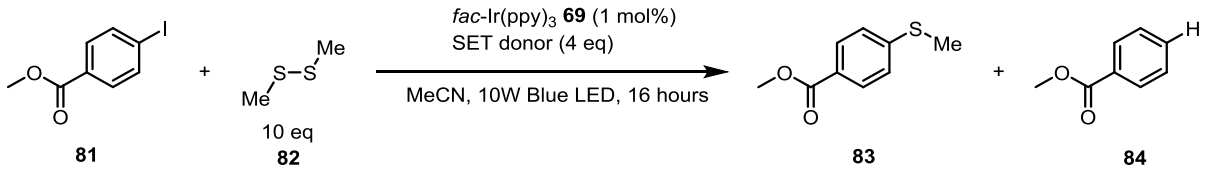

Entry	SET donor	Isolated yield (%)	Recovered SM (%)
1	DIPEA	50	0
2	Bu_3N	19	0
3	Et_3N	33	0
4	$^{i}Pr_3N$	41	0
5	2,6-Lutidine	N.R.	-
6	Ph_3N	N.R.	-
7	4-Methoxytriphenylamine	N.R.	-
8	3,5-Dimethoxytriphenylamine	N.R.	-

An alternative approach towards decreasing the rate of reductive dehalogenation requires the reduction of the mole equivalents of the SET donor, DIPEA. Table 5 illustrates the effect of reducing the mole equivalents of DIPEA from 4 to 1. It was observed that, as the equivalents of DIPEA were decreased, the yield of the disulfide reduced slightly from 50% to 45%. Furthermore, a reduction of the equivalents of DIPEA resulted in incomplete conversion of the aryl iodide (**81**), suggesting that the rate of conversion of 4-methyl iodobenzoate (**81**) was slowed. As conversion and the best yield were obtained when 4 equivalents of DIPEA were used, these conditions were used in further optimisation.

Table 2: Influence of DIPEA stoichiometry on aryl sulfide formation

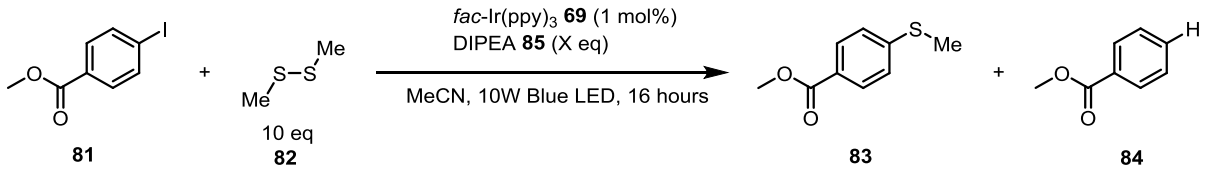

Entry	DIPEA (equiv.)[a]	Isolated yield (%)	Recovered SM (%)
1	1	45	25
2	2	40	8
3	3	50	0
4	4	50	0

a. Relative to 4-methyl iodobenzoate (**81**)

In the attempt to solve the problem of the unwanted reduction of the 4-methyl iodobenzoate (**81**), a slow addition of the SET donor, DIPEA, was investigated. Initially 1 equivalent of DIPEA was added to the reaction, with a further 3 equivalents slowly added over 12 hours via syringe pump. After 16 hours ^{1}H NMR spectroscopic analysis revealed that 20% of the product had formed with 48% of 4-methyl iodobenzoate (**81**) remaining. The slow addition of the DIPEA had slowed the overall reaction. This may suggest that insufficient quantities of DIPEA was available to turnover the photoredox catalytic cycle. In a further attempt, the experiment was repeated with 1.8 equivalents of DIPEA initially in the reaction solution with an additional 1 equivalent of DIPEA added over 12 hours by syringe pump. ^{1}H NMR spectroscopy analysis revealed 9% of product **83** was produced under these conditions. This observation led to the conclusion that slow addition of DIPEA was not a viable approach to ameliorate competitive reductive dehalogenation.

Table 3: The effect of the slow addition of DIPEA

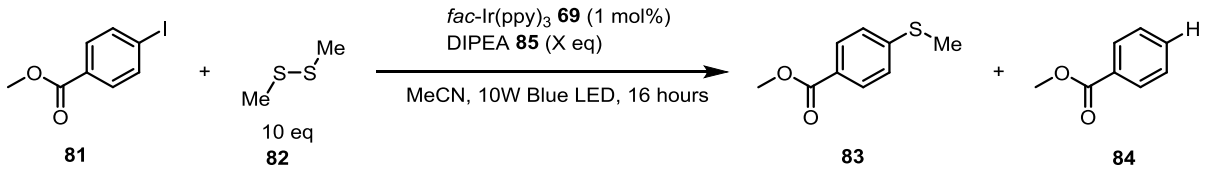

[1]H NMR yields calculated against internal standard (3-sulfolene)

Entry	Equivalents of DIPEA (initial)	Equivalents of DIPEA added	Yield of 83 (%)	% Conversion of 81
1	1	3	20	52
2	1.8	1	9	52

Given the limited success in preventing the competitive reduction of the aryl halide (**81**), it was proposed that increasing the equivalents of the disulfide, DMDS, may be more successful. This should increase the probability of interaction between the aryl radical formed and DMDS. Table 4 shows the influence of increasing the mole equivalent of DMDS from 10-20 mole equivalents (Table 4, entries 4 & 5). It was observed that with an increase in the equivalents of DMDS, the yield of the desired product did not increase by a significant amount. This may be attributed to the decreased solubility of 4-methyl iodobenzoate (**81**) with increasing concentration of DMDS. To test if solubility was a reason behind the poor conversion of 4-methyl iodobenzoate (**81**) to the desired aryl sulfide (**83**), the equivalents of DMDS were reduced. However, at 5 equivalents or less, an increase in reductive dehalogenated product was observed (Table 4, entries 1-3).

DMDS was also trialled neat. It was postulated that neat DMDS would limit reduction owing to a large excess of electrophilic disulfide. [1]H NMR spectroscopic analysis of the crude reaction mixture revealed that 20% of the desired product was formed and 64% of the 4-methyl iodobenzoate (**81**) was still present. This may be attributed to the insolubility of 4-methyl iodobenzoate (**81**) in DMDS. Due to poor solubility of reagents and corresponding poor conversion to products, the use of excess DMDS was not implemented and 10 equivalents of DMDS was deemed appropriate for further optimisation the reaction.

Table 4: Equivalents of DMDS

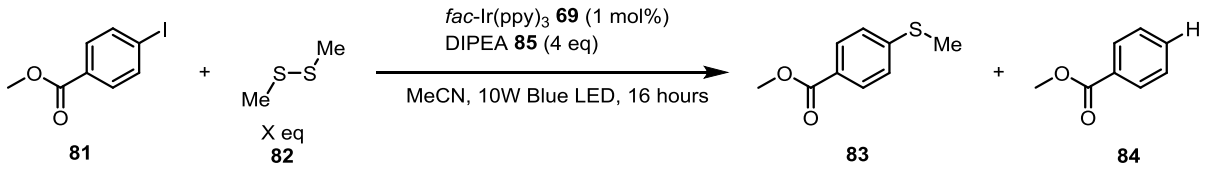

Entry	Equivalents of DMDS (Mole)	Isolated Yield of 83 (%)
1	1	19
2	2	12
3	5	41
4	10	50
5	20	55
6	Neat[a]	20

a) ^{1}H NMR Yields calculated against internal standard (3-sulfolene)

The influence of the reaction solvent is not thoroughly understood in visible light photoredox chemistry. However in general, it is believed that polar solvents can assist stabilise charged intermediates and can furthermore separate charged intermediates, thus preventing redundant electron transfer processes.

Accordingly, a solvent screen was undertaken to examine solvents effects and the influence of various solvents on the yield of **83** is shown in Table 5. As expected the nature of the solvents did significantly influence the reaction efficiency and selectivity with respect to competitive reduction. Consistent with previous reports, polar solvents (MeCN, DMF, DMSO and MeOH) gave good results for the synthesis of **83** (50%, 30%, 55% & 39% respectively) (Table 5, entries 1-3 & 8). The use of MeOH resulted in 39% product formation by isolated yield. However, as the polarity of the alcohol decreased, formation of product **83** also decreased. This was evidenced by the use of EtOH resulting 6% of the desired product **83** and ^{i}PrOH and ^{t}BuOH having no observed reaction (Table 5, entries 9-10 & 12). $CHCl_3$ and NMP also gave no reaction. Full conversion of the 4-methyl iodobenzoate (**81**) was only observed in the presence of three solvents: MeCN, DMF and DMSO, with DMSO and MeCN giving equivalent formation of the desired product **83**. Accordingly, MeCN was chosen as the optimal solvent for this reaction given the ease of isolating the product from MeCN compared to DMSO (Table 5, entries 1 & 3).

As all the solvents screened were thoroughly dried, wet solvents were screened to observe the effect of water in the reaction (Table 6). Wet MeCN was observed to give equivalent results to dry MeCN, illustrating a lack of sensitivity to water by this reaction. However, like dry MeCN, wet MeCN also resulted in a high amount of reduction of the 4-methyl iodobenzoate (**81**). So while a small amount of water was not detrimental to the reaction, it did not improve formation of the product.

Finally, the effect of oxygen was investigated by degassing dry MeCN using the freeze-pump-thaw method.[27] After 16 hours it was observed that only 32% of the desired product was formed, however all of the 4-methyl iodobenzoate (**81**) was consumed. It was proposed that oxygen does influence formation of the product, however the role and mechanism of oxygen participation was not investigated within the scope of this study.

Table 5: The Optimisation of Solvent

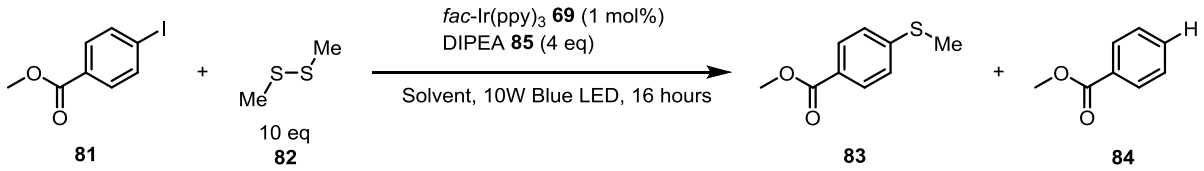

Entry	Solvent	Isolated yield 83 (%)	Recovered SM (%)
1	MeCN	50	0
2	DMF	30	0
3	DMSO	55	0
4	THF	3	52
5	DCM	23	40
6	DCE[a]	8	53
7	$CHCl_3$	N.R.	-
8	MeOH	39	15
9	EtOH[a]	6	67
10	$^{i}Pr_3N$	N.R.	-
11	NMP	N.R.	-
12	^{t}BuOH	N.R.	-
13	toluene	Trace	-

a) ^{1}H NMR Yields calculated against internal standard (3-sulfolene)

Table 6: Reaction Controls

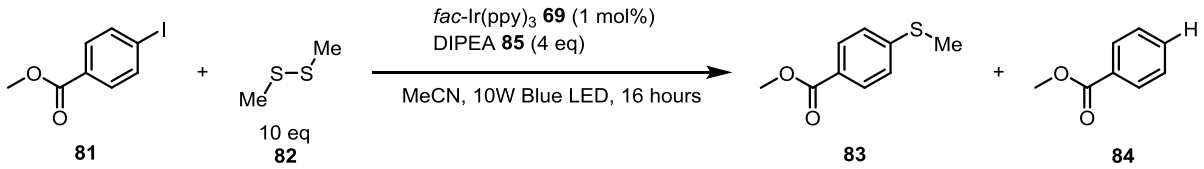

Entry	Solvent	Isolated yield 83 (%)	Recovered 81 (%)
1	MeCN - Wet	49	0
2	MeCN - Freeze-pump-thaw	32	-

Following studies to optimise the reaction in terms of screening SET donors, equivalents of DMDS and solvents, variation of these reaction parameters did not successfully reduce the competitive reduction of the aryl radical, and this unwanted reaction pathway appeared to be the major limitation of this method. It became evident that the rate of hydrogen atom abstraction was much higher than the rate of reaction of aryl radical with DMDS, however typical approaches to control the relative rates of these two processes were unsuccessful. Reducing the concentration of DIPEA affected catalyst turnover and therefore led to incomplete conversion of the 4-methyl iodobenzoate (**81**). On the other hand, increasing concentration of DMDS beyond 10 equivalents affected solubility of the aryl iodide substrate and possibly the catalyst, and did not lead to any significant improvements. It was therefore considered whether reducing the rate of formation of the aryl radical could change the effective ratio of the aryl radical to DMDS and therefore improve the yield of the target product **83**. Consequently, an investigation was undertaken to determine the influence of different photoredox catalysts.

The reduction potential of iodobenzene has been measured at -2.24 V versus SCE[28]. The reduction potential for 4-methyl iodobenzoate has not been reported. However, the presence of an electron withdrawing group should lower the reduction potential relative to iodobenzene, with related compounds having a redox potential of -1.77 and -1.87 V vs SCE[29] (4-iodoacetophenone and 4-ethyl iodobenzoate respectively). $Ir(ppy)_3$, with the highest reduction potential (1.73 V vs SCE), has been

reported to fully reduce 4-methyl iodobenzoate in 6 hours and has been demonstrated in this study to give 50% yield of desired product. Other commonly used catalysts that should be able to reduce the substrate include $Ir(dtbbpy)(ppy)_2$ (-0.96 V) and $Ir(dFppy)_3$ (-1.43 V). $Ru(bpy)_3$ (-0.81 V) was also included in this study, although there was little evidence that it should be effective.

$Ir(dFppy)_3$ and $Ir(dtbbpy)(ppy)_2$ both led to full conversion of the 4-methyl iodobenzoate (**81**) in 16 hours, with 51% and 37% product formation respectively. Interestingly, $Ru(bpy)_3Cl_2$, with the reduction potential of -0.81 V vs SCE, gave 9% yield of the **83**.

As a control, the reaction was conducted without catalyst resulting in the formation of 10% of **83** and 82% of recovered 4-methyl iodobenzoate (**81**). This illustrates that the 10W LED lights that have been used are able to homolytically cleave the $C(sp^2)$-I bond without the need of a catalyst giving a modest background reaction. The control provides evidence that $Ru(bpy)_3Cl_2$ does not catalyse the reduction of the $C(sp^2)$-I bond.

$Ir(ppy)_3$ and $Ir(dFppy)_3$ both gave equivalent results in the screen conducted, however due to better availability, $Ir(ppy)_3$ was chosen as the catalyst to continue with the optimisation of this reaction.

Table 7: Catalyst Screen

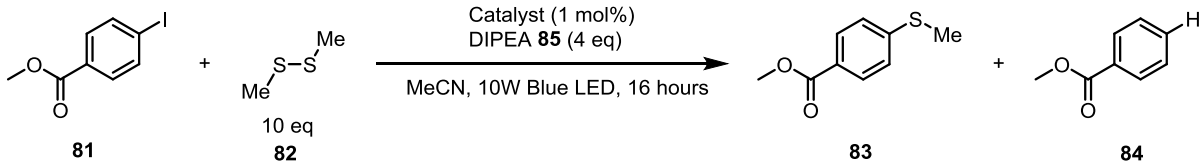

81 **82** **83** **84**

Entry	Catalyst	$E_{1/2}^{+}$ (Cat /Cat*) (V vs SCE)	Isolated yield 83 (%)	Recovered 81 (%)
1	$Ir(ppy)_3$	-1.73	50	0
2	$Ru(bpy)_3$	-0.81	9	59
3	$Ir(dFppy)_3$	-1.43[30]	51	0
4	$Ir(dtbbpy)(ppy)_2$	-0.96	37	0
5	No Catalyst[a]		10	82

a) ^{1}H NMR Yields calculated against internal standard (3-sulfolene)

$Ir(ppy)_3$ afforded the best yield of product (**83**) at 50%. However, under these conditions, 50% of the 4-methyl iodobenzoate (**81**) was reduced. The equivalents of $Ir(ppy)_3$ was also screened. As the loading of $Ir(ppy)_3$ was increased from 1 mol% to 3 mol% there was no significant change in the observed amount of aryl sulfide **83** formation (Table 8). This illustrates that the rate of radical formation is optimum at 1 mol% catalyst loading and this used for further optimisation.

Table 8: Equivalents of Photoredox Catalyst *fac*-$Ir(ppy)_3$

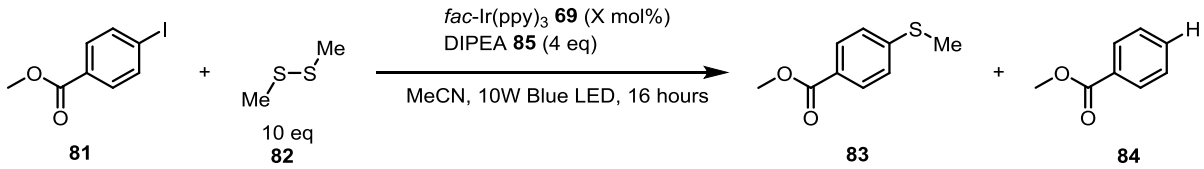

X mol% of $Ir(ppy)_3$	Yield 83 (%)	Recovered SM 81 (%)
1	50	0
2	47	0
3	46	0

In another approach to increase the rate of addition of the aryl radical to disulfide the Lewis acid activation of DMDS was investigated. Glorius *et al.* recently reported the use of $CuCl_2$ to activate disulfides to improve the thiolation of heteroarenes.[31] Glorius proposed that $CuCl_2$ coordinated to the disulfide bond to form a polarised complex (**90**) (Scheme 30). This polarised complex then underwent oxidative addition via nucleophilic attack by Pd[0] forming a very electrophilic complex (**92**). This complex would then react with the heteroarene via S_{EAr}. Reductive elimination would afford the desired sulfenylated product (**89**) and regenerate the catalyst.

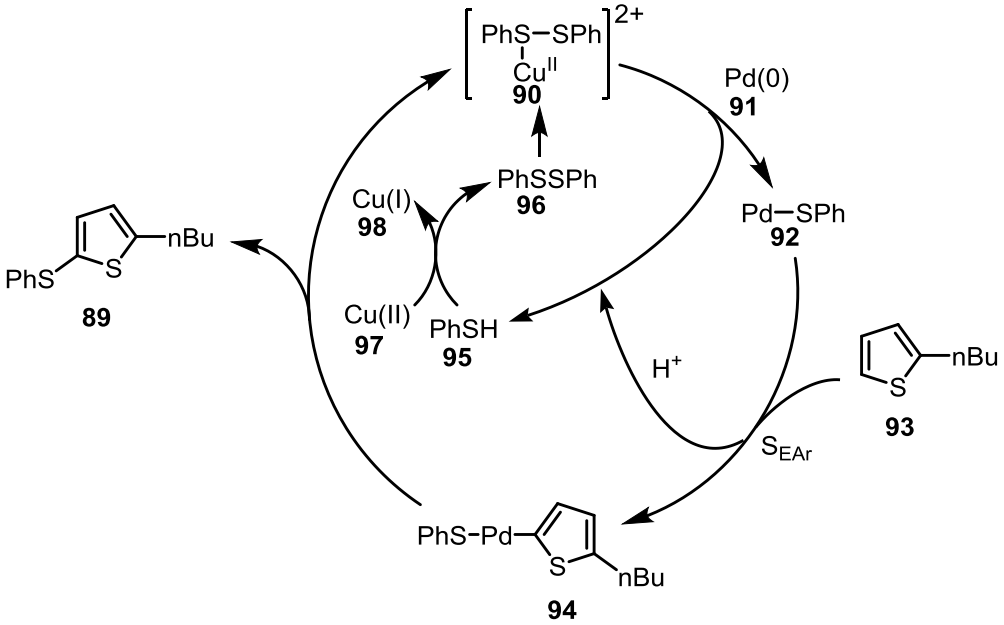

Scheme 30: The thiolation of heteroarenes by Glorius *et al*[31].

Inspired by Glorius' observation, various Lewis acids were trialled as additives to the reaction to activate the disulfide bond and thus increase product yield. 1, 5 and 10 equivalents of $CuCl_2$ were trialled, however no reaction was observed in all cases (Table 9, entries 1-3). This is believed to be caused by $CuCl_2$ rendering the reaction mixture black and opaque, thereby limiting light penetration into the reaction mixture, and preventing catalyst activation. CuCl also had a similar result. Furthermore, copper is very redox active, and it may have interfered with the photoredox cycle. Unsurprisingly, AgOAc formed a mirror around the reaction container when subjected to visible light. This resulted in only a trace amount of product being formed. $AlCl_3$ was observed to produce aryl sulfide **83** in 30% yield with 26% of the 4-methyl iodobenzoate (**81**) remaining (Table 9, entry 5). Although $AlCl_3$ did not fully inhibit the reaction from occurring, it was observed that it resulted in a higher amount of reduction of the 4-methyl iodobenzoate (**81**).

Table 9: Addition of Lewis Acids

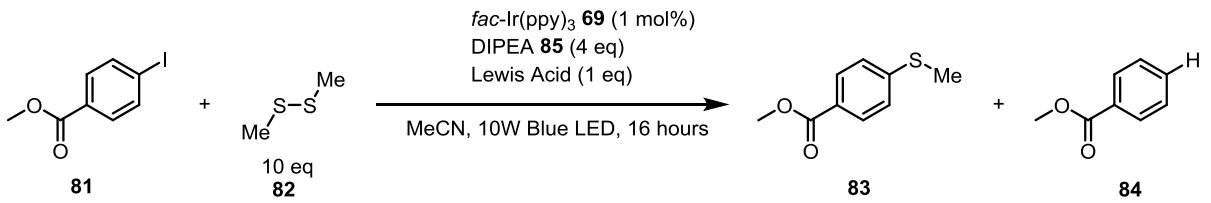

Entry	Lewis Acid	Yield 83 (%)	Recovered 81 (%)
1	$CuCl_2$ - 1 eq	N.R.	-
2	$CuCl_2$ - 5 eq	N.R.	-
3	$CuCl_2$ - 10 eq	N.R.	-
4	CuCl	N.R.	-
5	$AlCl_3$[a]	30	26
6	AgOAc	trace	

a) ^{1}H NMR Yields calculated against internal standard (3-sulfolene)

After further consideration, it was proposed that dimethyl disulfide may not stabilise the sulfur based radical following the addition of the aryl radical into the disulfide bond. Primary radicals have been shown to be less stable than secondary[32] and aryl radicals, therefore various disulfides were screened. Diethyl disulfide produced the desired product in 53% with full conversion of the 4-methyl iodobenzoate (**81**) (Table 10, entry 2). However, as the R substituent on the disulfide became larger, the yield of the corresponding arylsulfide decreased; dibutyl disulfide and the phenyl derivatives gave poor results. A trace of the desired product was observed by ^{1}H NMR analysis when dibenzyl disulfide was the coupling partner and bis(4-chlorophenyl) formed a thick black tar in the reaction container rendering isolation impossible. Phenyl disulfides derivatives have been reported to stablise the free radical more readily than any of the alkyl disulfides. This would result in a longer lived radical species and presumably side reactions like polymerisation due to these aryl radical thiols.

Table 10: Disulfide Scope

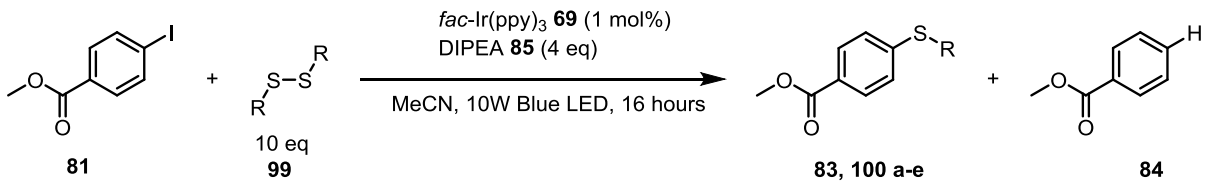

Entry	Disulfide (R=)	Isolated yield (113) (%)	Recovered 81 (%)
1	Dimethyl (**83**)	50	-
2	a) Diethyl	53	-
3	b) Dibutyl	0	-
4	c) Diphenyl	N.R.	-
5	d) Dibenzyl[a]	trace	-
6	e) Bis(4-chlorophenyl)	N.R.	-

The structure of the disulfide was found to significantly influence the reaction and structural variation in the disulfide was not well tolerated. As a consequence, the scope of the reaction was investigated with respect to structural and electronic variation of the aryl iodide. Aryl iodide substrates with *ortho* substitution were not well tolerated (Table 11) and all were observed to give poor yields for the respective products. The isolation of the 2-iodotoluene adduct was very difficult. Substrates with *para* substitution also gave modest yields and 4-Iodo-1-nitrobenzene and 4-iodophenol failed to react. However, 4-Iodoanisole was converted into the corresponding arylsufide in 20% yield. However, 4-chloro-iodobenzene was converted into the arylsufide in 41% yield.

A Hammett study was undertaken to determine the basis for observed reactivity pattern. Analysis of the Hammett sigma values showed a "Goldilocks' zone" for substrates that would successfully couple with DMDS under photo catalytic conditions. Figure 6 shows the percentage yield of aryl iodides against the corresponding Hammett value. From the graph an approximate bell-shaped-curve is observed, which leads to the best Hammett value for a substrate around 0.31. 4-Bromo-iodobenzene, 4-iodoacetophenone and 4-iodobenzaldehyde all had Hammett values close to 0.31 and these substrates afforded 36%, 47% and 58% of the desired product respectively. 1-Iodonapthalene afforded the desired product in 41% yield and 2-iodopyridine afforded the product in poor yield (18%)

Table 11: Substrate Scope

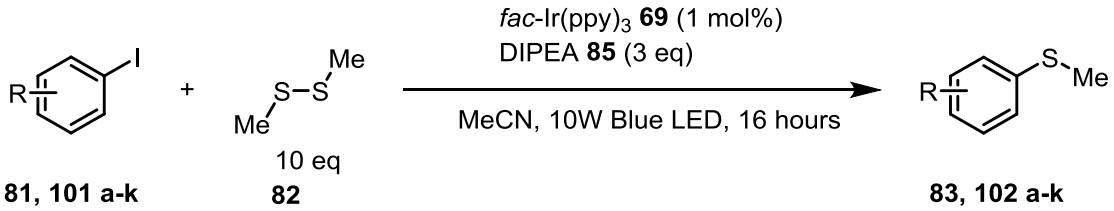

Entry	Substrate (R=)	Hammett Values[33]	Aryl Sulfide (%)[a]
1	4-Methyl ester (**81**)	0.31	50
2	a) 2-OMe	-0.27	4
3	b) 2-NO_2	0.81	17
4	c) 2-CF_3	0.53	9
5	d) 2-Me[b]	-0.14	10
6	e) 4-OMe[b]	-0.27	20
7	f) 4-Cl	0.24	41
8	g) 4-Br	0.26	36
9	h) 4-COMe	0.47	47
10	i) 4-COH	0.42	58
11	j) 1-iodonapthalene	-	41
12	k) 2-iodopyridine[b]	-	18

a) Isolated yields, b) ^{1}H NMR Yields calculated against internal standard (3-sulfolene)

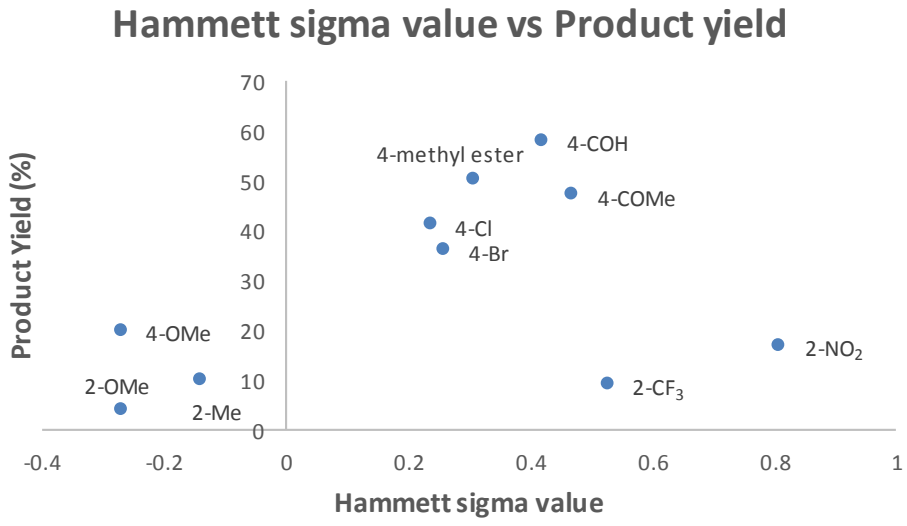

Figure 6: Hammett sigma value versus Product Yield

2.2 Mechanistic Studies

Investigating the scope of the reaction with both various disulfides and various aryl iodides illustrated that the reaction was sensitive to the electronics of the substrate and the disulfide. To fully understand the conversion of the 4-methyl iodobenzoate (**81**) to aryl sulfide **83**, the reaction was analysed by ^{1}H-NMR spectroscopy at time intervals. It was observed that initially the consumption of the 4-methyl iodobenzoate (**81**) was extremely fast but the rate plateaus after 2 hours of irradiation (Figure 7). It was also observed that the formation of the product and the reduction of 4-methyl iodobenzoate (**81**) occur contemporaneously. The plateau of product formation after 2 hours explains the results seen in the slow addition of DIPEA (Table 3). In Table 3 it was seen that if DIPEA was slowly added over 12 hours, the formation of product and the consumption of 4-methyl iodobenzoate (**81**) was retarded significantly and Figure 7 shows that the first 2 hours of the reaction is when the majority of product **83** is formed. This lack in reactivity after 2 hours may be due to catalyst deactivation, which has been observed in the presence of organosulfur compounds.[34]

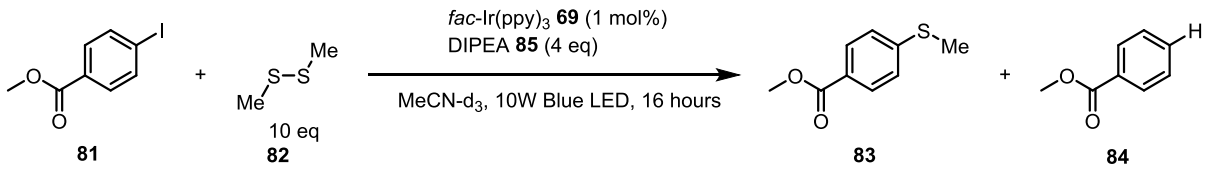

Scheme 31: Time delayed NMR analysis

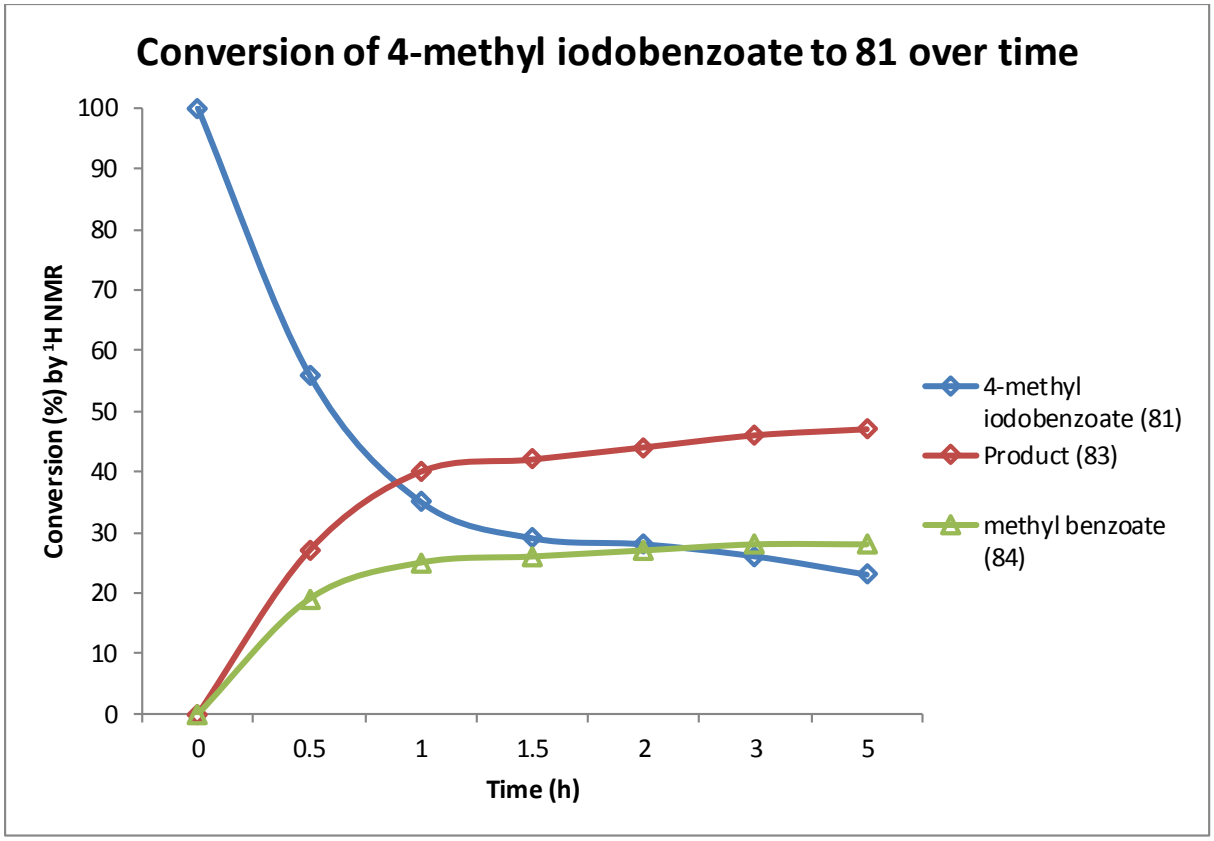

Figure 7: ^{1}H NMR spectroscopic analysis of the formation of product over time.

The influence of the light source on the reaction was also investigated. Two light sources were studied; a 10W LED blue light and a white 1W fluorescent light bulb. When the reaction was irradiated with a white 1W light source, the 4-methyl iodobenzoate (**81**) was consumed very slowly (13 days) and ^{1}H NMR analysis indicated presence of 86% of the desired product (Table 12, entry 1). More importantly, only 12% of the 4-methyl iodobenzoate (**81**) was unreacted and the reduction of the 4-methyl iodobenzoate (**81**) had been eliminated.

As a control experiment, the reaction was repeated in the absence of photocatalyst and irradiated by white light for 14 days. ^{1}H NMR analysis showed that the expected aryl sulfide (**83**) had not been produced (Table 12, entry 2). This suggests that white light does not initiate homolytic cleavage of the DMDS, eliminating the background reactions previously seen when the reaction was irradiated by 10W

blue light without photocatalyst (Table 7, entry 5, 10% yield of desired product, 82% of 4-methyl iodobenzoate (**81**)).

Table 12: Control reactions with white light

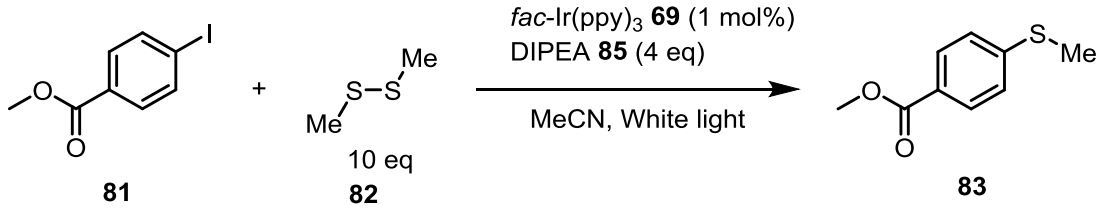

Entry	Control	Time (days)	Product Yield (%)[a]	4-methyl iodobenzoate (81) Yield (%)[a]
1	White Light	13	86	12
2	White Light	14	0	95

a) NMR yield calculated against internal standard

In view of the potential influence of the photo-induced homolytic cleavage of the disulfides in the reaction, further studies were undertaken to examine this reaction pathway by ^{1}H NMR analyses. The homolytic cleavage of diaryl disulfide bonds by blue light had been reported previously[35], in which diphenyl disulfide and di(*p*-tolyl) disulfide were irradiated by blue light and a cross over product was observed (Scheme 32). To determine if photo-induced homolytic cleavage was occurring with DMDS, a similar cross over experiment was conducted with dimethyl disulfide (**82**) and diphenyl disulfide (**96**) (Scheme 33). ^{1}H NMR spectroscopic analysis evidenced for the formation of methyl phenyl disulphide (**105**) within 30 minutes. GC/MS analysis of the reaction mixture also supported the formation of methyl phenyl disulfide. When this experiment was repeated without photocatalyst or DIPEA, ^{1}H NMR spectroscopic analysis showed a similar behaviour.

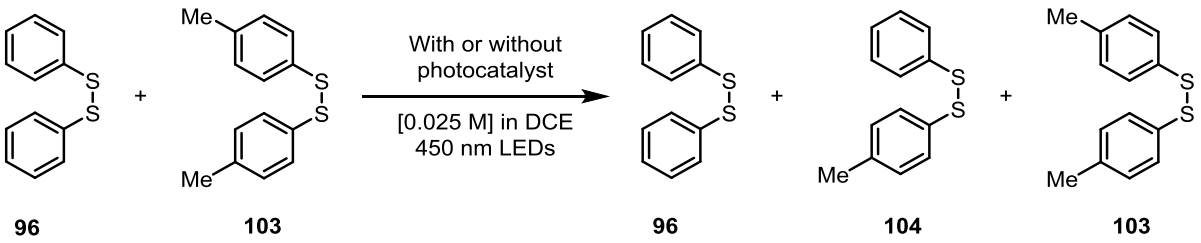

Scheme 32: Cross over experiment

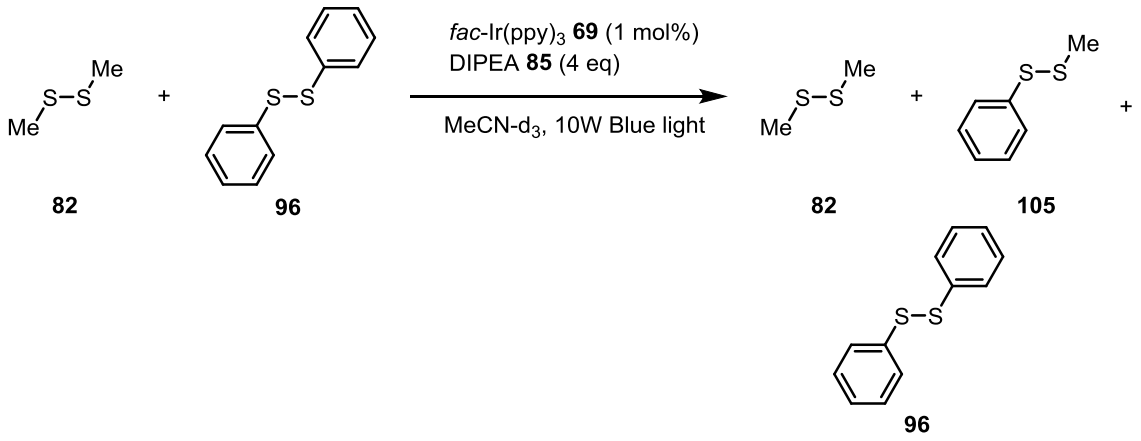

Scheme 33: Disulfide cross over experiment

The results from the cross over experiment illustrate that the 10W LED blue light source induces homolytic photo cleavage of the disulfide bond to afford the corresponding thiyl radicals which can subsequently recombine or undergo a cross coupling to form methyl phenyl sulfide (**105**). Although the photo-induced homolytic cleavage of disulfides was established, the influence of the formation of thiyl radicals as potential competitive reaction pathway remains unclear and further study is required to elucidate this pathway.

Figure 8 shows the proposed mechanism for the formation of the aryl sulfides via the developed reaction. The primary pathway for aryl sulfide formation proceeds via the photocatalytic cycle (Pathway 1). However, experimental evidence also supports contributions of pathways 2 and 3. Pathway 2

requires the homolytic cleavage of the C(sp^2)-I bond in methyl 4-iodobenzoate by irradiation. Once this bond is cleaved, the newly formed aryl radical can undergo electrophilic aromatic substitution with the disulfide affording the product. Pathway 3 requires the formation of the product from the combination of the aryl radical and thiol radical formed by homolytic cleavage induced by the blue light. The contributions of pathways 2 and 3 were not however, fully elucidated in this study.

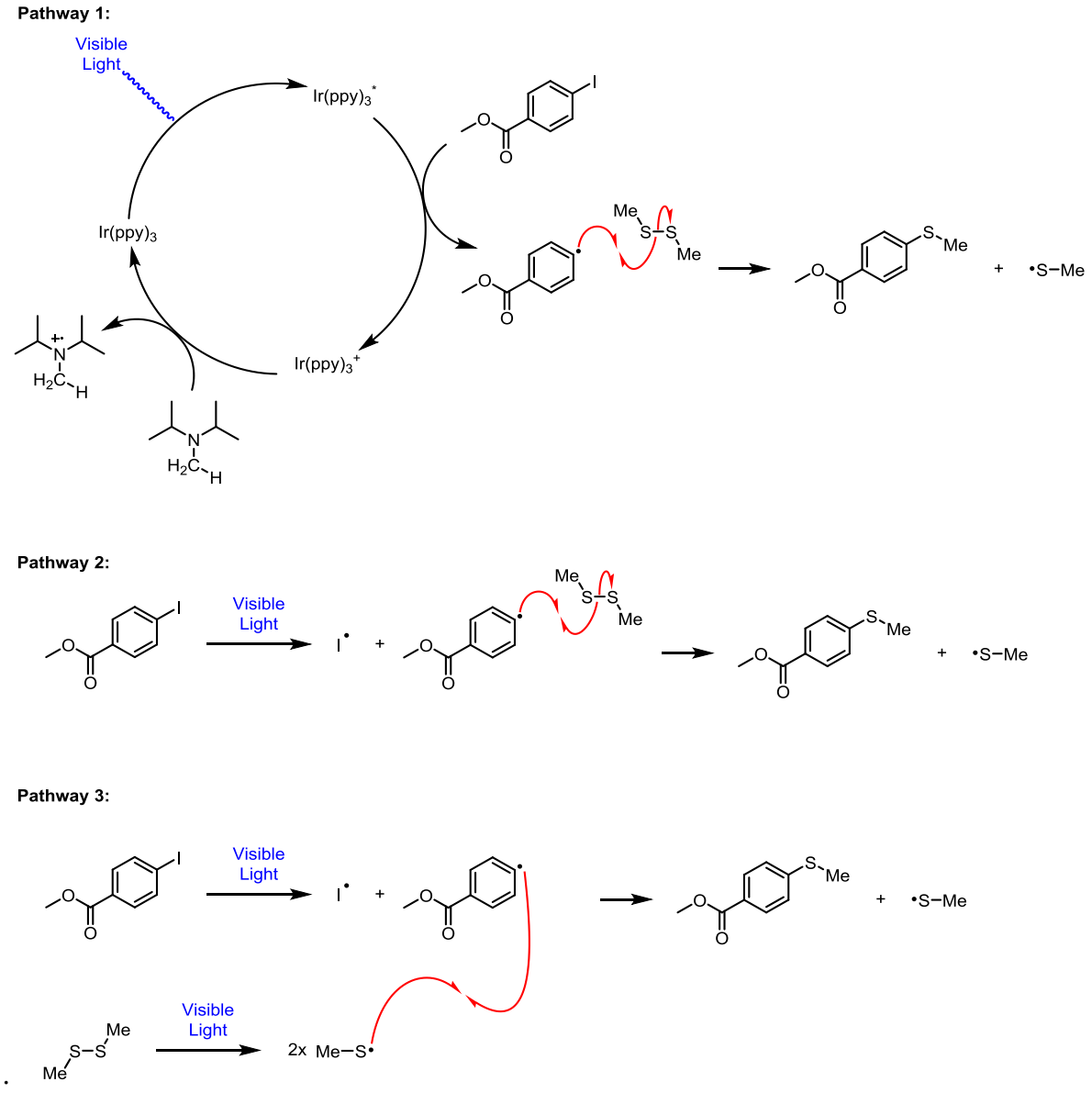

Figure 8: Proposed mechanism for the formation of aryl sulfide (**83**)

The use of the 1W fluorescent white light bulb resulted in the elimination of the competitive reductive dehalogenation of 4-methyl iodobenzoate (**81**) and this was very encouraging. However, irradiating with the 1W light source resulted in an unpractically long reaction time. To compensate for the slow reaction, a new reactor was built in which the power of the blue LED light could be adjusted (Table 13) resulting in a controlled intensity of irradiation. As the power of the LED was reduced, the yield of the product increased until a maximum of 66% was reached with 4W LED's (Table 13, entry 2).

Table 13: The influence of LED intensity

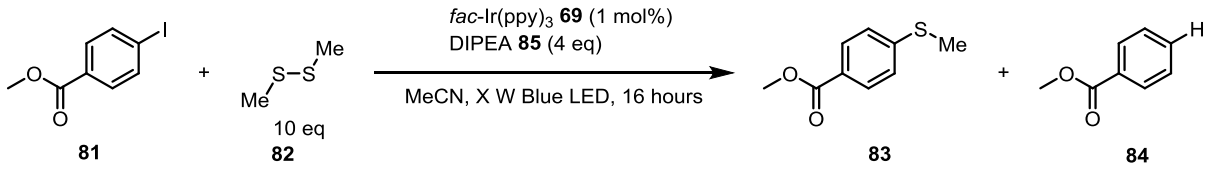

Entry	Power (W)	Yield 83 (%)
1	2	54
2	4	66
3	6	59
4	8	55
5	10	50

Flow chemistry has many advantages over batch chemistry in terms of increased safety, increased reactivity and decreased reaction times. These are due in part to the increased temperatures and pressures caused by the environment inside the tubes or microfluidic channels.[36] Conducting photoredox catalysis experiments in flow has been shown to dramatically reduce the time needed for the reaction to reach completion.[37] Given that continuous flow photochemical reactions imbue greater control over reactor conditions through temporal control of reagents (the time in which reactants and products are irradiated) it was anticipated that greater control could improve the reaction yields while simultaneously potentially eliminating competitive reductive dehalogenation.

A study was conducted to determine the influence of continuous flow processing on product yield and selectivity. A commercially available flow reactor platform was used for this study; Vapourtec R2+R4 photechmistry unit. The schematic for this reactor is shown in Figure 9.

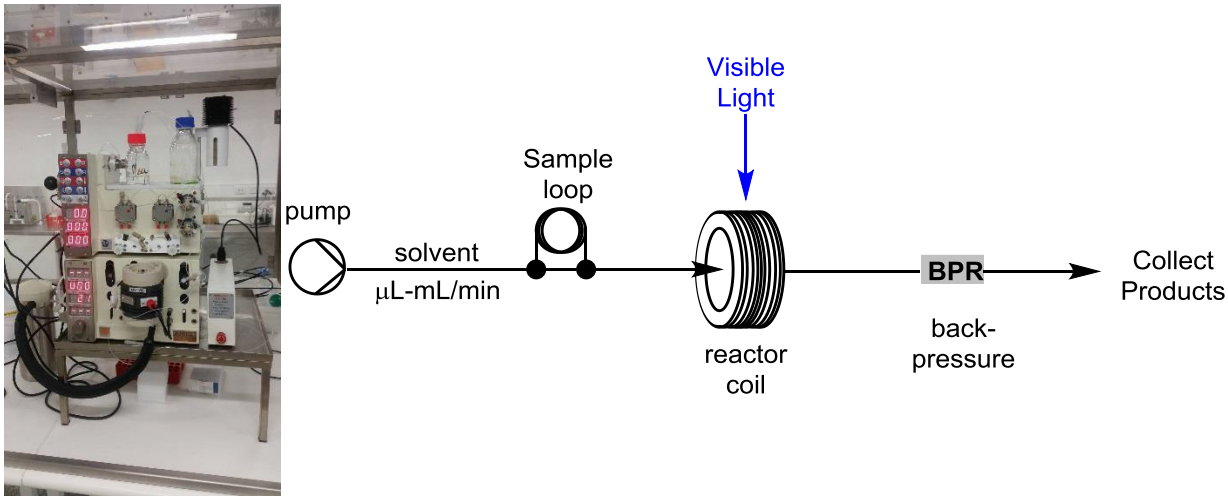

Figure 9: Flow reactor and schematic

The reaction was pumped through a flow reactor and through an inline blue light LED photo reactor. The flow reactor was a Vapourtec R2+ pumping system joined with an R4 heating/cooling module. Commercially available perfluoro alkoxy alkane (PFA) tubing with an internal diameter of 0.762 mm was chosen as a viable choice because it is chemically resistant and optically transparent. The R2+ pumping module uses piston pumps to pump solvent from a reservoir through a sample loop, containing the reaction mixture, and through the tubing through the R4 module containing the UV-150 reactor to irradiate the sample with blue LEDs.

As the 4W LED gave the highest conversion to product in batch, the inline photo reactor was set to the lowest setting (50%, 75W) and the reaction was irradiated for 1 hour. ^{1}H NMR spectroscopic analysis of the crude material showed 41% conversion to the desired product. It was also observed that 12% of the 4-methyl iodobenzoate (**81**) was unconverted. This would mean that 47% of the 4-methyl

iodobenzoate (**81**) was reduced and subsequently removed *in vacuo* before ^{1}H NMR spectroscopic analysis. It was observed that the conversion of 4-methyl iodobenzoate (**81**) to product did not increase with the increase in power of the LED light, however reduction of the 4-methyl iodobenzoate (**81**) increased. While flow did accelerate the rate of reduction of the 4-methyl iodobenzoate (**81**), it gave comparable conversion of the 4-methyl iodobenzoate (**81**) to aryl sulfide **83** in 1 hour compared to 16 when conducted in batch. Thus although the reaction time was significantly reduced, the selectivity was not improved under flow conditions.

Table14: Flow Reaction

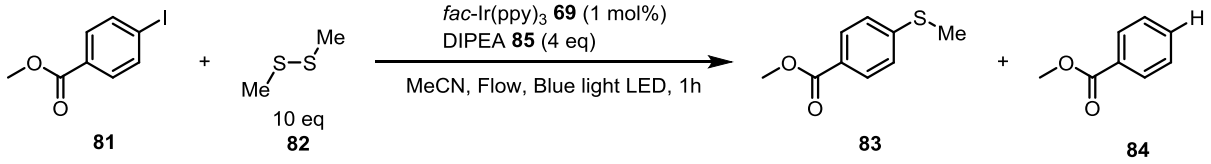

Entry	LED intensity (%)	Product 83 Yield (%)	Reduced Product 84 (%)	Recovered 4-methyl iodobenzoate (81) (%)
1	50	41	13	12
2	75	41	50	6
3	99	40	34	6

Chapter 3:

Summary and Future Work

3.0 Conclusion and Future Work

In this study a new method for the synthesis of aryl sulfides from aryl iodides via visible light photoredox catalysis was established. In the presence of 1 mol% $Ir(ppy)_3$ and blue LED's, a series of aryl sulfides were readily prepared in a maximum of 66% yield. The mechanism for this reaction was proposed to be the reduction of the aryl iodide from the excited state of $Ir(ppy)_3$, to form an carbon based aryl radical (Figure 10). This aryl radical would then undergo electrophilic aromatic substitution with dimethyl disulfide to form the product. The addition of the formed aryl radical to disulfide was proposed to be the rate determining step as the major by-product for the reaction, methyl benzoate (**84**), was from the competing reductive dehalogenation pathway. This observed by the elimination of reductive dehalogenation pathway when the formation of aryl radicals was slowed by changing the irradiation source from blue LED's to a 1W white light bulb.

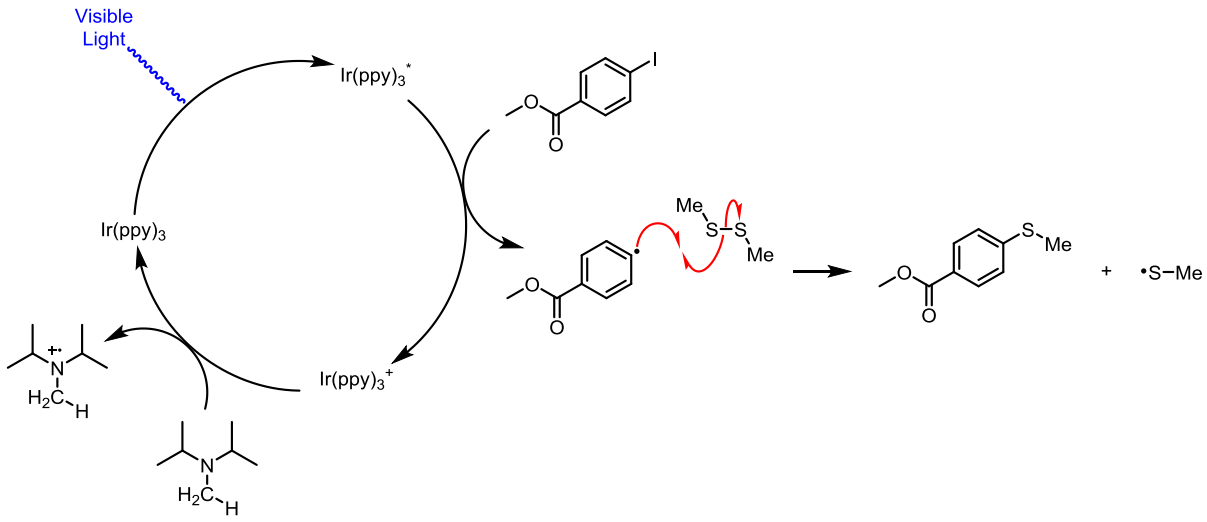

Figure 10: Proposed mechanism for the synthesis of aryl sulfide via visible light catalysis

The use of a 1W white light bulb prepared aryl sulfides in yields up to 86%. The extended reaction times under these conditions (13 days) is impractical for synthetic use, however the irradiation with 4W

blue LEDs results acceptable reaction times of approximately 16 hours, however, with a comparative reduction in yield of 66%.

There are a number of solutions to address the limitations of this reaction:

Firstly, the use of a more powerful white light could be used to improve the time taken for the reaction to reach completion (Scheme 33). The increase from 1W to 10W would result in a more practical reaction time for this reaction, while also keeping yields high. As discussed in Chapter 2.2, continuous flow processing can decrease the reaction time as evidenced by completion of the reaction in 1 hour compared to 16 in batch. The flow experiments used blue LED's and the formation of reductive dehalogenation product could not be eliminated. The use of white light LED's in the flow reactor, may afford a more expedient time frame while ensuring high yields of aryl sulfide and low yield of reductive dehalogenation product.

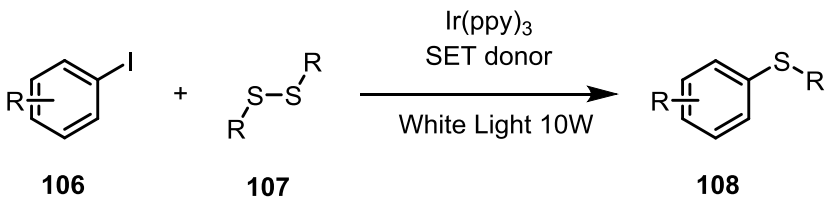

Scheme 34: White light Catalysed Aryl sulfide synthesis

As seen in Chapter 2.2, the use of blue LEDs resulted in the homolytic cleavage of the disulfides. Although the effect is unclear it would be of interest to screen other electrophilic thiolating agents. For example N-(arylthio)succinimides (**110**), as recently reported by Cossy *et al.*[22] (Scheme 34).

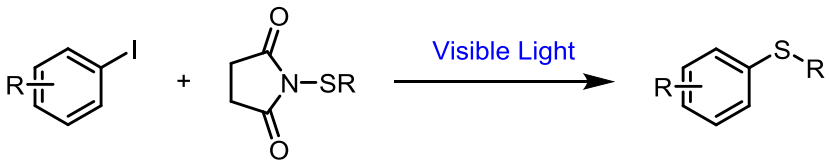

109 **110** **111**

Scheme 35: Possible aryl sulfide synthesis from N-(arylthio)succinimides

The SET donors used in this reaction requires further investigation. The SET donor is believed to be the major H-atom donor leading to the unwanted dehalogenative reduction. The use of triaryl amine as SET donor would eliminate reduction of the starting material. Although, triaryl amines investigated in this project gave no reaction (probably because of incompatible redox potentials with $Ir(ppy)_3$). The use of triphenyl amines with matched redox potential may solve this challenge. Electron rich amines such as 4,4'-Bis(4-methoxy)triphenylamine (**112**) and 4,4',4"-Tris(4-methoxy)triphenylamine (**113**) (Figure 11) may be investigated.

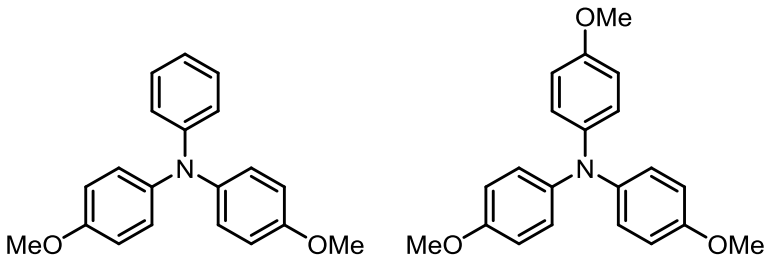

112 **113**

Figure 11: 4,4'-Bis(4-methoxy)triphenylamine and 4,4',4"-Tris(4-methoxy)triphenylamine

If successful, these modifications could successfully meet the goal of synthesising aryl sulfides in practical yields and reaction times.

Chapter 4:

Experimental

4.0 Experimental

Photoreactor:

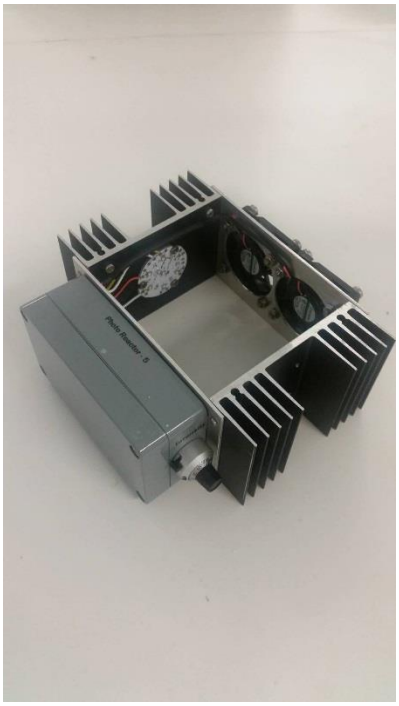

The photoreactor (pictured above) was made from 2 Luxeon Star LEDs Royal-Blue (447.5nm) Rebel ES LED on a SinkPAD-II 40mm Round 7-Up base (7210 mW @ 700 mA) LED diodes positioned, facing each other, 100 mm apart, with 2 heat sinks and fans attached. Reactor also had a tuneable power source that could tune power from 0-100%. The reactor was designed and built at CSIRO, Clayton, Australia.

The flow photoreactor (pictured above) was a vapourtec UV-150 photochemical reactor. The reactor was fitted with blue LEDs and is able to have the power controlled from 75 watts to 150 watts during operation. The reactor was constantly cooled with a nitrogen gas line to keep the reactor at room temperature.

NMR Time-Course Experimental:

To a 20 mL flask, 4-methyl iodobenzoate (0.3 mmol), $Ir(ppy)_3$ (1 mol%), DIPEA (4 eq) and dimethyl disulfide (10 eq) were added. Dry MeCN-d_3 was added (3 mL, 0.1 M) then the flask was sealed and placed within the photoreactor. Samples of the reaction mixture, of 50 µL, were taken at time equals 0, 15, 30, 45, 60, 90 and 120 minutes, then every hour after. To each sample 50 µL of a 0.1 M solution of 3-sulfolene in MeCN-d_3 was added as internal standard. Each sample was then placed into an NMR flask, topped up with MeCN-d_3. Each sample was then analysed by ^{1}H NMR spectroscopy. Comparison of the signals of 4-methyl iodobenzoate, methyl benzoate and 4-methyl (methylthio)benzoate to 3-sulfolene gave percentages of each in the reaction.

Flow Experimental:

To a 20 mL flask, 4-methyl iodobenzoate (0.3 mmol), $Ir(ppy)_3$ (1 mol%), DIPEA (4 eq) and dimethyl disulfide (10 eq) were added. Dry MeCN was added (3 mL, 0.1 M) then mixed. 2 mL of the reaction

was removed by syringe and added to the solvent loop of the Vapourtec R2+ pump module system. The sample was flowed through a Vapourtec R4 reactor heater/cooler module with attached Vapourtec UV-150 reactor, with blue LED strip insert, with MeCN for 1 hour at 25 ºC. The reaction was collected in a 50 mL round bottom flask before the solvent was removed *in vacuo* and product was isolated by flash chromatography (EtOAc in Heptane, 1 – 10%).

Chromatography:

Analytical Thin Layer Chromatography (TLC) was carried out using aluminium-backed Merck Kieselgel KG60 F_{254} silica plates. The plates were visualised by irradiation with short-wave ultraviolet light. Flash chromatography was performed on Grace Davidson Davisil LC60A 40-63 micron silica gel.

Reagents and Solvents:

All reagents and solvents were purchased from commercial sources and used without further purification.

Instrument Conditions:

Infra-red (IR) spectra were obtained on a Thermo Scientific Nicolet 6700 FT-IR spectrometer and are reported as wavenumbers (cm^{-1}). Spectra were recorded from solid supported samples dissolved in $CDCl_3$.

Melting Points were obtained on a John Morris Scientific Stuart SMP30.

NMR spectra were obtained on Bruker 400 Ultrashield (400 MHz), Ascend 400 (400 MHz) and Avance III 500 (500 MHz) spectrometers running Brucker Topspin v3 software at CSIRO, Clayton. The data was acquired and processed using Topspin 3.1 software. Chemicals shifts are expressed as parts per million (PPM) and are referenced to the internal standard.

GC-mass spectra were obtained with a Thermo Scientific TSQ 8000 TRACE 1310 GC mass spectrometer using electron impact ionisation in the positive ion mode with an ionisation energy of 70 eV. The gas chromatography was performed with a SGE SOLGEL-1MS column (30 m x 0.25 mm ID, 0.25 µm film thickness), with a temperature program of 50°C for 2 minutes, then heating at 23°C/min to 300°C where the temperature was held for 7 minutes with a splitless injection, an injector temperature of 300°C and the transfer line was set to 300°C. High-purity helium was used as carrier gas with a flow rate of 1 ml/min.

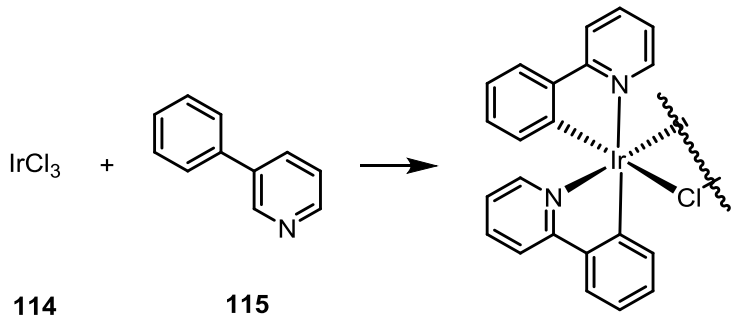

114 **115** **116**

Iridium µ-Cl-Diamer

Experimental: To a Schlenk flask equipped with a magnetic stir bar was added $IrCl_3$ hydrate (200 mg, 0.67 mmol) and dissoleved in 2.6 mL of water. Ethoxyethanol (8 mL) was added, then ligand, 2-phenyl pyridine (428 mg, 1.65 mmol). The mixture was then sparged for 30 minutes with N_2. The flask was equipped with a cold water condenser and then heated with stirring to 120 °C for 20 hours, during which time a yellow precipitate was observed to form. After cooling to room temperature, the precipitate was collected by vacuum filtration. The filter cake was washed copiously with H_2O (75 mL), EtOH (10-20

mL) and then Heptane (30 mL) to afford iridium μ-Cl-diamer as a fine yellow powder. The diamer was used without further purification.

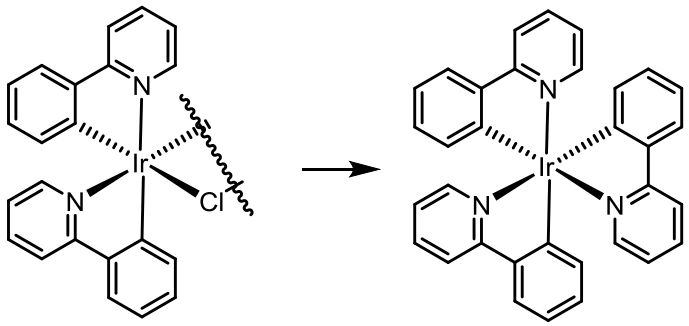

116 **117**

Tris[2-phenylpyridinato-C^2,*N*]iridium (III)[38]

Experimental: To a schlenk flask equipped with a magnetic stir bar was added Iridium diamer (126 mg, 0.12 mmol) and 2,2'-bipyridine (45 mg, 0.29 mmol). The reaction components were diussolved in ethylene glycol (6 mL) and the flask was sparged with N_2 for 20 minutes. The flask was then attached to a reflux condenser and heated with stirring at 150 °C for 24 hours. Upon cooling to room temperature, the reation mixture was diluted with deionized H_2O and transferred to a separatory funnel. The aqueous phase was washed with heptanes resulting in a yellow solid being formed. The solid was dried by vacuum filtration, washing with Heptane (50 mL). The solid was dissolved in DCM and then the solvent was removed *in vacuo* resulting in the formation of a fine yellow precipitate that was further dried under high vacuum (11.1 mg, 0.017 mmol, 14% yield over 2 steps).

^{1}H NMR (400 MHz, CD_2Cl_2): δ 7.92 (d, *J* = 8.2 Hz, 1H), 7.66 (m, 2H), 7.57 (d, *J* = 4.8 Hz, 1H), 6.91 (m, 2H), 6.77 (m, 2H)

^{13}C NMR (400 MHz, CD_2Cl_2): δ 166.83, 161.40, 147.58, 144.24, 137.14, 136.63, 130.05, 124.42, 122.51, 120.25, 119.26

IR: 3035, 1599, 1580, 1560, 1545, 1471, 1451, 1435, 1413, 1300, 1261, 1160, 1058, 1031, 752, 732 cm^{-1}

General experimental for aryl sulfides:

To a 20 mL flask, Aryl iodide (0.3 mmol), catalyst (1 mol%), amine (4 eq) and disulfide (10 eq) were added. Dry solvent was added (3 mL, 0.1 M) then the flask was sealed and placed within the photoreactor for 16 hours. Solvent was removed *in vacuo* and product was isolated by flash chromatography (EtOAc in Heptane, 1 – 10%).

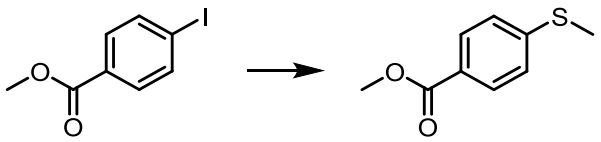

81 **83**

Methyl 4-(methylthio)benzoate

^{1}H NMR (400 MHz, $CDCl_3$): δ 7.93 (dt, *J* = 8.8 Hz, 2H), 7.24 (dt, *J* = 8.7 Hz, 2H), 3.89 (s, 3H), 2.50 (s, 3H)

^{13}C NMR (400 MHz, $CDCl_3$): δ 166.96, 145.54, 129.98, 126.37, 125.02, 52.12, 14.92

IR: 2994, 2947, 2845, 1708, 1594, 1560, 1492, 1433, 1404, 1369, 1308, 1279, 1196, 1188, 1116, 1014, 986, 967, 853, 837, 830, 759, 690 cm^{-1}

MP: 77-79 °C

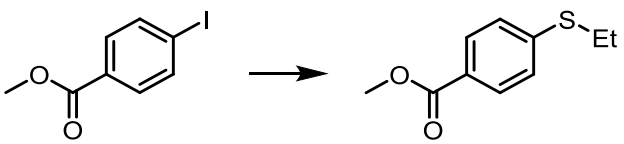

81 **100b**

Methyl 4-(ethylthio)benzoate

^{1}H NMR (400 MHz, $CDCl_3$): δ 7.89 (dt, *J* = 8.8 Hz, 2H), 7.25 (dt, *J* = 8.7 Hz, 2H), 3.86 (s, 3H), 2.98 (q, *J* = 7.4, 7.4 Hz, 2H), 1.33 (t, *J* = 7.4 Hz, 3H)

^{13}C NMR (400 MHz, $CDCl_3$): δ 166.94, 144.27, 130.02, 126.72, 126.42, 52.14, 26.25, 14.04

IR: 2976, 2951, 2932, 1716, 1597, 1492, 1434, 1402, 1381, 1314, 1289, 1278, 1185, 1113, 1014, 963, 843, 757, 733, 691 cm^{-1}

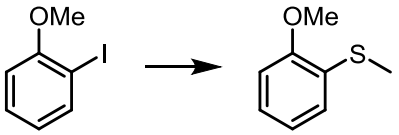

101a **102a**

2-Methylthioanisole[39]

^{1}H NMR (400 MHz, $CDCl_3$): δ 7.15 (m, 2H), 6.96 (td, *J* = 7.6, 1.2 Hz, 1H), 6.84 (dd, *J* = 8.0, 1.0 Hz, 1H), 3.90 (s,3H), 2.43 (s,3H)

^{13}C NMR (400 MHz, $CDCl_3$): δ 126.33, 126.07, 121.31, 110.20, 55.90, 14.90

IR: 3003, 2950, 2835, 1716, 1594, 1578, 1478, 1463, 1433, 1285, 1274, 1240, 1182, 1111, 1092, 1073, 1044, 1025, 967, 842, 826, 791, 745, 679 cm^{-1}

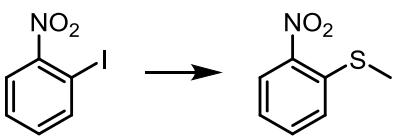

101b **102b**

2-(methylthio)-nitrobenzene[23]

^{1}H NMR (400 MHz, $CDCl_3$): δ 8.26 (dd, *J* = 8.4, 1.4 Hz, 1H), 7.59 (td, *J* = 7.7, 1.5 Hz, 1H), 7.38 (d, *J* = 8.1 Hz, 1H), 7.25 (td, *J* = 7.8, 1.3 Hz, 1H), 2.50 (s, 3H)

^{13}C NMR (400 MHz, $CDCl_3$): δ 145.60, 139.44, 133.82, 126.32, 125.78, 124.30, 16.09

IR: 3109, 3087, 2989, 2921, 1593, 1563, 1504, 1455, 1441, 1427, 1363, 1337, 1305, 1277, 1249, 1171, 1153, 1105, 1062, 1046, 970, 947, 854, 780, 729, 711, 681, 653 cm^{-1}

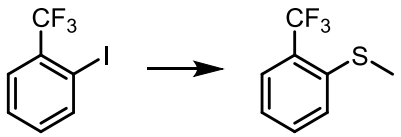

101c **102c**

2-(methylthio)-benzotrifluoride[23]

^{1}H NMR (400 MHz, $CDCl_3$): δ 7.63 (d, *J* = 7.8 Hz, 1H), 7.48 (t, *J* = 8.0 Hz, 1H), 7.38 (d, *J* = 8.0 Hz, 1H), 7.23 (t, *J* = 7.7 Hz, 1H), 2.52 (s, 3H)

^{13}C NMR (400 MHz, $CDCl_3$): δ 132.14, 127.55, 126.85, 126.80, 124.83, 16.49

IR: 2928, 1594, 1572, 1472, 1442, 1313, 1257, 1172, 1116, 1035, 759 cm^{-1}

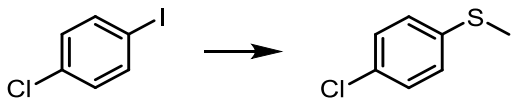

101f **102f**

4-Chlorophenyl methyl sulfide[23]

^{1}H NMR (400 MHz, $CDCl_3$): δ 7.25 (dt, *J* = 7.4, 2.4 Hz, 2H), 7.17 (dt, *J* = 8.8, 2.2 Hz, 2H), 2.47 (s, 3H)

^{13}C NMR (400 MHz, $CDCl_3$): δ 137.13, 131.03, 129.04, 128.04, 16.24

IR: 2986, 2920, 1477, 1437, 1389, 1320, 1179, 1096, 1011, 968, 809, 747 cm^{-1}

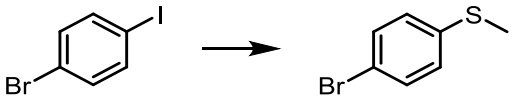

101g **102g**

4-Bromophenyl methyl sulfide[23]

^{1}H NMR (400 MHz, $CDCl_3$): δ 7.39 (dt, *J* = 8.7, 2.7 Hz, 2H), 7.12 (dt, *J* = 8.6, 2.0 Hz, 2H), 2.46 (s, 3H)

^{13}C NMR (400 MHz, $CDCl_3$): δ 137.84, 131.93, 128.26, 118.75, 16.07

IR: 2920, 2852, 1473, 1435, 1387, 1319, 1181, 1093, 1070, 1007, 967, 806 cm^{-1}

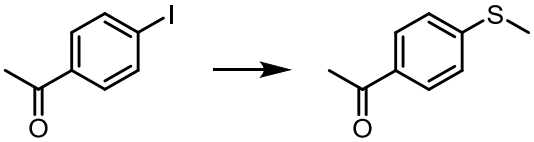

101h **102h**

4'-(Methylthio)-Acetophenone[40]

^{1}H NMR (400 MHz, $CDCl_3$): δ 7.87 (dt, *J* = 8.6, 2.0 Hz, 2H), 7.27 (dt, *J* = 8.6, 2.0 Hz, 2H), 2.57 (s, 3H), 2.52 (s, 3H)

^{13}C NMR (400 MHz, $CDCl_3$): δ 197.31, 146.02, 133.65, 128.87, 125.11, 26.57, 14.92

IR: 2922, 2251, 1671, 1592, 1556, 1490, 1429, 1398, 1360, 1288, 1268, 1187, 1128, 1102, 1071, 1012, 957, 909, 818, 731 cm^{-1}

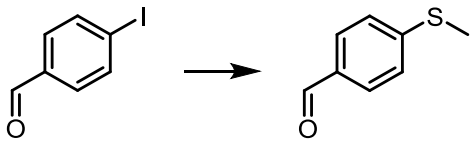

101i **102i**

4'-(methylthio)-Benzaldehyde[41]

^{1}H NMR (400 MHz, $CDCl_3$): δ 9.92 (s, 1H), 7.77 (dt, *J* = 8.6, 1.9 Hz, 2H), 7.32 (dt, *J* = 8.4, 2.0 Hz, 2H), 2.54 (s, 3H)

^{13}C NMR (400 MHz, $CDCl_3$): δ 191.37, 148.04, 133.09, 130.13, 125.33, 14.83

IR: 2924, 2853, 2736, 1740, 1696, 1673, 1592, 1561, 1490, 1437, 1389, 1322, 1302, 1215, 1170, 1093, 838, 812 cm^{-1}

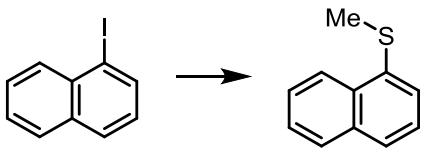

101j **102j**

1-Thiomethyl naphthalene[23]

^{1}H NMR (400 MHz, $CDCl_3$): δ 8.30 (d, *J* = 7.8, 0.6 Hz, 1H), 7.85 (dd, *J* = 7.6, 1.8 Hz, 1H), 7.69 (d, *J* = 7.8 Hz, 1H), 7.54 (pd, *J* = 7.8, 2.0 Hz, 2H), 7.42 (m, 2H), 2.59 (s, 3H)

^{13}C NMR (400 MHz, $CDCl_3$): δ 135.94, 133.74, 131.77, 128.65, 126.35, 126.26, 125.95, 125.80, 124.40, 123.74, 16.33

IR: 3053, 2985, 2918, 1590, 1564, 1504, 1426, 1383, 1334, 1316, 1257, 1205, 1143, 1024, 978, 787, 768, 663 cm^{-1}

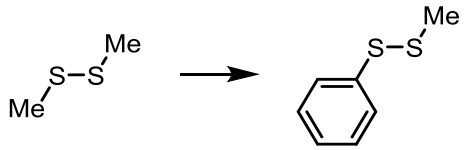

82 **105**

Methyl phenyl disulphide[35]

^{1}H NMR (400 MHz, CD_3CN): δ7.56-7.54 (2H, m), 7.4-7.36 (2H, m), 7.30-7.26 (1H, m), 2.46 (3H, s)

Mass Spec: R.T. 4.7 mins. Peaks: 159.1, 156.7, 140.9, 109.0, 77.0

Chapter 5:

Spectra

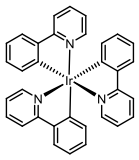

129

7.93
7.91
7.68
7.68
7.67
7.66
7.66
7.65
7.64
7.63
7.57
7.57
7.56
6.94
6.94
6.93
6.93
6.92
6.91
6.91
6.90
6.89
6.88
6.87
6.87
6.81
6.81
6.79
6.79
6.77
6.77
6.76
6.75
6.74
6.73
14 13 12 11 10 9 8 7 6 5 4 3 2 1 0 ppm
1.000
1.971
0.965
2.005
1.962

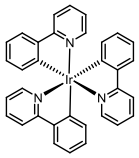

129

166.83
161.40
147.58
144.24
137.14
136.63
130.05
124.42
122.51
120.25
119.26
240 230 220 210 200 190 180 170 160 150 140 130 120 110 100 90 80 70 60 50 40 30 20 10 ppm

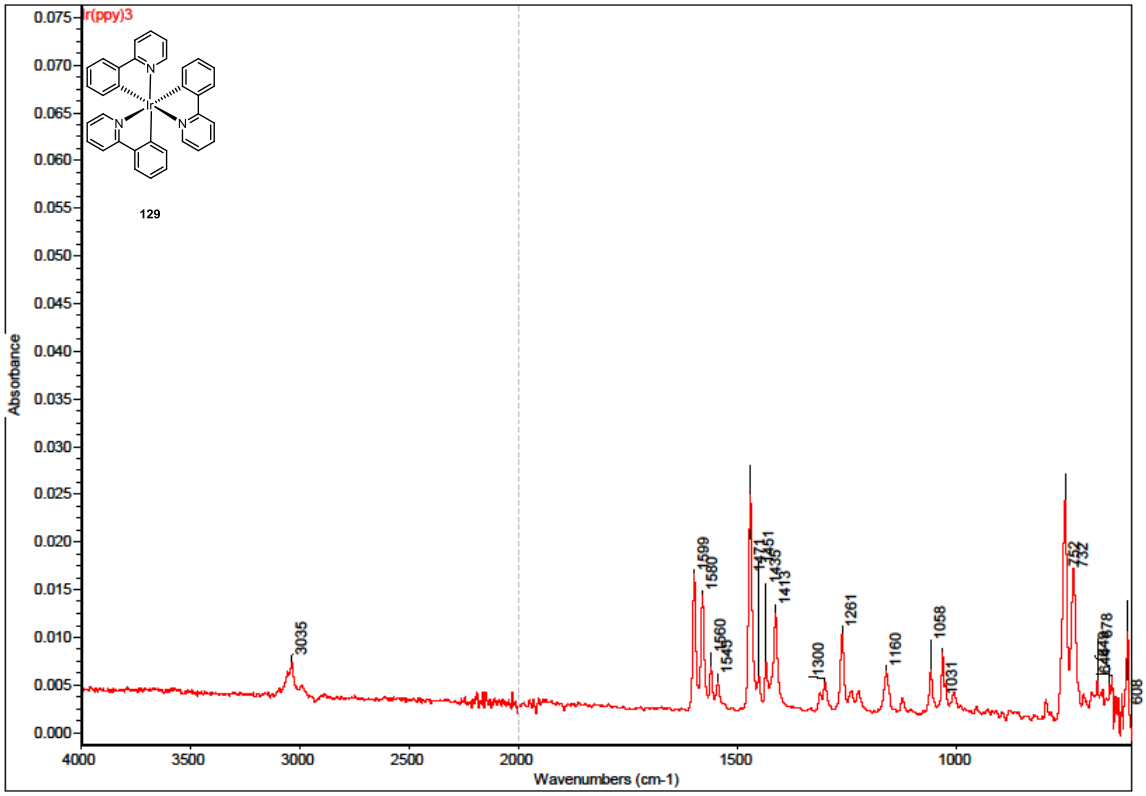
Ir(ppy)3
129
Absorbance
Wavenumbers (cm-1)
3035
1599
1580
1560
1545
1471
1451
1435
1413
1300
1261
1160
1058
1031
752
732
608

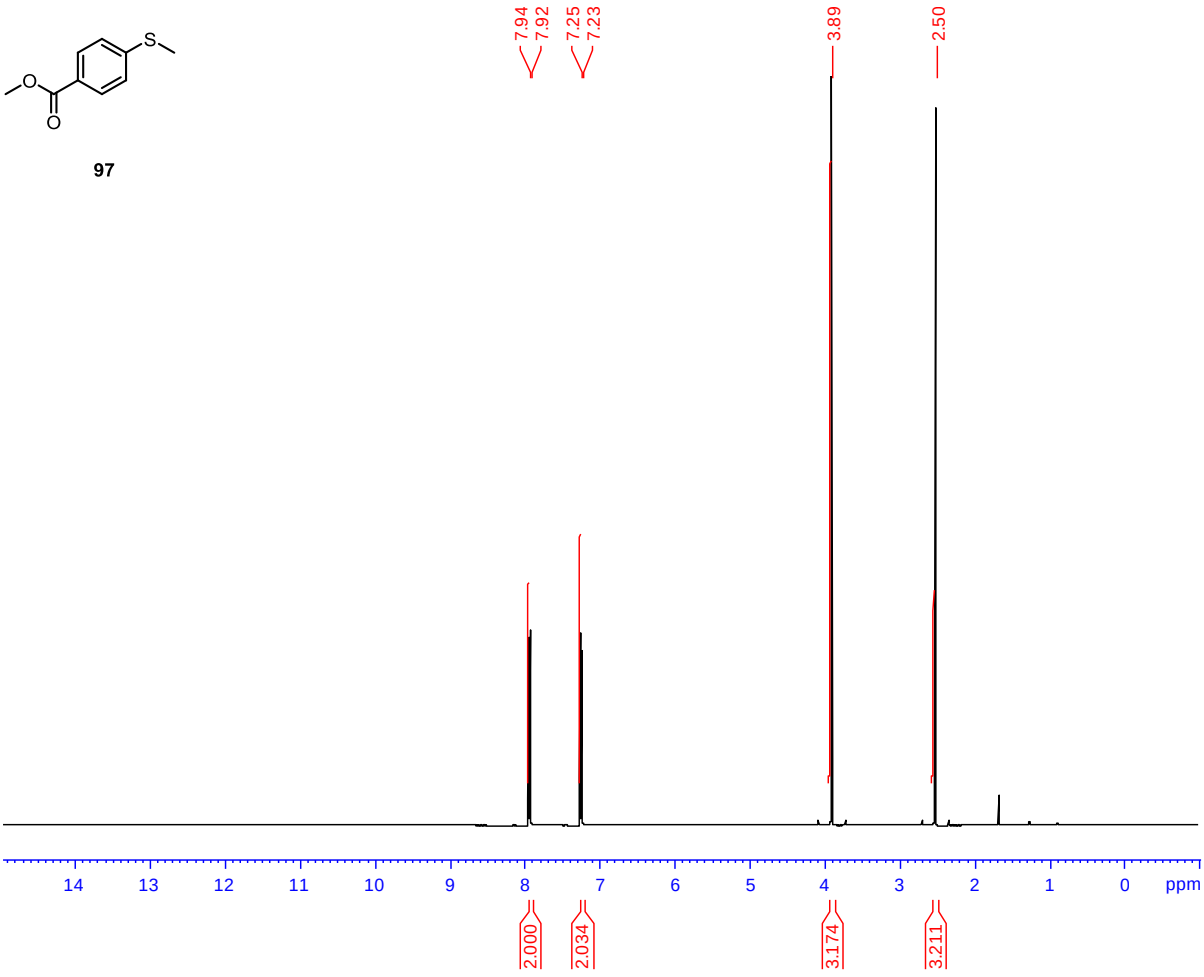
97
7.94
7.92
7.25
7.23
3.89
2.50
ppm
2.000
2.034
3.174
3.211

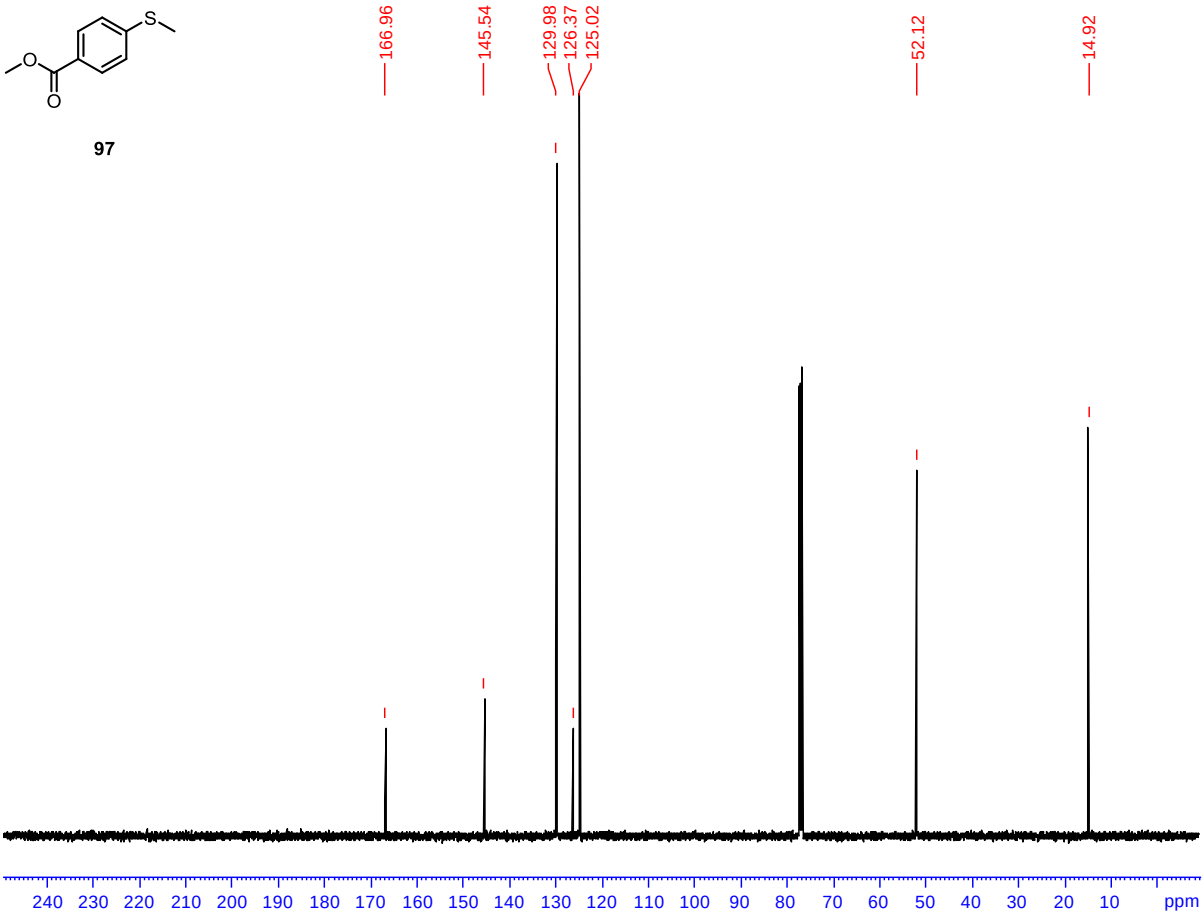
166.96
145.54
129.98
126.37
125.02
52.12
14.92
97
240 230 220 210 200 190 180 170 160 150 140 130 120 110 100 90 80 70 60 50 40 30 20 10 ppm

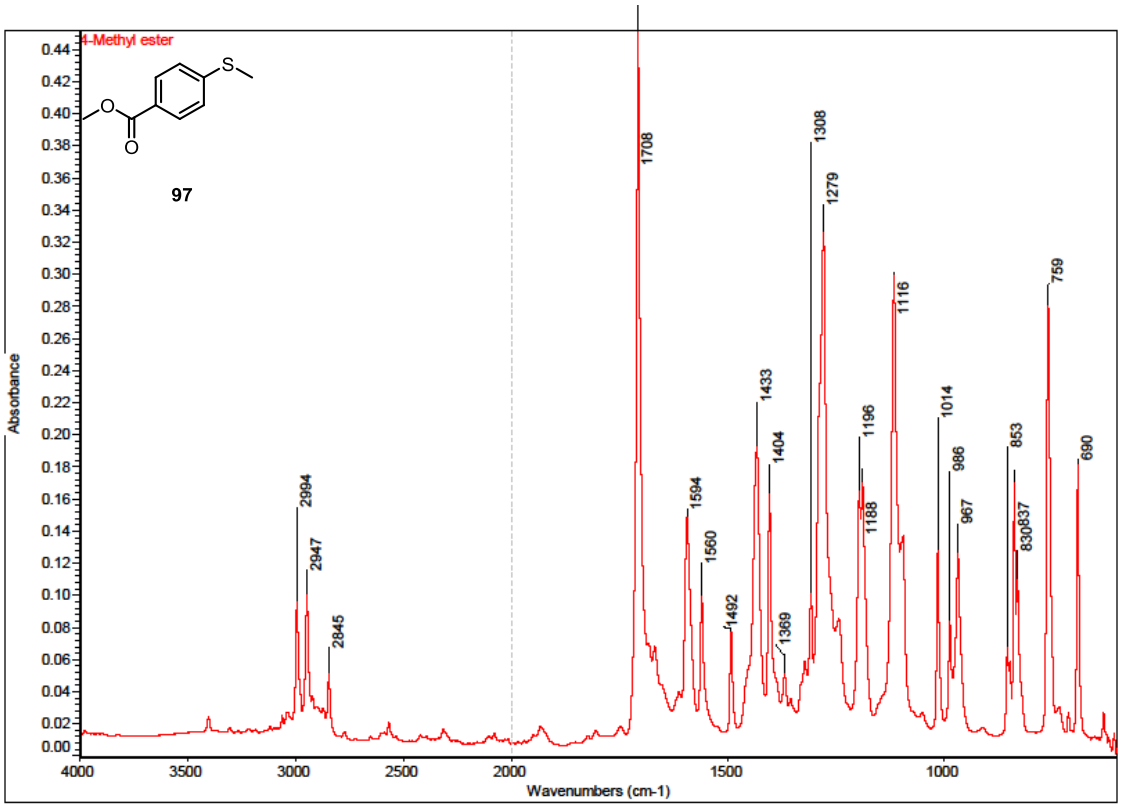
4-Methyl ester
97
Absorbance
Wavenumbers (cm-1)
4000 3500 3000 2500 2000 1500 1000
2994
2947
2845
1708
1594
1560
1492
1433
1404
1369
1308
1279
1196
1188
1116
1014
986
967
853
830837
759
690

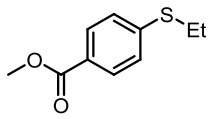
S
Et
O
O

100b

7.90
7.88
7.26
7.24
3.86
3.01
2.99
2.97
2.95
1.35
1.33
1.31
14
13
12
11
10
9
8
7
6
5
4
3
2
1
0
ppm
2.000
2.157
3.121
2.074
3.105

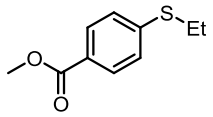
S
Et
O
O

100b

166.94
144.27
130.02
126.72
126.42
52.14
26.25
14.04
240
230
220
210
200
190
180
170
160
150
140
130
120
110
100
90
80
70
60
50
40
30
20
10
ppm

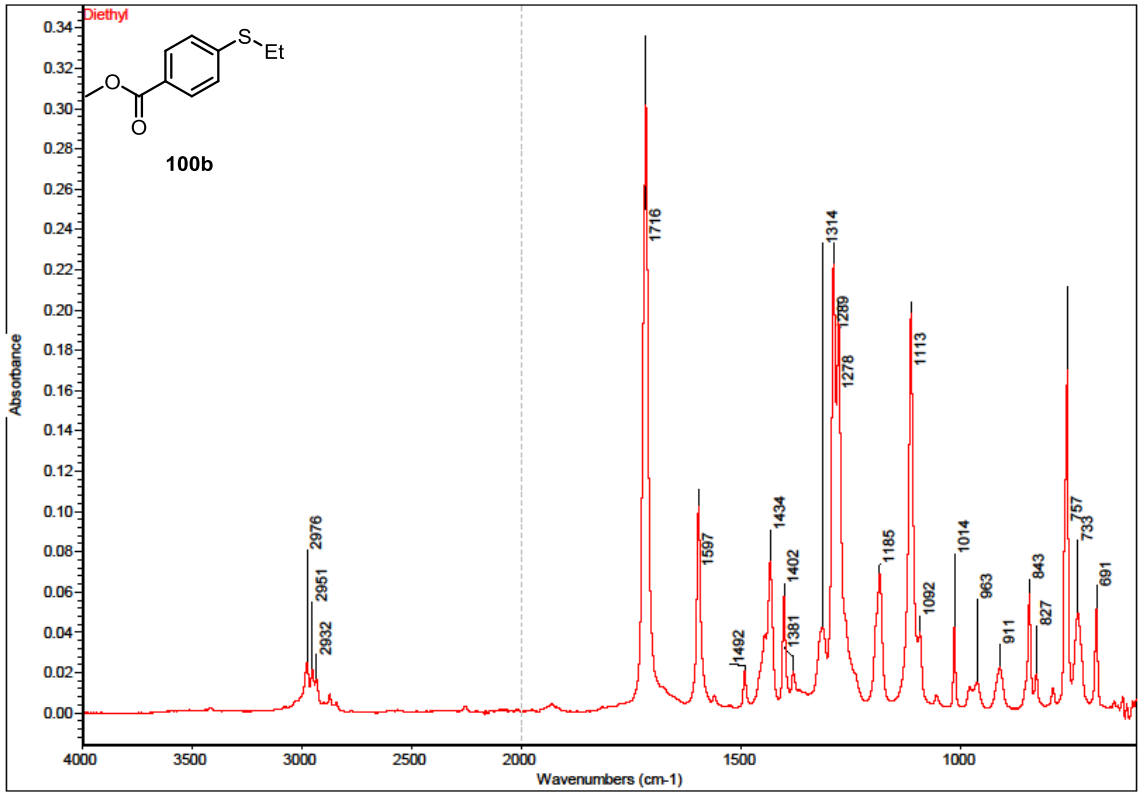
Diethyl
S
Et
O
O
100b
Absorbance
Wavenumbers (cm-1)
4000
3500
3000
2500
2000
1500
1000
0.34
0.32
0.30
0.28
0.26
0.24
0.22
0.20
0.18
0.16
0.14
0.12
0.10
0.08
0.06
0.04
0.02
0.00
2976
2951
2932
1716
1597
1492
1434
1402
1381
1314
1289
1278
1185
1113
1092
1014
963
911
843
827
757
733
691

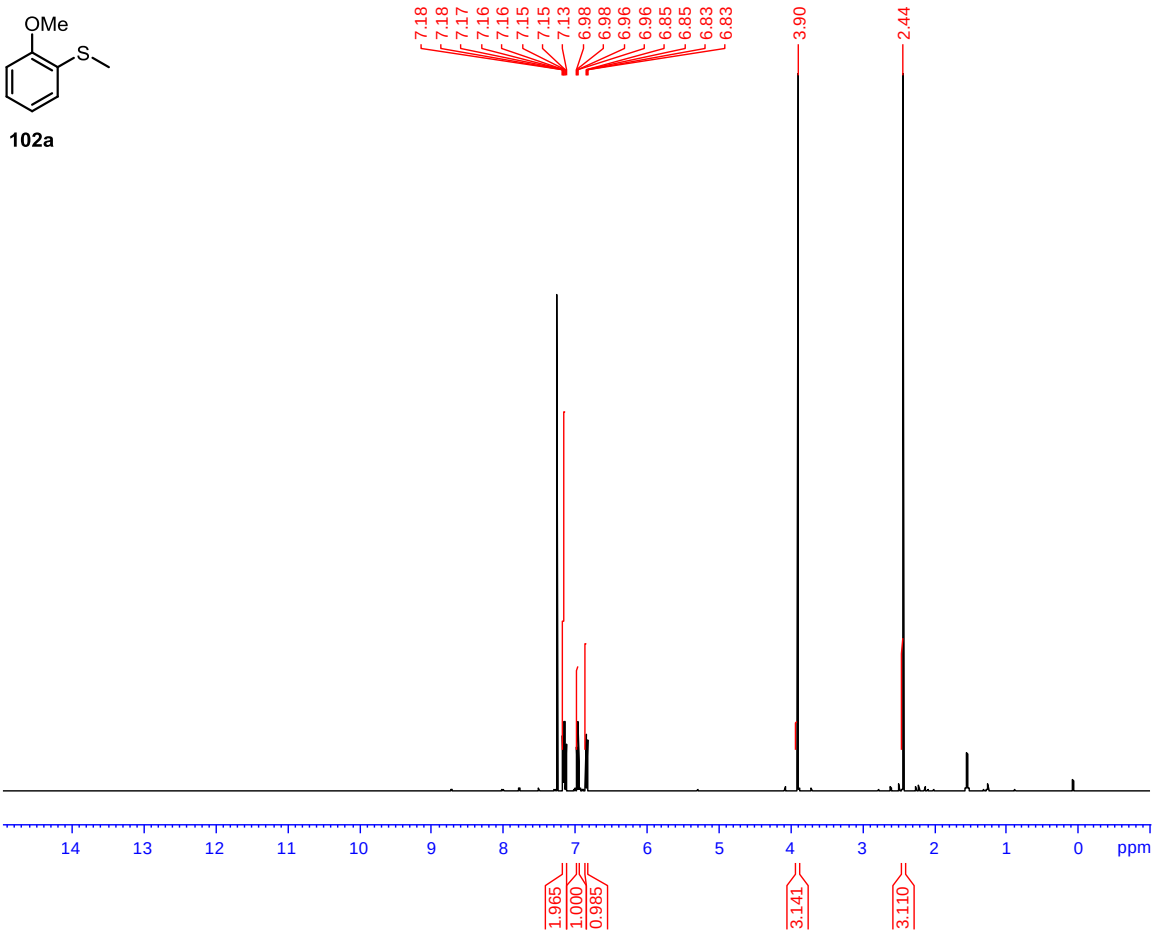
OMe
S
102a
7.18
7.18
7.17
7.16
7.16
7.15
7.15
7.13
6.98
6.98
6.96
6.96
6.85
6.85
6.83
6.83
3.90
2.44
14
13
12
11
10
9
8
7
6
5
4
3
2
1
0
ppm
1.965
1.000
0.985
3.141
3.110

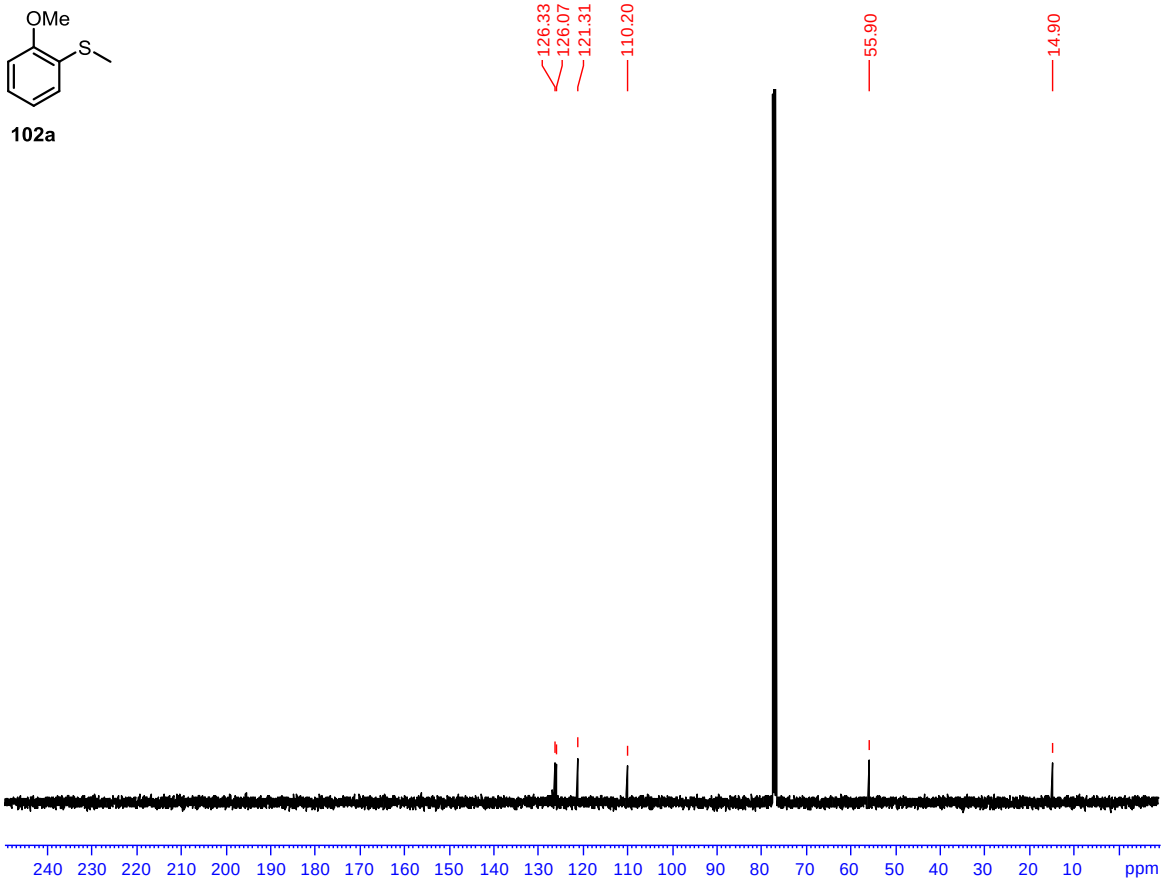
OMe
S
102a
126.33
126.07
121.31
110.20
55.90
14.90
240 230 220 210 200 190 180 170 160 150 140 130 120 110 100 90 80 70 60 50 40 30 20 10 ppm

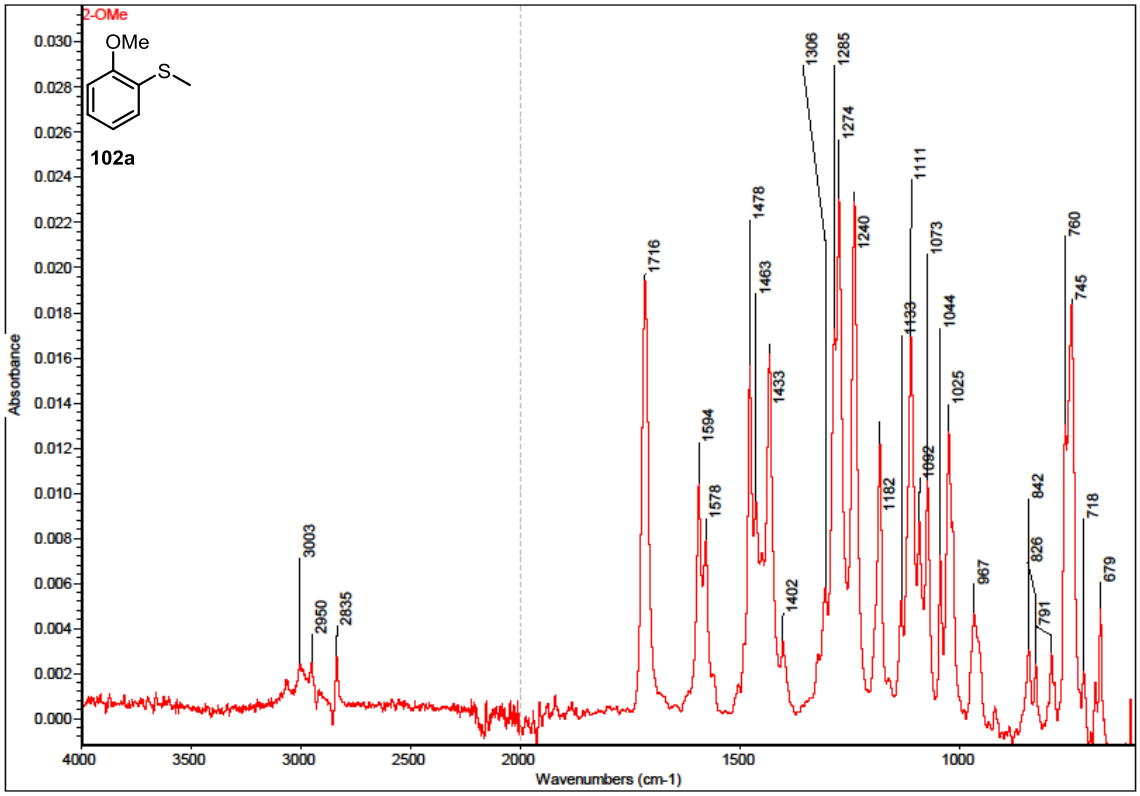
2-OMe
OMe
S
102a
Absorbance
Wavenumbers (cm-1)
4000 3500 3000 2500 2000 1500 1000
0.030 0.028 0.026 0.024 0.022 0.020 0.018 0.016 0.014 0.012 0.010 0.008 0.006 0.004 0.002 0.000
3003
2950
2835
1716
1594
1578
1478
1463
1433
1402
1306
1285
1274
1240
1182
1133
1111
1092
1073
1044
1025
967
842
826
791
760
745
718
679

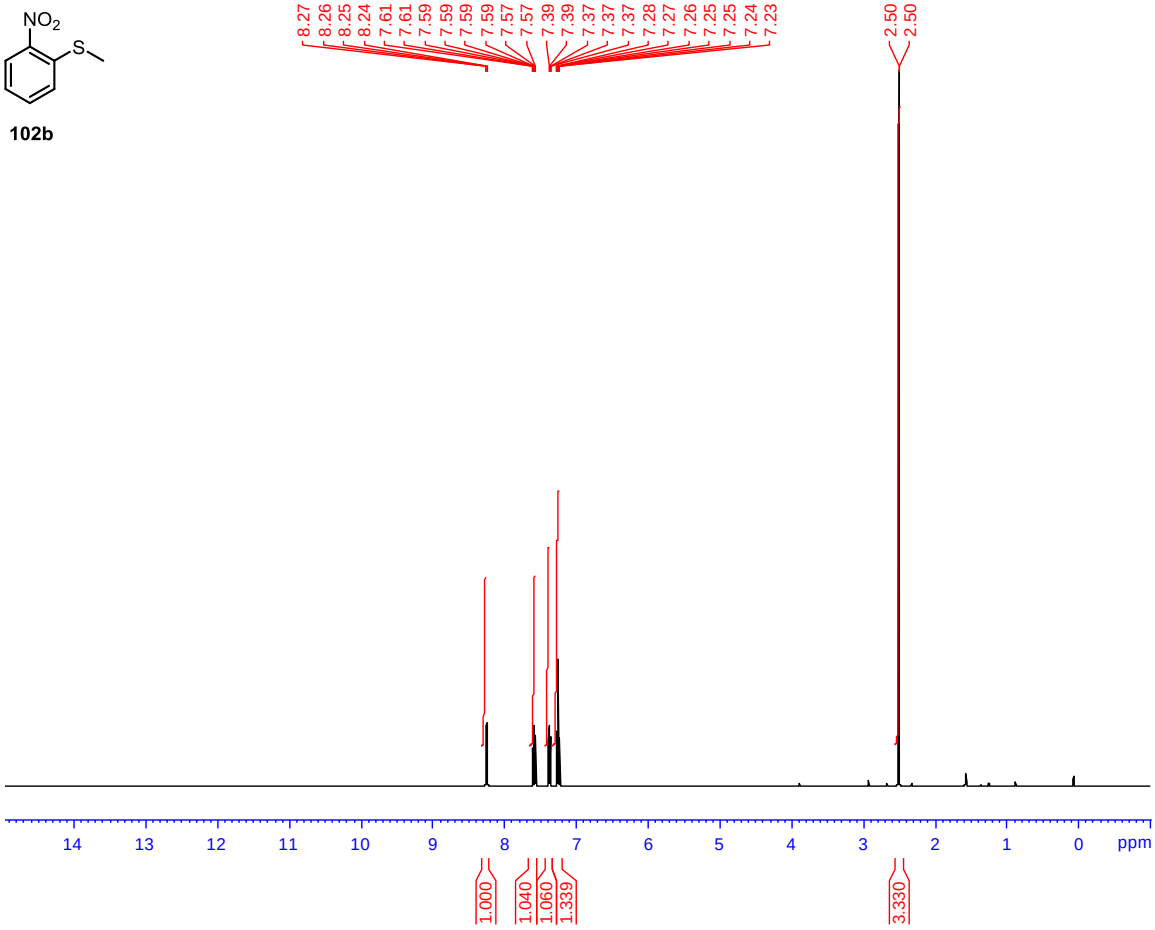
NO2
S
102b
8.27
8.26
8.25
8.24
7.61
7.61
7.59
7.59
7.59
7.59
7.59
7.57
7.57
7.39
7.39
7.37
7.37
7.37
7.28
7.27
7.26
7.25
7.25
7.24
7.23
2.50
2.50
14 13 12 11 10 9 8 7 6 5 4 3 2 1 0 ppm
1.000
1.040
1.060
1.339
3.330

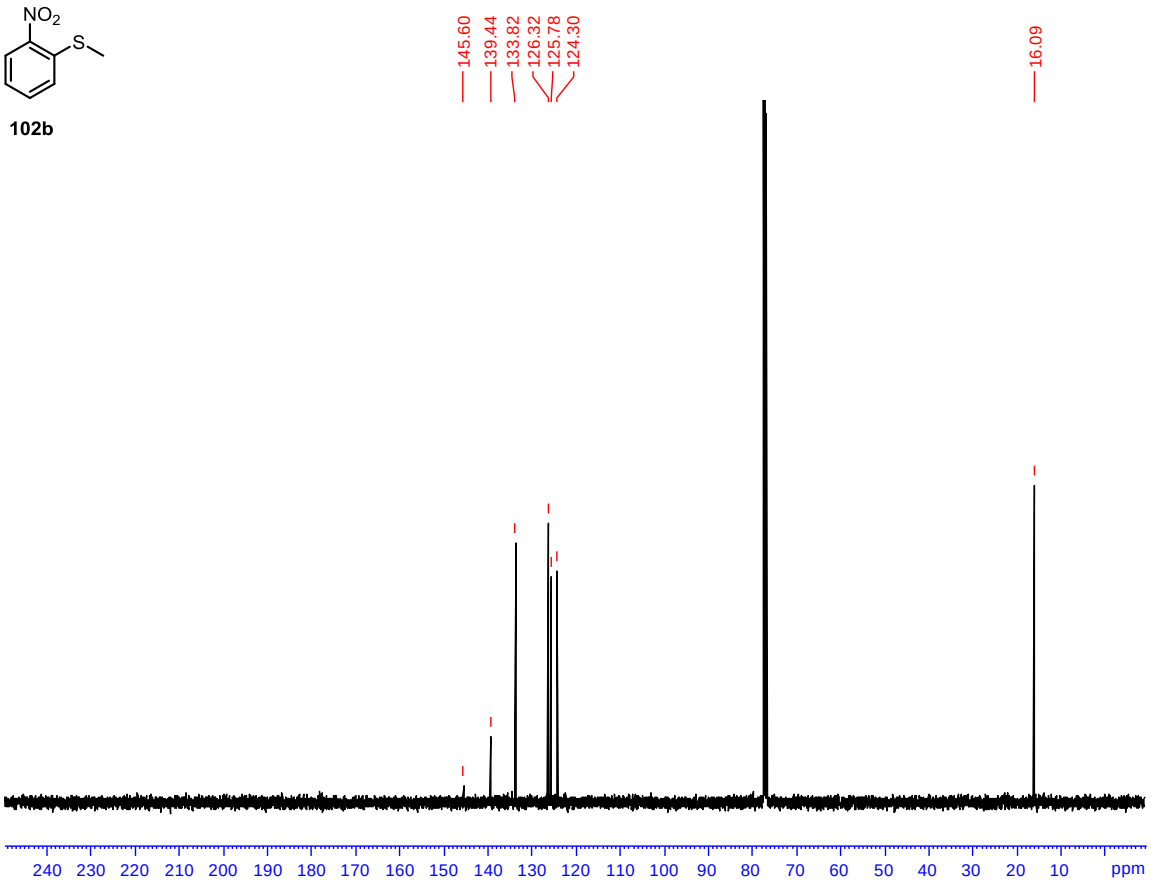
NO2
S
102b
145.60
139.44
133.82
126.32
125.78
124.30
16.09
240 230 220 210 200 190 180 170 160 150 140 130 120 110 100 90 80 70 60 50 40 30 20 10 ppm

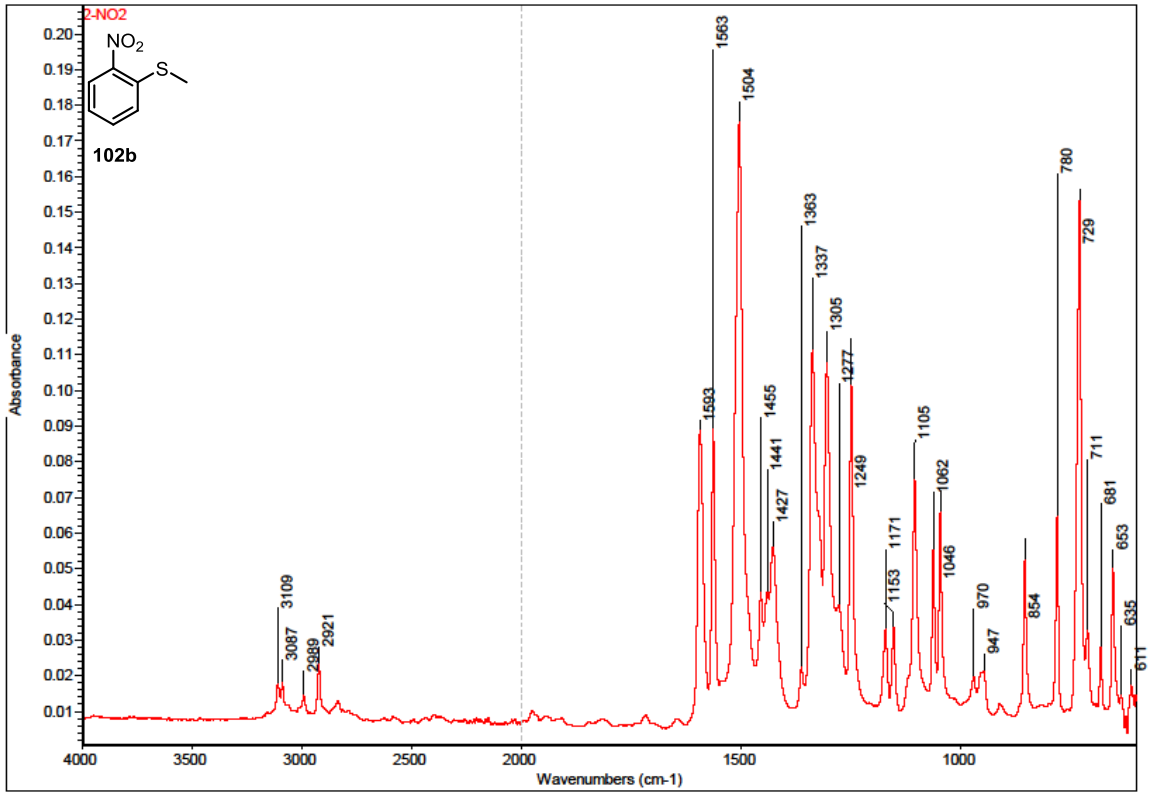
2-NO2
NO2
S
102b
Absorbance
Wavenumbers (cm-1)
4000
3500
3000
2500
2000
1500
1000
3109
3087
2989
2921
1593
1563
1504
1455
1441
1427
1363
1337
1305
1277
1249
1171
1153
1105
1062
1046
970
947
854
780
729
711
681
653
635
611

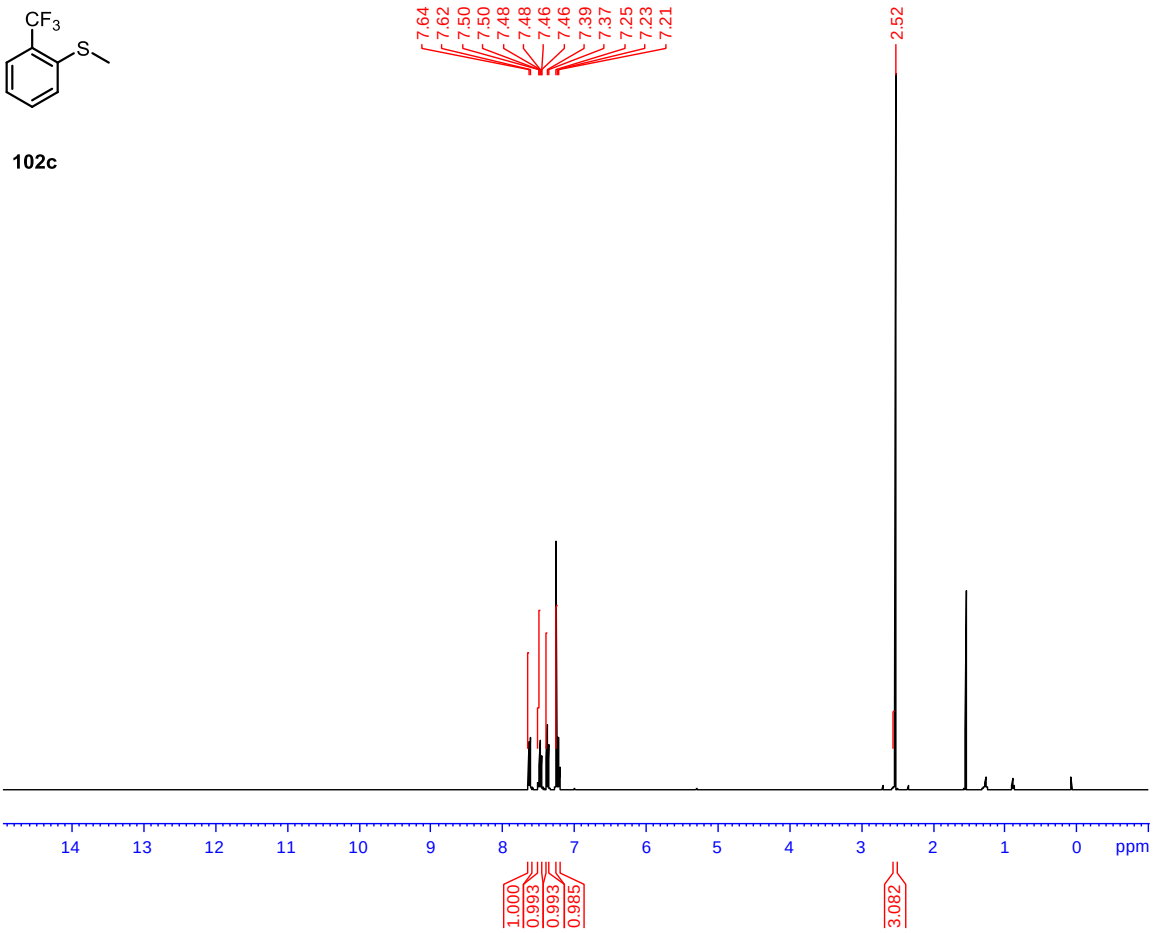
CF3
S
102c
7.64
7.62
7.50
7.50
7.48
7.48
7.46
7.46
7.39
7.37
7.25
7.23
7.21
2.52
ppm
1.000
0.993
0.993
0.985
3.082

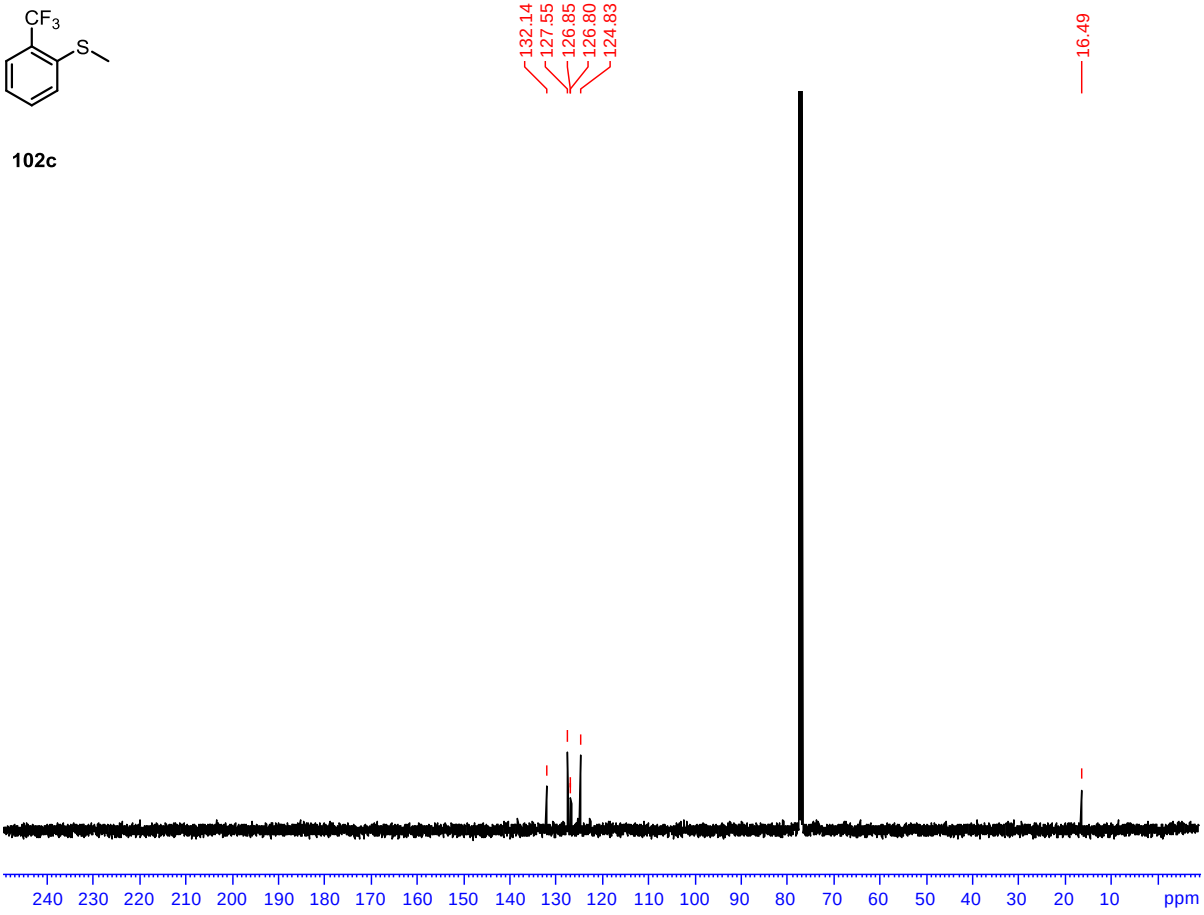
CF3
S
102c
132.14
127.55
126.85
126.80
124.83
16.49
240 230 220 210 200 190 180 170 160 150 140 130 120 110 100 90 80 70 60 50 40 30 20 10 ppm

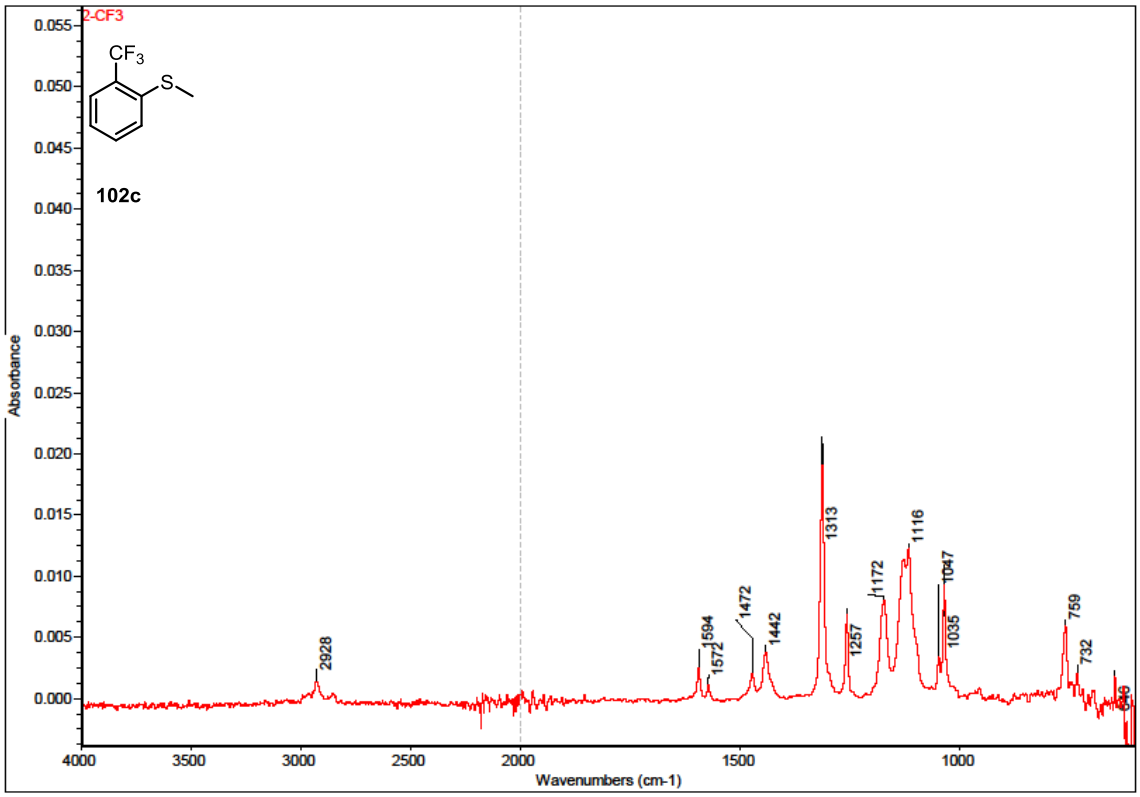
2-CF3
CF3
S
102c
Absorbance
0.055
0.050
0.045
0.040
0.035
0.030
0.025
0.020
0.015
0.010
0.005
0.000
2928
1594
1572
1472
1442
1313
1257
1172
1116
1047
1035
759
732
4000 3500 3000 2500 2000 1500 1000
Wavenumbers (cm-1)

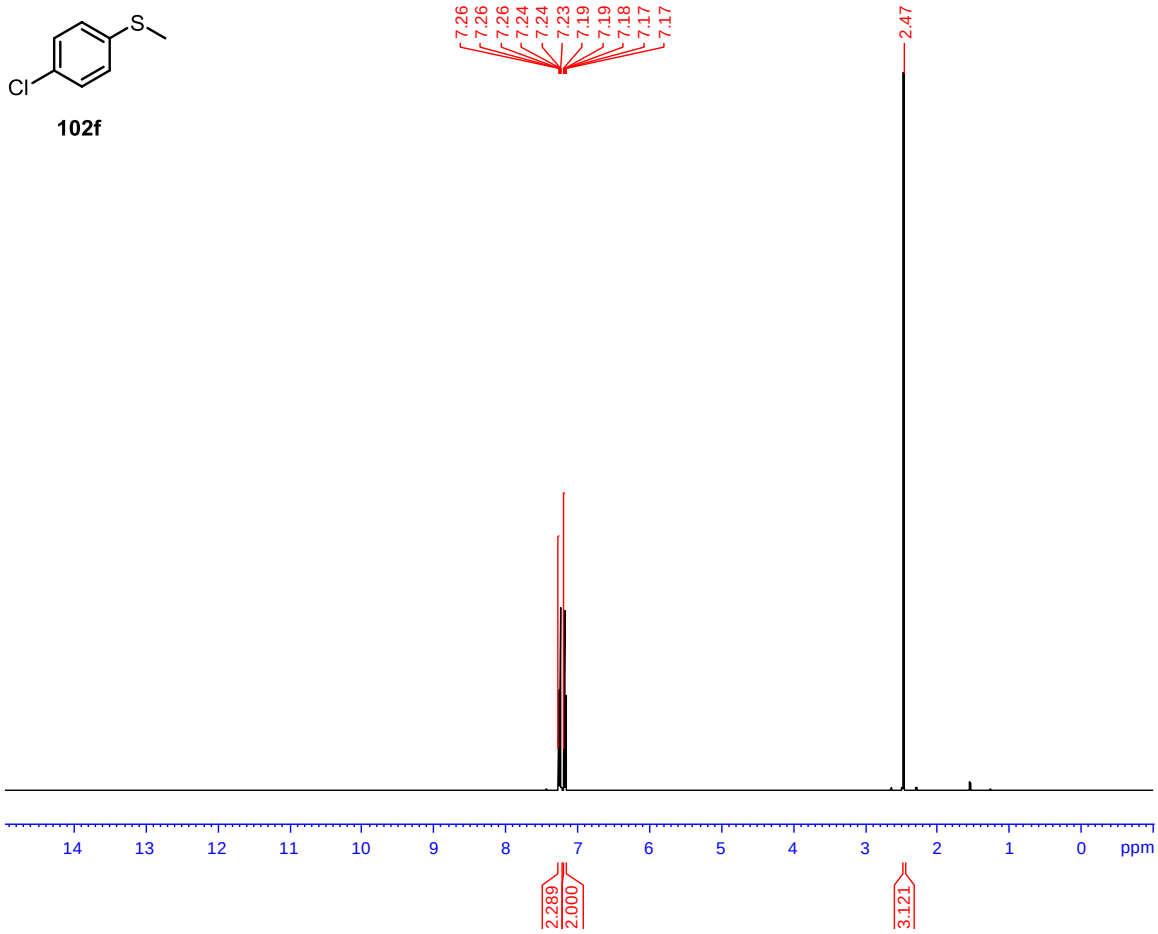
Cl
S
102f
7.26
7.26
7.26
7.24
7.24
7.23
7.19
7.19
7.18
7.17
7.17
2.47
14 13 12 11 10 9 8 7 6 5 4 3 2 1 0 ppm
2.289
2.000
3.121

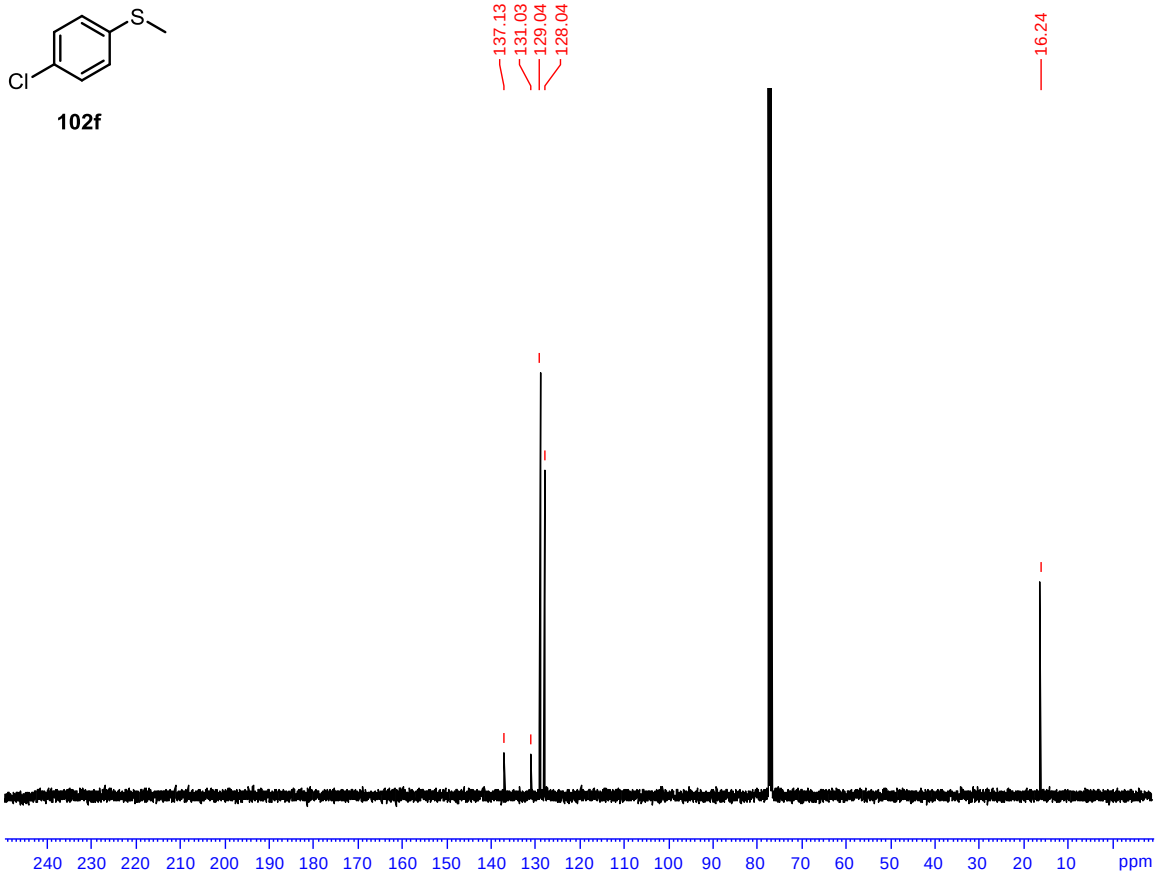
Cl
S
102f
137.13
131.03
129.04
128.04
16.24
240 230 220 210 200 190 180 170 160 150 140 130 120 110 100 90 80 70 60 50 40 30 20 10 ppm

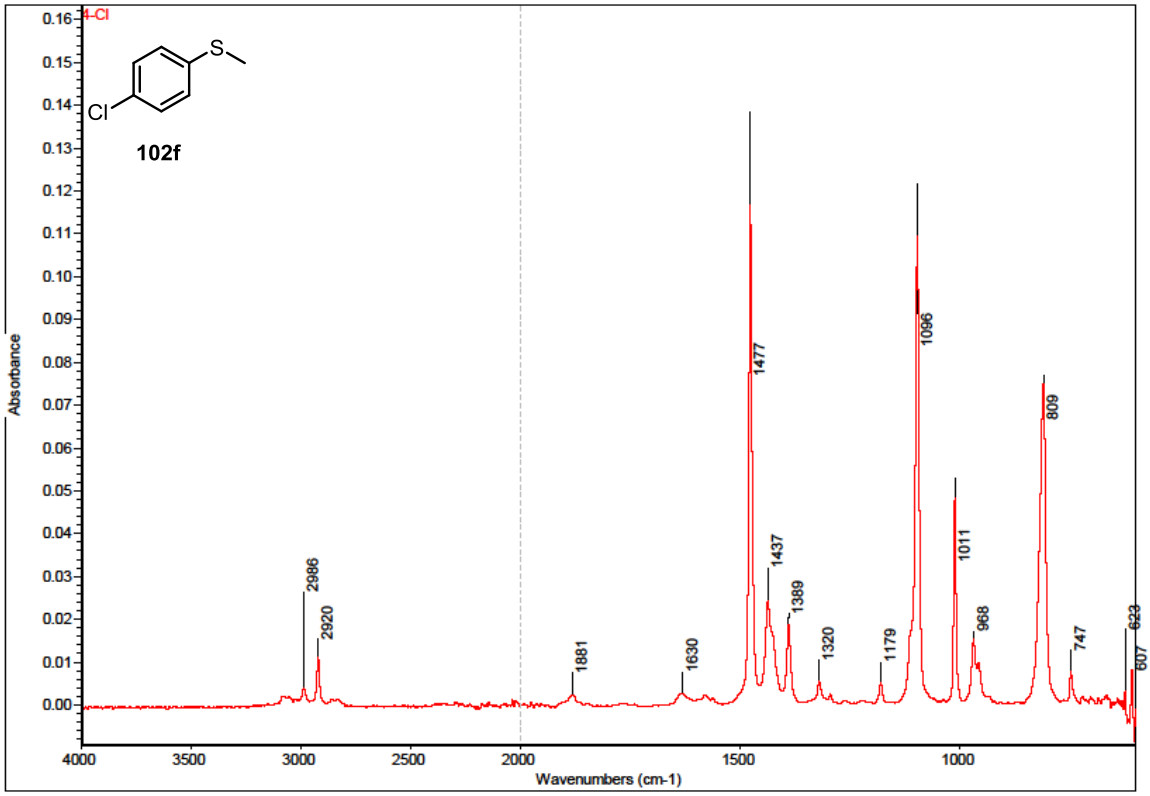
4-Cl
Cl
S
102f
Absorbance
Wavenumbers (cm-1)
2986
2920
1881
1630
1477
1437
1389
1320
1179
1096
1011
968
809
747
623
607

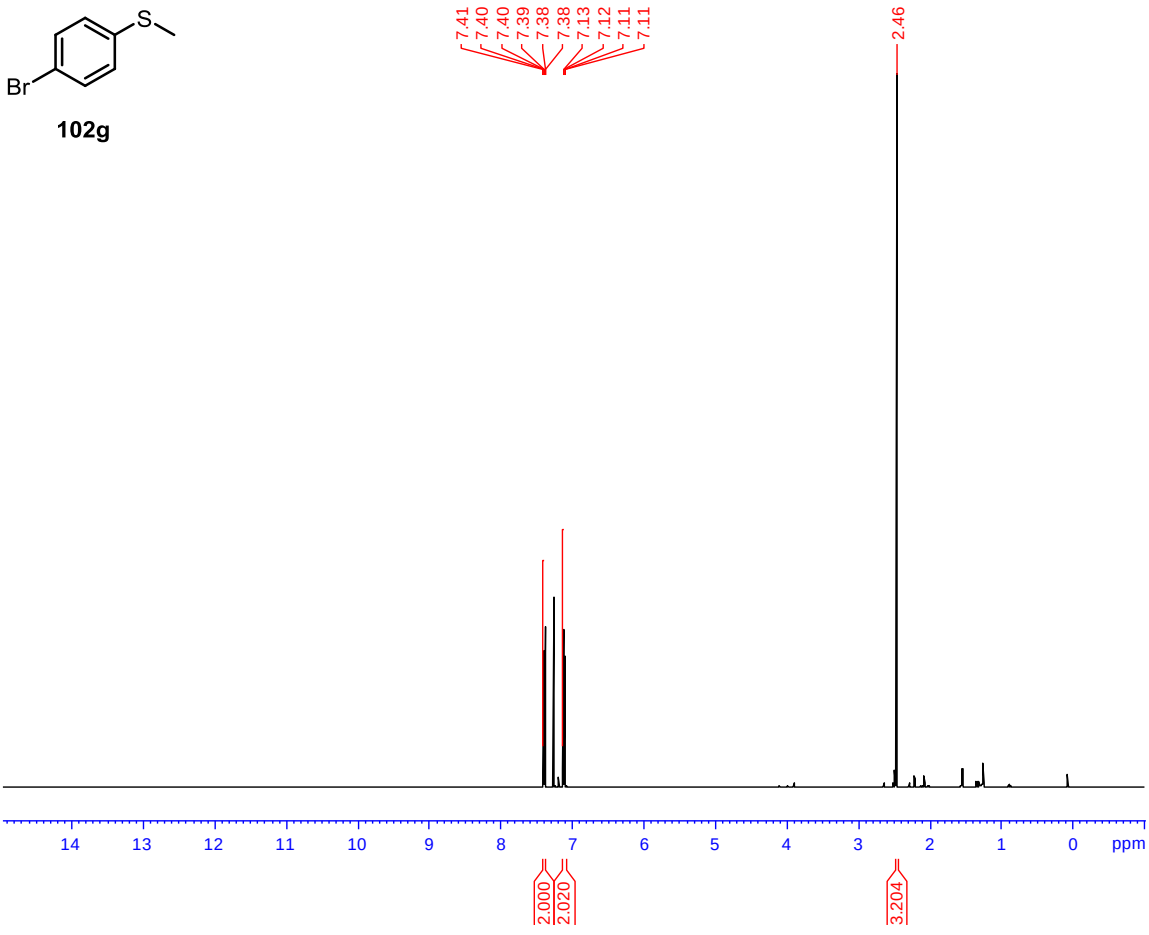
Br
S
102g
7.41
7.40
7.40
7.39
7.38
7.38
7.13
7.12
7.11
7.11
2.46
ppm
2.000
2.020
3.204

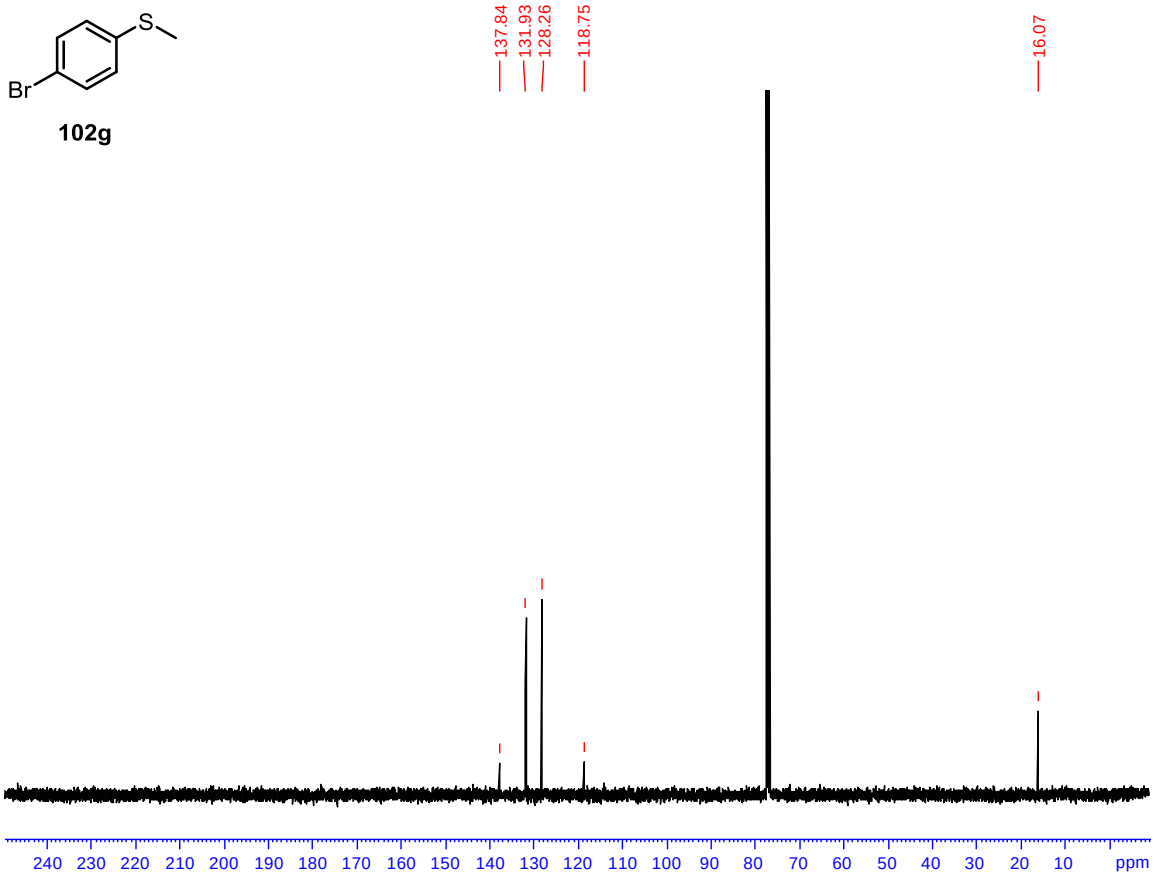
Br
S
102g
137.84
131.93
128.26
118.75
16.07
240 230 220 210 200 190 180 170 160 150 140 130 120 110 100 90 80 70 60 50 40 30 20 10 ppm

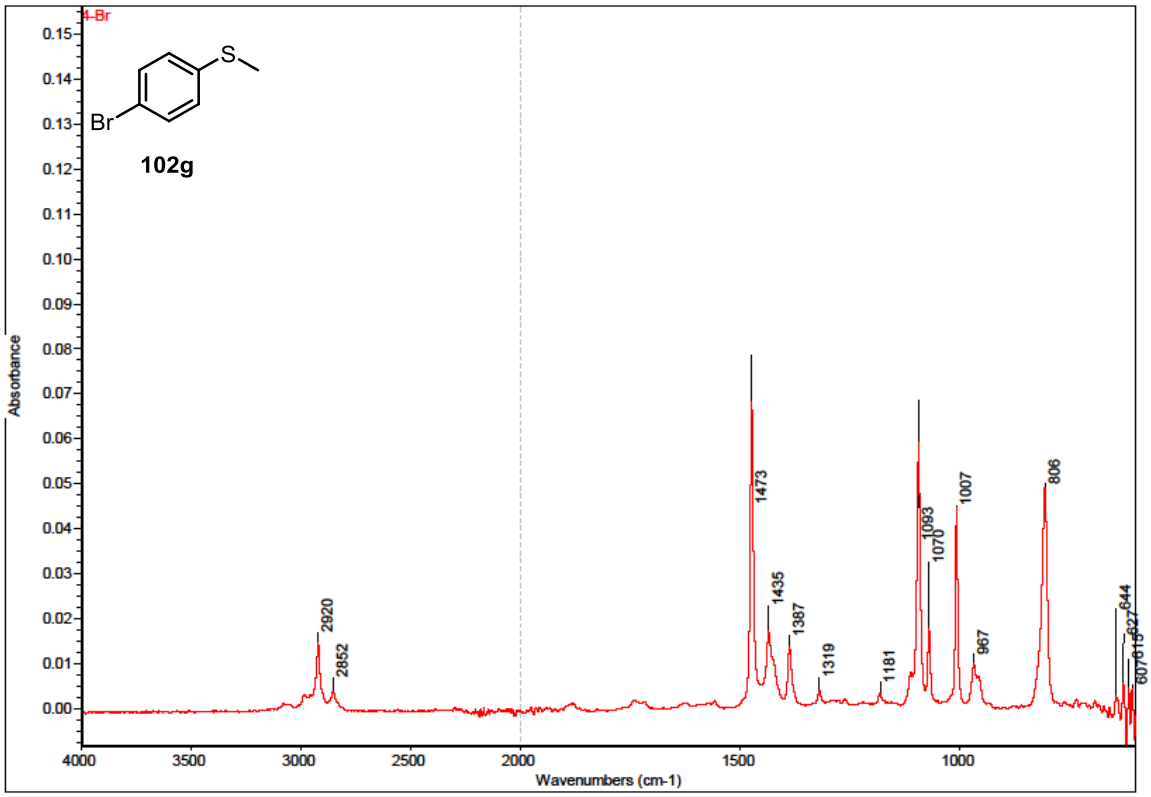
4-Br
Br
S
102g
Absorbance
Wavenumbers (cm-1)
4000 3500 3000 2500 2000 1500 1000
0.15 0.14 0.13 0.12 0.11 0.10 0.09 0.08 0.07 0.06 0.05 0.04 0.03 0.02 0.01 0.00
2920
2852
1473
1435
1387
1319
1181
1093
1070
1007
967
806
644
607

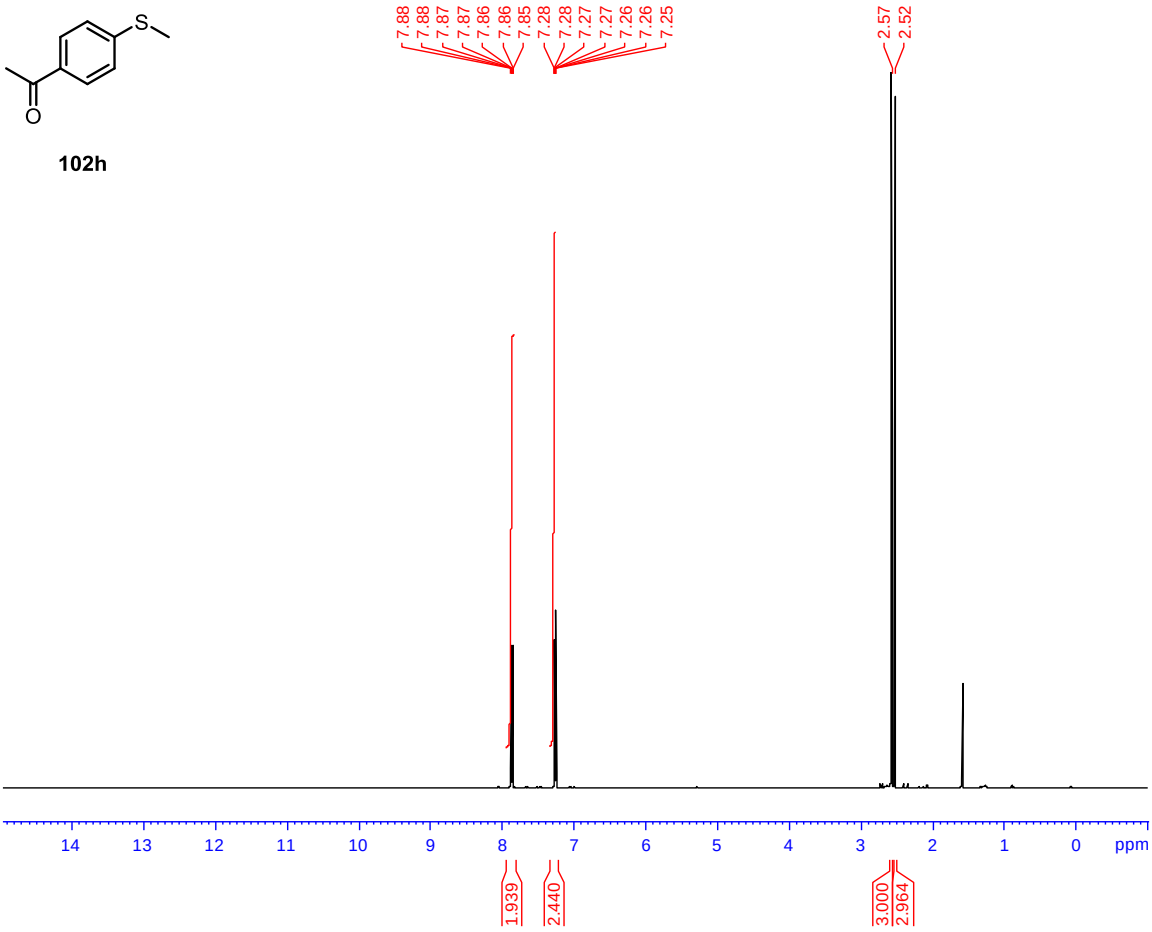
S
O
102h
7.88
7.88
7.87
7.87
7.86
7.86
7.85
7.28
7.28
7.27
7.27
7.26
7.26
7.25
2.57
2.52
14
13
12
11
10
9
8
7
6
5
4
3
2
1
0
ppm
1.939
2.440
3.000
2.964

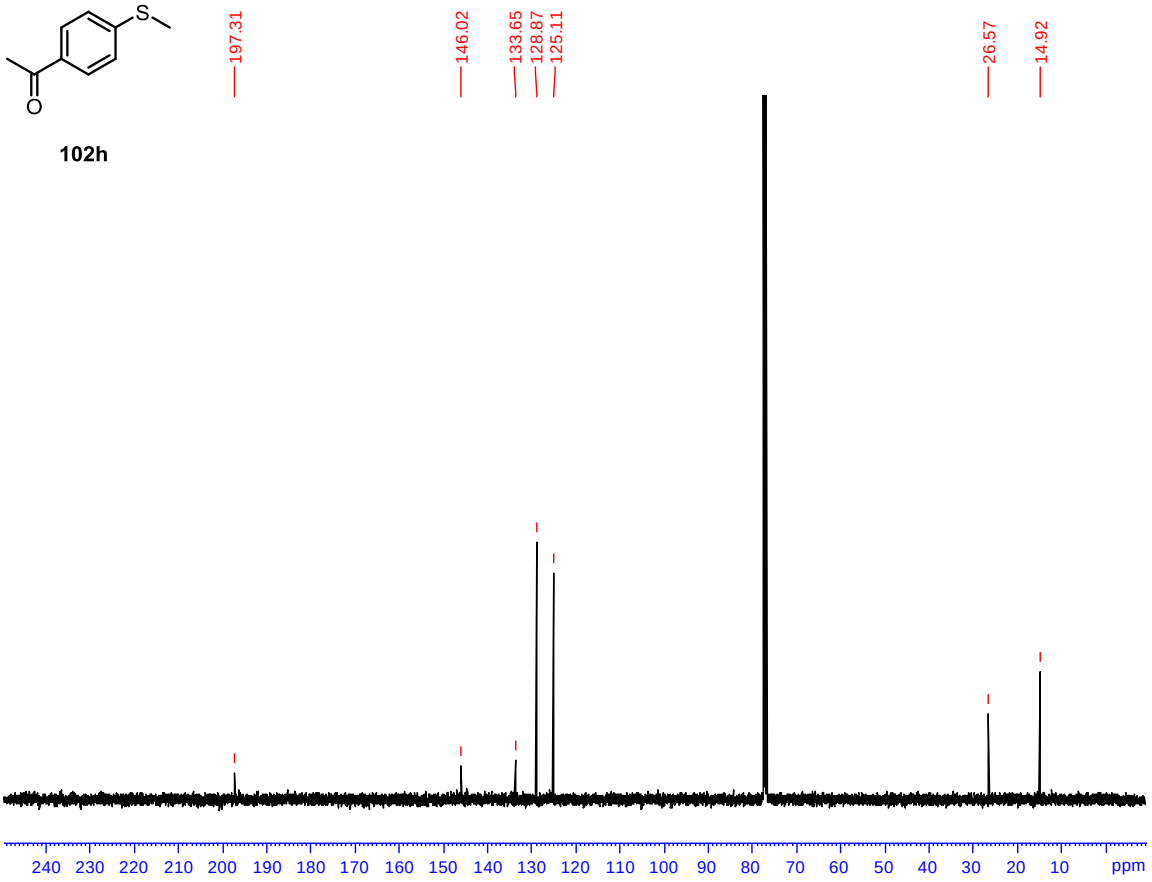
S
O
102h
197.31
146.02
133.65
128.87
125.11
26.57
14.92
240
230
220
210
200
190
180
170
160
150
140
130
120
110
100
90
80
70
60
50
40
30
20
10
ppm

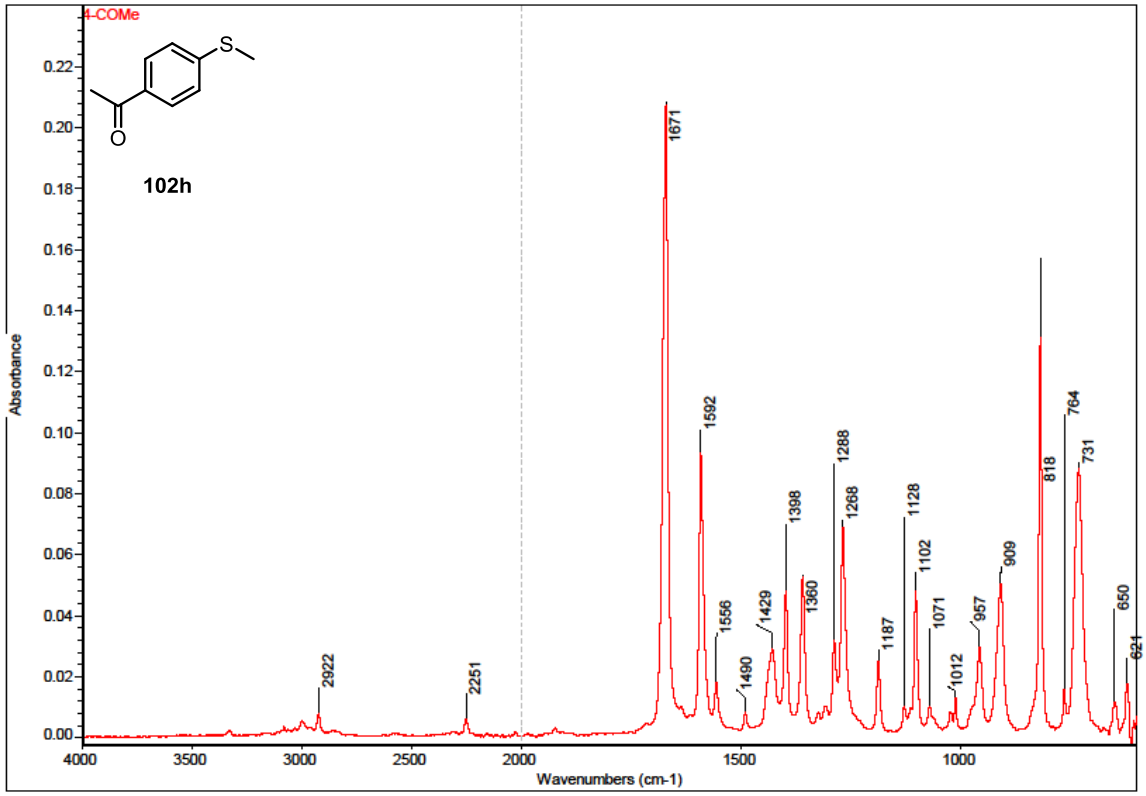
4-COMe
102h
Absorbance
Wavenumbers (cm-1)
2922
2251
1671
1592
1556
1490
1429
1398
1360
1288
1268
1187
1128
1102
1071
1012
957
909
818
764
731
650
621

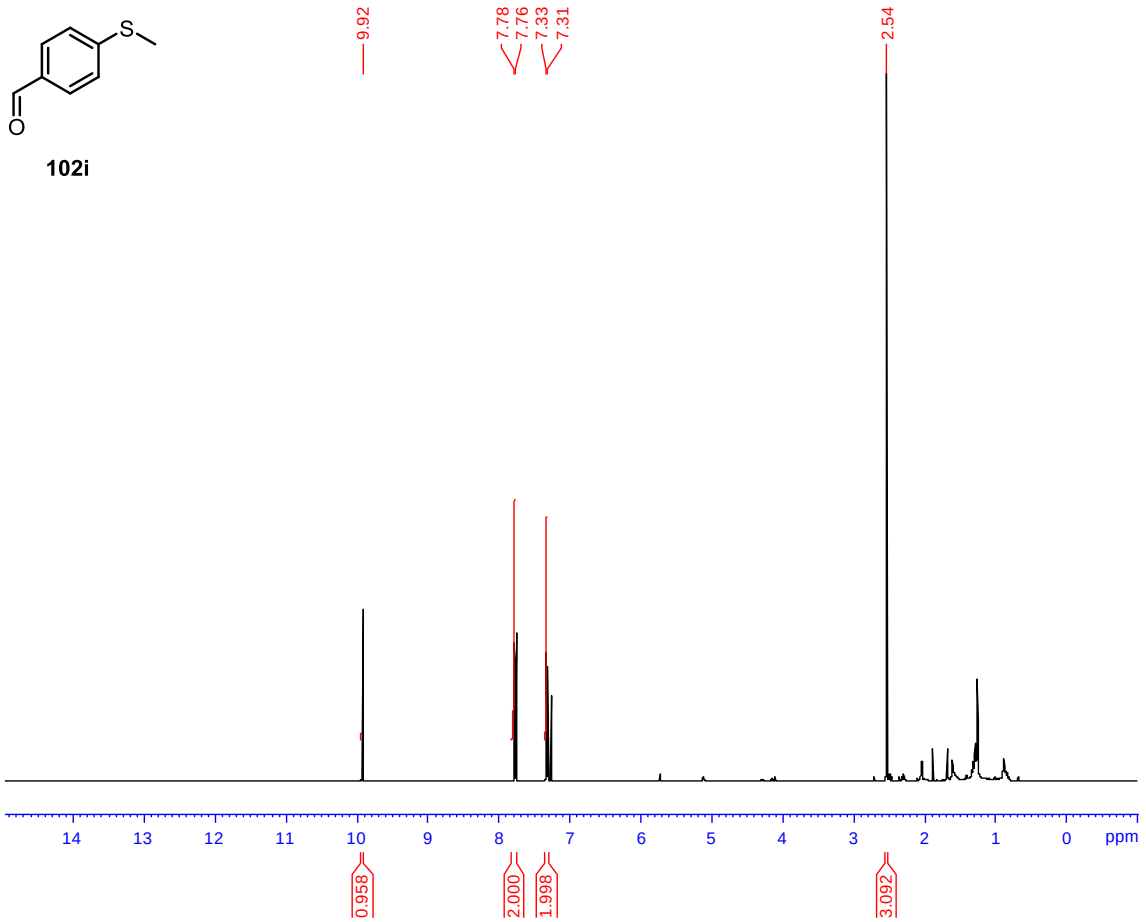
102i
9.92
7.78
7.76
7.33
7.31
2.54
ppm
0.958
2.000
1.998
3.092

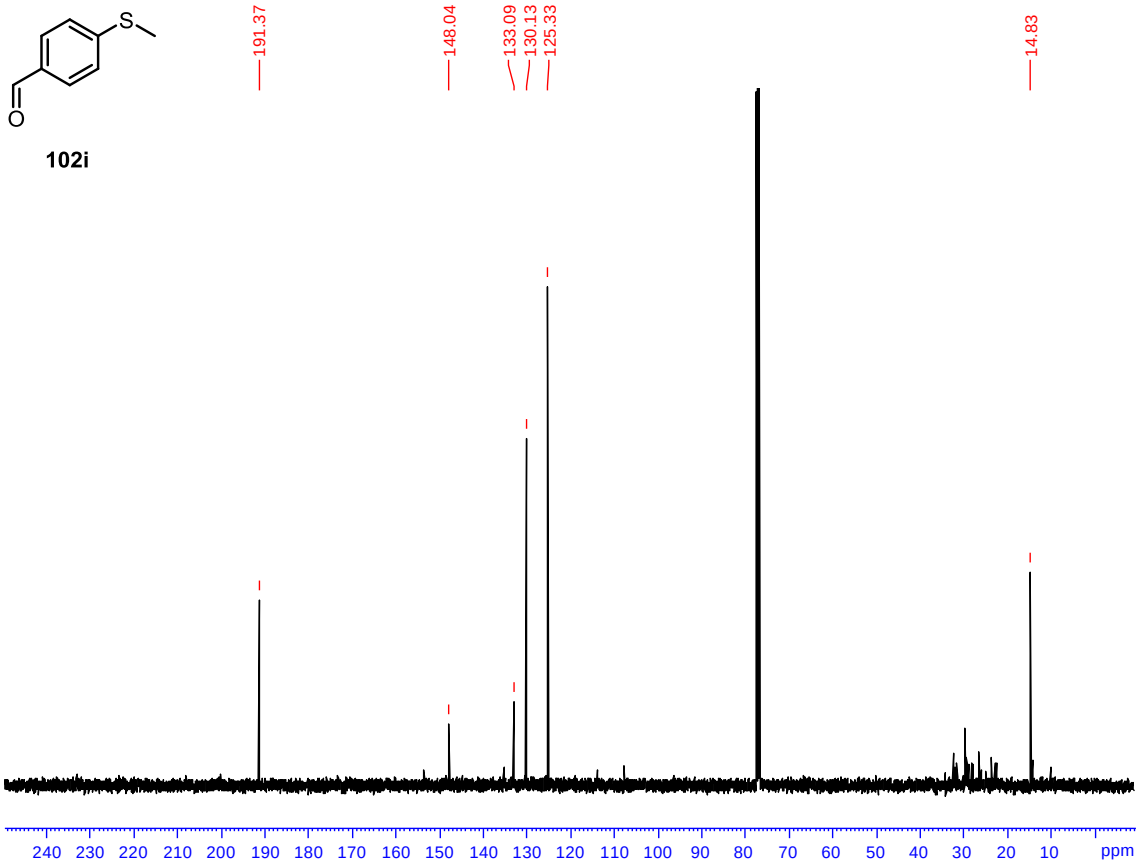
191.37
148.04
133.09
130.13
125.33
14.83
102i
240 230 220 210 200 190 180 170 160 150 140 130 120 110 100 90 80 70 60 50 40 30 20 10 ppm

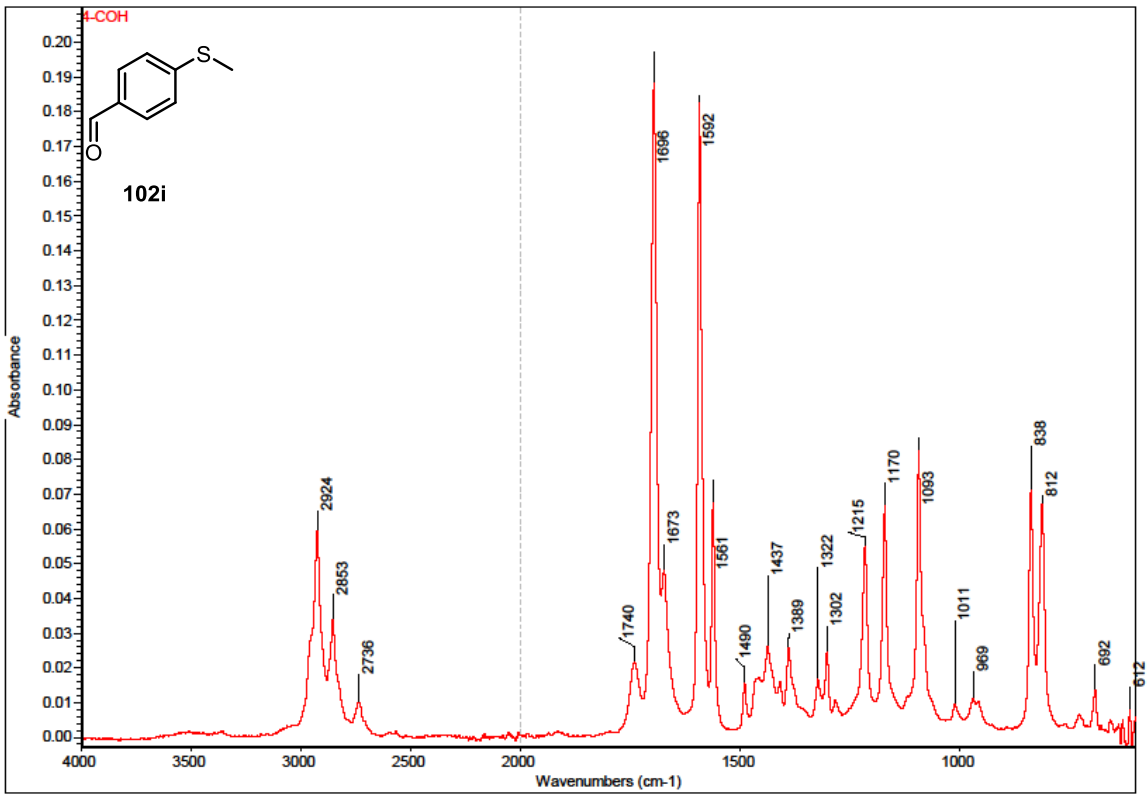
4-COH
102i
Absorbance
Wavenumbers (cm-1)
4000 3500 3000 2500 2000 1500 1000
2924
2853
2736
1740
1696
1673
1592
1561
1490
1437
1389
1322
1302
1215
1170
1093
1011
969
838
812
692
612

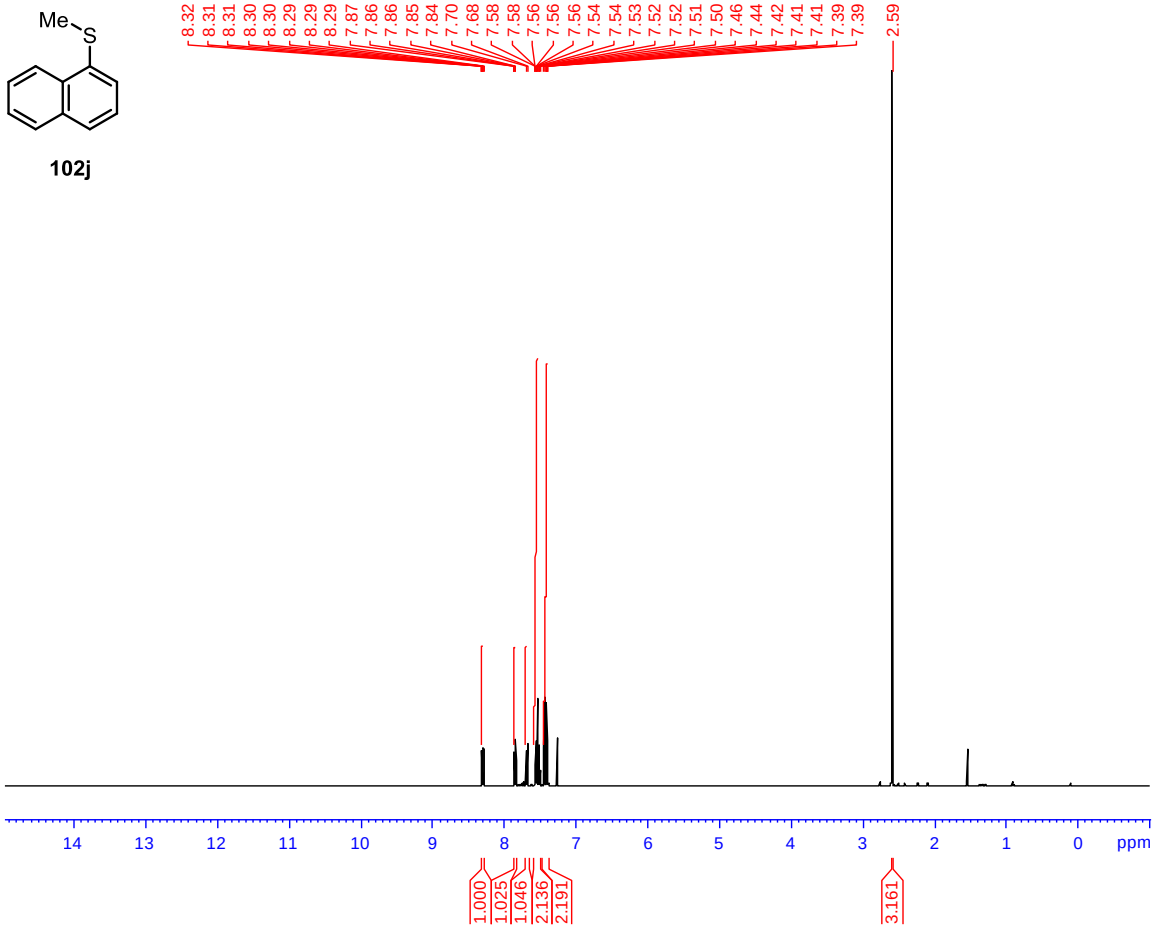
Me
S
102j
8.32
8.31
8.31
8.30
8.30
8.29
8.29
8.29
7.87
7.86
7.86
7.85
7.84
7.70
7.68
7.58
7.56
7.56
7.56
7.54
7.54
7.53
7.52
7.52
7.51
7.50
7.46
7.44
7.42
7.41
7.41
7.39
7.39
2.59
14 13 12 11 10 9 8 7 6 5 4 3 2 1 0 ppm
1.000
1.025
1.046
2.136
2.191
3.161

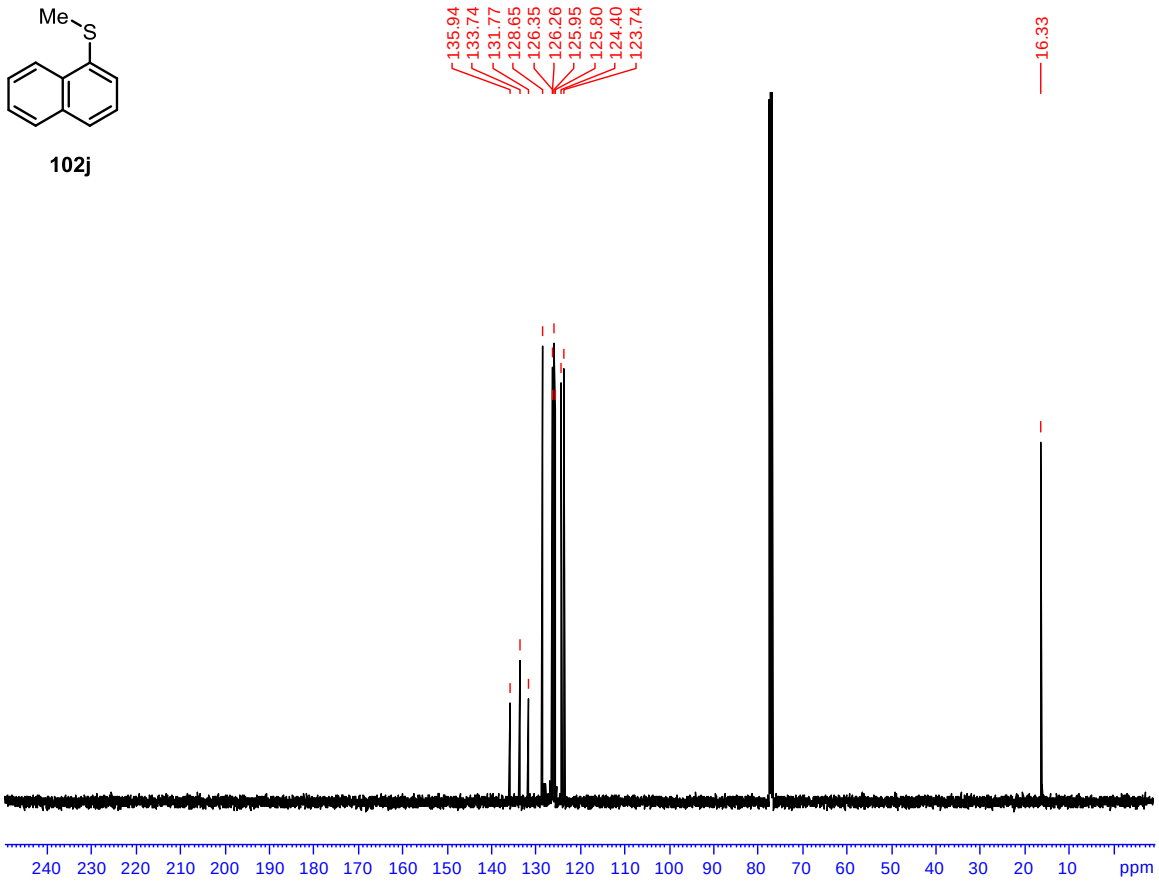
Me
S
102j
135.94
133.74
131.77
128.65
126.35
126.26
125.95
125.80
124.40
123.74
16.33
240 230 220 210 200 190 180 170 160 150 140 130 120 110 100 90 80 70 60 50 40 30 20 10 ppm

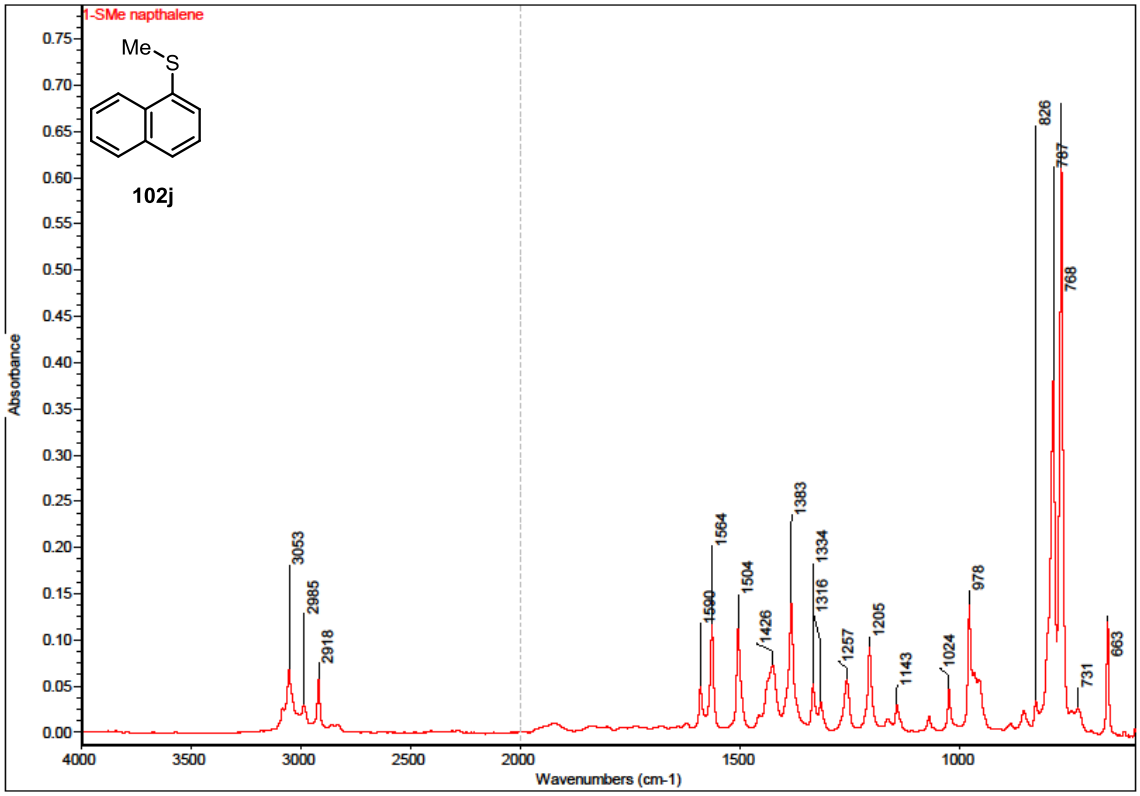
1-SMe napthalene
Me
S
102j
Absorbance
Wavenumbers (cm-1)
4000
3500
3000
2500
2000
1500
1000
0.75
0.70
0.65
0.60
0.55
0.50
0.45
0.40
0.35
0.30
0.25
0.20
0.15
0.10
0.05
0.00
3053
2985
2918
1590
1564
1504
1426
1383
1334
1316
1257
1205
1143
1024
978
826
787
768
731
663

6.0 References:

1. (a) Sun, Z. Y.; Botros, E.; Su, A. D.; Kim, Y.; Wang, E.; Baturay, N. Z.; Kwon, C. H., *J. Med. Chem.* **2000,** *43*, 4160-4168; (b) Otzen, T., Wempe, E. G., Kunz, B., Bartels, R., Lehwark-Yvetot, G., Hansel, W., Schaper, K. J., Seydel, J. K., *J. Med. Chem.* **2004,** *47*, 240-253; (c) Alcaraz, M. L.; Atkinson, S.; Cornwall, P.; Foster, A. C.; Gill, D. M.; Humphries, L. A.; Keegan, P. S.; Kemp, R.; Merifield, E.; Nixon, R.; Noble, A. J.; O'Beirne, D.; Patel, Z. M.; Perkins, J.; Rowan, P.; Sadler, P.; Singleton, J. T.; Tornos, J.; Watts, A. J.; Woodland, I. A., *Org. Process Res. Dev.* **2005,** *9*, 555-569
2. (a) Liu, G.; Huth, J. R.; Olejniczak, E. T.; Mendoza, R.; DeVries, P.; Leitza, S.; Reilly, E. B.; Okasinski, G. F.; Fesik, S. W.; von Geldern, T. W., *J. Med. Chem.* **2001,** *44*, 1202-1210; (b) Llauger, L.; He, H.; Kim, J.; Aguirre, J.; Rosen, N.; Peters, U.; Davies, P.; Chiosis, G., *J. Med. Chem.* **2005,** *48*, 2892-2905; (c) Ueda, M., Murakami, N., Nakagawa, Y., *Chem. Pharm. Bull.* **1968,** *16* (2), 345-351
3. Molinski, T. F.; Ireland, C. M., *J. Org. Chem.* **1989,** *54* (17), 4256-4259
4. Kosugi, M.; Shimizu, T.; Migita, T., *Chem. Lett.* **1978**, 13-14
5. Murata, M.; Buchwald, S. L., *Tetrahedron* **2004,** *60* (34), 7397-7403
6. Fernandez-Rodrıguez, M.; Shen, Q.; Hartwig, J. F., *J. Am. Chem. Soc.* **2006,** *128*, 2180-2181
7. Bastug, G.; Nolan, S. P., *J. Org. Chem.* **2013,** *78* (18), 9303-9308
8. Fu, C.-F.; Liu, Y.-H.; Peng, S.-M.; Liu, S.-T., *Tetrahedron* **2010,** *66* (12), 2119-2122
9. Droge, T.; Glorius, F., *Angew. Chem. Int. Ed.* **2010,** *49* (39), 6940-6952
10. Cristau, H. J.; Chabaud, B.; Chene, A.; Christol, H., *Synthesis* **1981**, 892/894
11. Taniguchi, N., *J. Org. Chem.* **2004,** *69*, 6904-6906
12. Baldovino-Pantaleón, O.; Hernández-Ortega, S.; Morales-Morales, D., *Adv. Synth. Catal.* **2006,** *348* (1-2), 236-242
13. (a) Chan, D. M. T.; Monaco, K. L.; Wang, R. P.; Winters, M. P., *Tetrahedron Lett.* **1998,** *39*, 2933-2936; (b) Evans, D.; Katz, J. L.; West, T. R., *Tetrahedron Lett.* **1998,** *39*, 2937-2940; (c) Lam, P. Y. S.; Clark, C. G.; Saubern, S.; Adams, J.; Winters, M. P.; Chan, D. M. T.; Combs, A., *Tetrahedron Lett.* **1998,** *39*, 2941-2944
14. Soria-Castro, S. M.; Penenory, A. B., *Beilstein J Org Chem* **2013,** *9*, 467-75
15. Uyeda, C.; Tan, Y.; Fu, G. C.; Peters, J. C., *J. Am. Chem. Soc.* **2013,** *135* (25), 9548-9552
16. Wong, Y. C., Jayanth, T. T., Cheng, C. H., *Org. Lett.* **2006,** *8* (24), 5613-5616
17. Reddy, V. P., Kumar, A. V., Swapna, K., Rao, K. R., *J. Org. Chem.* **2009,** *74*, 3189-3191
18. Wu, J. R.; Lin, C. H.; Lee, C. F., *Chem Commun (Camb)* **2009,** (29), 4450-4452
19. Arisaw, M., Suzuki, T., Ishikawa, T., Yamaguchi, M., *J. Am. Chem. Soc.* **2008,** *130*, 12214-12215
20. Jean, M.; Renault, J.; van de Weghe, P.; Asao, N., *Tetrahedron Lett.* **2010,** *51* (2), 378-381
21. Reddy, V. P., Kumar, A. V., Swapna, K., Rao, K. R., *Org. Lett.* **2009,** *11* (8), 1697-1700
22. Hostier, T., Ferey, V., Ricci, G., Pardo, D. G., Cossy, J., *Org. Lett.* **2015,** *17*, 3898-3901
23. Majek, M., von Wangelin, A., J.,, *ChemComm* **2013,** *49*, 5507-5509
24. Prier, C. K.; Rankic, D. A.; MacMillan, D. W., *Chem. Rev.* **2013,** *113* (7), 5322-5363
25. Narayanam, J. M.; Stephenson, C. R., *Chem. Soc. Rev.* **2011,** *40* (1), 102-113
26. Nguyen, J. D., D'Amato, E. M., Narayanam, J. M. R., Stephenson, C. R. J., *nature chemistry* **2012,** *4*, 854-859
27. Leonard, J.; Lygo, B.; Procter, G., *Advanced Practical Organic Chemistry*. 3 ed.; CRC Press Taylor & Francis Group: Boca Raton, Fl, 2013; p 142-143.
28. (a) Fry, A. J.; Krieger, R. L., *J. Org. Chem.* **1976,** *41*, 54-57; (b) Pause, L.; Robert, M.; Save´ant, J. M., *J. Am. Chem. Soc.* **1999,** *121*, 7158-7159
29. Enemaerke, R. J.; Christensen, T. B.; Jensen, H.; Daasbjerg, K., *Journal of the American Chemical Society Perkins Transactions 2* **2001,** (9), 1620-1630
30. Doeven, E. H.; Zammit, E. M.; Barbante, G. J.; Francis, P. S.; Barnett, N. W.; Hogan, C. F., *Chemical Science* **2013,** *4*, 977-982
31. Vasquez-Cespedes, S.; Ferry, A.; Candish, L.; Glorius, F., *Angew. Chem. Int. Ed.* **2015,** *54* (19), 5772-5776

32. Oderinde, M. S.; Frenette, M.; Robbins, D. W.; Aquila, B.; Johannes, J. W., *J. Am. Chem. Soc.* **2016,** *138* (6), 1760-1763
33. (a) McDaniel, D. H.; Brown, H., *J. Org. Chem.* **1958,** *23*, 420-427; (b) Anslyn, E. V.; Dougherty, D. A., *Modern Physical Organic Chemistry*. University Science Books: 2006.
34. Hegedus, L. L.; McCabe, R. W., *Catalyst Poisoning*. Marcel Dekker: New York, 1984.
35. Romero, N. A.; Nicewicz, D. A., *J. Am. Chem. Soc.* **2014,** *136* (49), 17024-17035
36. Polyzos, A., *Chemistry* **2006,** *12* (23), 5972-5990
37. Tucker, J. W.; Zhang, Y.; Jamison, T. F.; Stephenson, C. R., *Angew. Chem. Int. Ed.* **2012,** *51* (17), 4144-4147
38. Tamayo, A. B.; Alleyne, B. D.; Djurovich, P. I.; Lamansky, S.; Tsyba, I.; Ho, N. N.; Bau, R.; E., T. M., *J. Am. Chem. Soc.* **2003,** *125*, 7377-7387
39. Luo, F.; Pan, C.; Li, L.; Chen, F.; Cheng, J., *Chem. Comm.* **2011,** *47* (18), 5304-5306
40. Jang, Y.; Kim, K. T.; Jeon, H. B., *J. Org. Chem.* **2013,** *78* (12), 6328-6331
41. Iinuma, M.; Moriyama, K.; Togo, H., *Eur. J. Org. Chem.* **2014,** *2014* (4), 772-780